RS1 STRUCTURE-FUNCTION RELATIONSHIPS:
ROLES IN RETINAL ADHESION AND
X-LINKED RETINOSCHISIS

by

WINCO WING-HO WU

B.Sc., The University of British Columbia, 2000

A THESIS SUBMITTED IN PARTIAL FULFILLMENT OF THE
REQUIREMENTS FOR THE DEGREE OF

DOCTOR OF PHILOSOPHY

in

THE FACULTY OF GRADUATE STUDIES

BIOCHEMISTRY AND MOLECULAR BIOLOGY

THE UNIVERSITY OF BRITISH COLUMBIA

October 2005

ABSTRACT

X-linked retinoschisis is a form of macular degeneration that can result in visual loss in young males or in females with both copies of the gene defective. The *RS1* gene associated with X-linked retinoschisis was positionally cloned in 1997. The gene was found to encode RS1, a 224-amino acid protein containing a discoidin domain that spans most of the protein. Discoidin domains are found in a wide variety of proteins that are involved mainly in cell adhesion. This thesis investigation examined the structure-function relationships in RS1 and their roles in maintaining retinal cell adhesion and in causing X-linked retinoschisis. Results showed that RS1 exists as a single disulfide-linked homo-octamer formed by intermolecular disulfide bonds between C59 and C223. C40-C40 intermolecular disulfide bonds further result in disulfide-linked dimer formation within this octameric complex. Within the discoidin domain, C63-C219 and C110-C142 form intramolecular disulfide bonds to allow for proper protein folding and stability of the discoidin domain, and C83 exists as a free cysteine. To allow for RS1 secretion into the extracellular matrix, each RS1 subunit is cleaved after S23 by signal peptidase. The main molecular mechanisms that cause X-linked retinoschisis can be grouped into four categories: mutations in the leader sequence prevent proper RS1 targeting to the endoplasmic reticulum; most mutations in the discoidin domain prevent proper protein folding and secretion; mutations in C59 or C223 prevent octameric assembly; and R141H within the discoidin domain causes abnormal oligomer formation. A suspected polymorphism D158N was shown to behave similarly to wildtype RS1. To identify the component that RS1 interacts with, known ligands of discoidin family proteins

were tested for their ability to bind RS1. Unlike Factor V, RS1 did not bind

phospholipids; however, similar to discoidin I, RS1 bound to D-galactose. This

interaction depended on the octameric form of RS1, as dimers or monomers

interacted weakly with galactose. Isopropyl β-D-1-thiogalactopyranoside eluted RS1

from a galactose-agarose column. This property was used to purify RS1 from retinal

membranes. In summary, RS1 is a lectin whose function critically depends on the

proper folding of its discoidin domain and disulfide-linked octamerization.

TABLE OF CONTENTS

LIST OF TABLES

LIST OF FIGURES

LIST OF ABBREVIATIONS

AD	autosomal dominant
AMD	age-related macular degeneration
AR	autosomal recessive
CRD	cone-rod dystrophy
DMEM	Dulbecco's modified Eagle media
DOPC	1,2 dioleoyl-*sn*-glycero-3-phosphocholine
DOPE	1,2 dioleoyl-*sn*-glycero-3-phosphoethanolamine
DOPS	1,2 dioleoyl-*sn*-glycero-3-phosphoserine
DTT	dithiothreitol
EBNA	Epstein-Barr nuclear antigen
EC	extracellular cadherin
EDTA	ethylene diamine tetraacetic acid
ER	endoplasmic reticulum
ERG	electroretinogram
GAG	glycosaminoglycan
h	hour
HEK	human embryonic kidney
IAM	iodoacetamide
ILM	inner limiting membrane
IgG	immunoglobulin
INL	inner nuclear layer
IPL	inner plexiform layer

IPTG	isopropyl β-D-1-thiogalactopyranoside
IS	inner segment
kDa	kilodalton
LC	liquid chromatography
MALDI-TOF	matrix-assisted laser desorption/ionization time-of-flight
min	minutes
MS	mass spectrometry
NEM	N-ethyl maleimide
NMR	nuclear magnetic resonance
OLM	outer limiting membrane
ONL	outer nuclear layer
OPL	outer plexiform layer
OS	outer segment
PAGE	polyacrylamide gel electrophoresis
PBS	phosphate-buffered saline
PCR	polymerase chain reaction
RP	retinitis pigmentosa
rWT	recombinant wildtype RS1
SDS	sodium dodecyl sulfate
TBS	Tris-buffered saline
Tris	Tris [hydroxymethyl]aminomethane
WT	wildtype
XL	X-linked

ACKNOWLEDGEMENTS

CHAPTER 1: INTRODUCTION

1.1 The Eye and the Retina

The eye is the main window through which humans perceive the outside world through vision. The eye is one of the most useful organs developed throughout evolution (Fernald, 2004), playing a key role in helping the organism obtain food or carry out other key activities required for survival. The vertebrate eye is an example of such an optimized structure that can transduce light into electrical signals which are further processed by the brain into a sharp image.

1.1.1 Anatomy of the Vertebrate Eye

Each eyeball consists of three main layers (Fig. 1.1): the sclera, choroid, and retina (McIlwain, 1996; Rodieck, 1973). The sclera is the tough outer layer of the eye, comprised of mainly collagen. The sclera surrounds the eye, and the clear cornea is continuous with the sclera at the front of the eye. The middle choroid layer contains the blood vessels that nourish the outer retina. The central retinal artery, which flows in from the optic nerve, nourishes the inner retina. The iris and ciliary body are continuous with the choroid. The iris allows a varying amount of light to enter the eye, while the ciliary body adjusts the shape of the lens. Finally, the innermost layer is the retina, the light-transducing tissue, which enables electrical signals to be transmitted and imaged by the brain. Before any light can reach the retina at the back of the eye, light must first pass through the cornea, aqueous humor, lens, and vitreous humor. Each of these layers helps to refract and focus the light rays reflected from an image onto the retina.
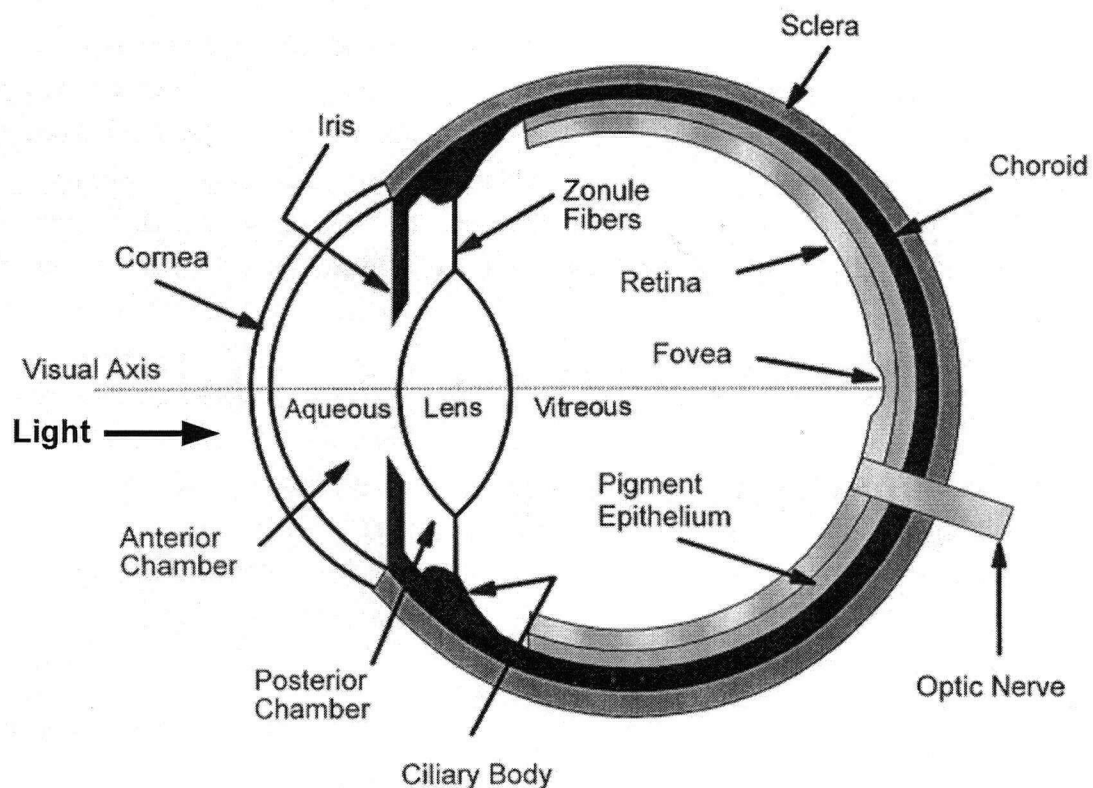
Figure 1.1. Anatomy of the vertebrate eye. Each eyeball is composed of three
layers. The outer layer known as the sclera provides structure to the whole eye.
The layer underneath the sclera is the choroid, which contains the blood vessels and
supplies the retinal pigment epithelium and part of the retina with nutrients. The
innermost layer is the retina, which contains the molecular components to transduce
the energy of light into that of chemical and electrical energy, which can be
transmitted to the brain through the optic nerve and processed as vision. Light must
first pass through the cornea, aqueous humor, lens, and vitreous humor before
reaching the retina. Modified from McIlwain, 1996.

1.1.2 The Retina

The retina is a delicate structure composed of three main layers of neuronal cells from the central nervous system (Fig. 1.2): the photoreceptors, bipolar cells, and ganglion cells (Buser and Imbert, 1992; Cohen, 1963; Dowling, 1987; Kolb, 1994; McIlwain, 1996). These three layers of retinal cells contain two synaptic layers – the outer and inner plexiform layers. The outermost layer of the retina, located under the choroid and the retinal pigment epithelium, consists of photoreceptors. Rod photoreceptor cells function under dim lighting and cone photoreceptors function under normal lighting and in color vision. The outer segments of photoreceptors are responsible for phototransduction. Under the photoreceptor cells is the layer of secondary neurons including bipolar, horizontal, and amacrine cells. Bipolar cells relay messages from the photoreceptors to the ganglion cells. Horizontal and amacrine cells transfer messages laterally within the synaptic regions of the outer and inner plexiform layers, respectively. Finally, the third layer, under the secondary neurons, is the ganglion cell layer, whose axons form the optic nerve connecting the retina to the brain. The outer and inner limiting membranes limit the diffusion of substances into and out of the retina. The outer limiting membrane is formed by contacts between photoreceptor inner segments and Müller cells, a type of glial cell that spans several layers within the retina. The inner limiting membrane is formed by contacts between Müller cells and their associated basement membrane.

The human retina contains a central region responsible for sharp visual acuity, which allows individuals to perform activities such as reading and writing.
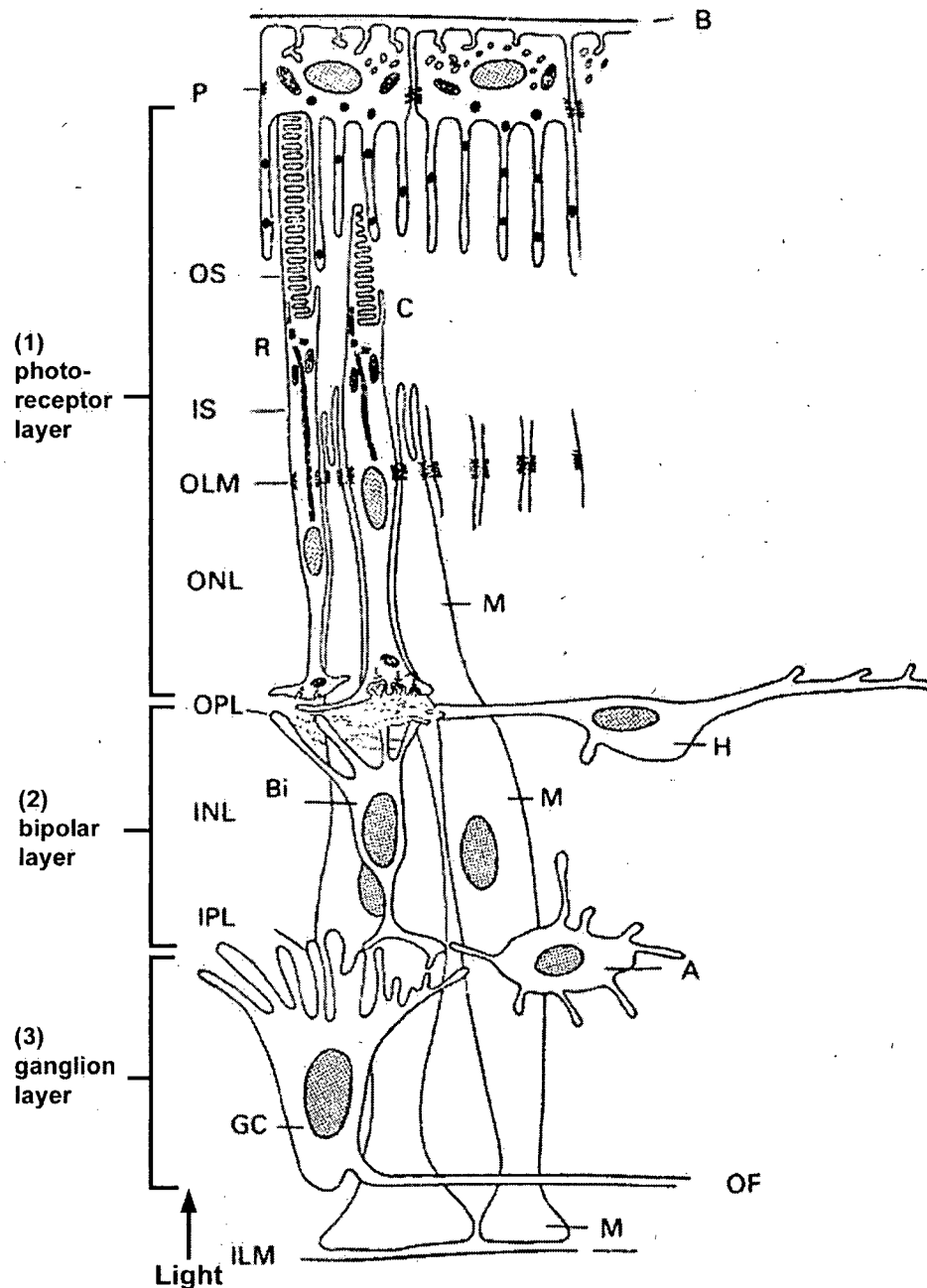
Figure 1.2. Organization of the vertebrate retina. The retina possesses three main layers of cells: the photoreceptor cell layer, bipolar cell layer, and ganglion cell layer. Signals are transmitted from the photoreceptors, to the bipolar cells, and finally to the ganglion cells, which relay the message to the brain. The abbreviations used are as follows: ILM –inner limiting membrane, GC –ganglion cells, OF –optic nerve fiber, IPL –inner plexiform layer, INL –inner nuclear layer, A –amacrine cells, Bi –Bipolar cells, M –Müller cells, H –horizontal cells, OPL –outer plexiform layer, ONL –outer nuclear layer, OLM –outer limiting membrane, IS –inner segment, OS –outer segment, R –rod cells, C –cone cells, P –retinal pigment epithelial cells, B – Bruch's membrane. Modified from Cohen, 1963.

This region is known as the macula lutea (or macula), with the centre of the macula known as the fovea or foveal pit (Bessant et al., 2001; McIlwain, 1996; Yamada, 1969). At the centre of the foveal pit, only the inner and outer segments of cones, and some of their cell bodies, are present. This is because the second and third layers of retinal cells are displaced to the edges of the pit. Outside this central macular region is the peripheral retina, where there is an abundance of rod photoreceptor cells. This region is responsible for peripheral vision and motion detection, as well as vision in dim light.

1.2 Retinal Degenerative Diseases

As the retina is a key component in the visual process, retinal degeneration represents a severe compromise to vision in individuals. Retinal degenerative diseases can take many forms, most of which eventually lead to photoreceptor death (Chang et al., 1993; Portera-Cailliau et al., 1994; Wenzel et al., 2005).

1.2.1 Age-related Macular Degeneration

Age-related macular degeneration is the most common cause of blindness in the developed world (Congdon et al., 2004; Kahn et al., 1977). As its name suggests, the degeneration is strongly associated with aging: There is a dramatic increase in its prevalence in European-derived populations from less than 1% in their sixth decade of life to more than 15% in their ninth decade (Congdon et al., 2004). Age-related macular degeneration has a strong genetic component (Edwards et al., 2005; Haines et al., 2005; Klaver et al., 1998; Klein et al., 2005;

Meyers and Zachary, 1988; Seddon et al., 2005), so studying inherited retinal dystrophies (see below) may also help elucidate mechanisms of age-related macular degeneration.

The most convincing environmental factor to be correlated with age-related macular degeneration is smoking (Smith et al., 1996; Vingerling et al., 1996). Studies with other environment factors, such as diet and sunlight exposure, have been controversial (van Leeuwen et al., 2003). However, it is now generally accepted that supplementation with antioxidant nutrients in high-risk individuals may be a useful form of preventive therapy (Comer et al., 2004; Hogg and Chakravarthy, 2004).

Age-related macular degeneration can be classified into two forms – dry (nonexudative) and wet (exudative) (Comer et al., 2004; Penfold et al., 2001). In the dry form, the retina contains atrophic and hypertrophic lesions in the macula, as well as deposits of drusen beneath the retinal pigment epithelium caused by degeneration of the retinal pigment epithelium and retina. In the wet form, neovascularization of choroidal vessels occurs, and the resulting haemorrhage beneath the retinal pigment epithelium causes lipid extravasation and fibrovascular tissue proliferation. Therapy for age-related macular degeneration has centered on thermal laser photocoagulation or verteporfin photodynamic therapy, both of which are treatments only for the wet form (Comer et al., 2004).

1.2.2 Inherited Retinal Dystrophies

As shown in Table 1.1 many genes have been implicated in various forms of inherited macular dystrophies (Bessant et al., 2001; Michaelides et al., 2003). The

Table 1.1 Selected inherited retinal dystophies.

More than 150 genes have been found to be associated with various inherited retinal dystrophies. Shown are selected disease-associated proteins and their corresponding retinal dystrophy. A more comprehensive list can be obtained from Retnet, http://www.sph.uth.tmc.edu/Retnet/disease.htm (Daiger et al., 1998). Abbreviations used: AD, autosomal dominant; AR, autosomal recessive; XL, X-linked; RP retinitis pigmentosa; CRD, cone-rod dystrophy; AMD, age-related macular degeneration. Modified from Bessant et al., 2001 and Michaelides et al., 2003.

Disease-Associated Protein	Inheritance Pattern	Inherited Retinal Dystrophies
Phototransduction cascade		
Rhodopsin	AD	RP, congenital stationary night blindness
GNAT1	AD	congenital stationary night blindness
Phosphodiesterase α	AR	RP
Phosphodiesterase β	AR	RP
Cyclic Nucleotide Gated Channel α	AR	RP
Recovery phase		
Arrestin	AR	Oguchi disease
Rho kinase	AR	Oguchi disease
GCAP	AD	Cone dystrophy
RetGC	AD	CRD
	AR	Leber congenital amaurosis
Structural proteins		
Peripherin	AD	RP, macular dystrophies
	Digenic	RP
ROM1	Digenic	RP
Prominin-like 1	AR	RP
Retinol (vitamin A) metabolism		
RLBP1	AR	RP
RDH5	AR	Fundus albipunctatus
RPE65	AR	Leber congenital amaurosis
ABCA4	AR	Stargardt dystrophy, CRD,RP, AMD
Transcription factors		
CRX	AD	CRD
	AR	Leber congenital amaurosis
NRL	AD	RP
NR2E3	AR	enhanced S-cone syndrome
Extracellular Proteins		
RS1	XL	X-linked retinoschisis
TIMP3	AD	Sorsby fundus dystrophy
NDP	XL	Norrie disease

following will briefly discuss inherited retinal dystrophies associated with rhodopsin, peripherin-2, and ABCA4.

More than one hundred different mutations of the gene encoding the key phototransduction protein, rhodopsin, have been identified (Daiger et al., 1998). Most of these mutations are associated with autosomal dominant retinitis pigmentosa, a genetically heterogeneous form of blindness due to abnormalities mainly in rod photoreceptors (Bessant et al., 2001; Kennan et al., 2005). For example, within different rhodopsin mutations, considerable phenotypic heterogeneity has been observed (Bessant et al., 2001). A number of phenotype-genotype studies have been performed on rhodopsin. For example, it has been reported that mutations affecting the C-terminal cytoplasmic tail of rhodopsin are particularly severe, having the fastest average rates of decline of visual field area and electroretinogram amplitude (Berson et al., 2002). This is because the C-terminal tail is a highly important region for the proper targeting of rhodopsin to rod outer segments (Sung et al., 1994; Tam et al., 2000). Therapeutically, there may be hope for the treatment of some mutations, as gene delivery of ribozymes have been used in animal models to show reduced photoreceptor loss and improved retinal function in a rhodopsin animal mutant (Lewin et al., 1998).

Mutations in the gene encoding peripherin-2, a protein present abundantly in the outer segment of rod and cone photoreceptors, can result in a variety of retinal dystrophies, including retinitis pigmentosa (Keen and Inglehearn, 1996). Especially useful to study abnormalities in this protein is the existence of a naturally-occurring disease mouse model called the rds (retinal degeneration slow) mouse (Connell et

al., 1991; Sanyal and Jansen, 1981). This rds mouse contains an insertion of viral DNA into an exon of the *Rds* gene, producing an abnormally large mRNA transcript with no detectable protein expression (Ma et al., 1995; Travis et al., 1989). Mutations in the human *RDS (or Prph2)* gene have been found to result in improper targeting of peripherin-2 to the outer segment or to exert a dominant negative effect on photoreceptor outer segment instability (Kedzierski et al., 1997; Loewen et al., 2003). A more complex type of retinal dystrophy is seen during abnormal subunit assembly of a peripherin-2 mutant protein with ROM-1, a protein which shares sequence homology with peripherin-2 (Bascom et al., 1992). This abnormal assembly results in a digenic type of retinal dystrophy (Goldberg and Molday, 1996; Kajiwara et al., 1994). Hope for treatment is also on the horizon for peripherin-associated visual loss, as investigators have found that diseased animals show improved photoreceptor structure and function using gene therapy with *Prph2* (Ali et al., 2000; Schlichtenbrede et al., 2003).

Mutations in *ABCA4*, which encodes another outer segment protein, are responsible for autosomal recessive Stargardt dystrophy (Allikmets et al., 1997) and other related retinal diseases (Cremers et al., 1998; Klevering et al., 1999; Martinez-Mir et al., 1998). ABCA4 (also known as ABCR) is expressed in rod and cone photoreceptors (Illing et al., 1997; Molday et al., 2000), where it co-localizes with peripherin-2 at the disc rim. In Stargardt disease, a compound called lipofuscin accumulates, which causes retinal pigment epithelium apoptosis (Delori et al., 1995; Wolf, 2003). This is due to defective ABCA4 because *ABCA4* knockout mice display increased levels of *N*-retinylidene-phosphatidylethanolamine (*N*-retinylidene-PE), the

major fluorescent constituent of lipofuscin (Weng et al., 1999). Normally, ABCA4 participates in the recycling of 11-*cis* retinal, the chromophore in rhodopsin which starts the phototransduction cascade (Glazer and Dryja, 2002): When a photon hits 11-*cis* retinal, it is converted to all-*trans* retinal. All-*trans* retinal then leaves rhodopsin and combines with phosphatidylethanolamine (PE) to form *N*-retinylidene-PE. ABCA4 subsequently transports *N*-retinylidene-PE from the lumen to the cytoplasmic side of the disc membrane (Beharry et al., 2004; Sun et al., 1999). After dissociation of *N*-retinylidene-PE to all-*trans* retinal and PE, all-*trans* retinal is reduced to all-*trans* retinol and subsequently transported to the retinal pigment epithelium, where it is converted back to 11-*cis* retinal (Rando, 2001). Consequently, ABCA4 plays a key role in facilitating the removal of all-*trans* retinal from disc membranes following photobleaching of rhodopsin.

1.2.3 Defects in Retinal Adhesion

Absolute alignment and preservation of the structural architecture of the retina is required for vision to occur. Defects in retinal adhesion, especially in the macular or central region of the retina responsible for sharp visual acuity, can be particularly detrimental. Retinal detachment and retinoschisis are two common forms of defects in retinal adhesion that lead to a loss of vision. Retinal detachment occurs in the region between the retinal pigment epithelium and photoreceptors (Ghazi and Green, 2002; Richards et al., 2002). A less common but still serious retinal adhesion lesion that occurs in the macular region is retinoschisis (George et al., 1995b; Tantri et al., 2004). In retinoschisis, the splitting occurs within the various layers of the retina.

There are several types of retinal detachment: rhegmatogenous, tractional, and exudative (Cavallerano, 1992; Gariano and Kim, 2004; Ghazi and Green, 2002). In all three types there is an accumulation of subretinal fluid. Rhegmatogenous retinal detachment is the most common, deriving its name from the Greek "rhegma," meaning "break". A prerequisite for rhegmatogenous retinal detachment is the presence of a liquefied vitreous. This in turn can cause tractional forces which produce and maintain a break, leading to the entry of fluid into the subretinal space and detachment of the retina from the retinal pigment epithelium. Rhegmatogenous retinal detachment may be caused by high myopia, lattice degeneration (a form of peripheral retinal degeneration), trauma, diabetes, cataract surgery, or certain inherited diseases. In tractional retinal detachment, detachment occurs due to fibrous membranes in the vitreous and a pulling away of the retina from the retinal pigment epithelium. The most common causes of tractional retinal detachment are proliferative diabetic retinopathy, sickle cell disease, advanced retinopathy of prematurity, and penetrating trauma. In exudative retinal detachment, detachment occurs when subretinal fluid accumulates and causes detachment without retinal breaks or traction. The fluid usually comes from the retinal blood vessels, choroid, or both. The etiologic factors of exudative detachments are usually tumor growth or inflammation.

Retinoschisis can also be subclassified into three types: degenerative, secondary, and hereditary (Madjarov et al., 1995; Tantri et al., 2004). In degenerative retinoschisis, also known as acquired or senile retinoschisis, retinal splitting occurs due to age. Foveal schisis is rare in degenerative retinoschisis, as

peripheral schisis is more common. Degenerative retinoschisis can be divided into two classes: typical and reticular. In typical degenerative retinsochisis splitting occurs mainly at the outer plexiform layer, while in reticular degenerative retinsochisis splitting occurs at the inner retinal layers. In secondary retinoschisis, retinal splitting occurs secondary to some disease. However, retinoschisis in these diseases is only a rare complication. Diseases include proliferative diabetic retinopathy, malignant melanoma, and blunt trauma. Interestingly, retinal detachment may lead to retinoschisis as a secondary effect, and retinoschisis can also lead to retinal detachment. Finally, hereditary retinoschisis, also called X-linked retinsochisis, is the congenital form of retinoschisis. This form is discussed in Section 1.4 in more detail.

1.3 Structural and Functional Features of Extracellular Matrix Components

The extracellular environment has recently been shown not only to mediate structural and adhesive contacts in the extracellular spaces between cells, but also to be a highly dynamic compartment that can regulate events inside the cell, including events within the nucleus (Carson, 2004; Reichardt, 1999; Reichardt et al., 1992). Examples of cellular processes mediated by the extracellular matrix include cell growth, development, differentiation, apoptosis, cell migration, tissue remodeling, tissue repair, and adhesion. The extracellular environment contains fibrous material rich in carbohydrate and glycoproteins (Venstrom and Reichardt, 1993). The environment is oxidizing, and as such, proteins often contain disulfide

bonds or crosslinked amino acids that stabilize their structure (Moriarty-Craige and Jones, 2004). Major classes of extracellular molecules will be discussed below.

One of the key themes especially apparent in the extracellular matrix is the modular component of extracellular proteins (Bork et al., 1996). Many proteins are formed by multiple modules, or repeating domains, each of which has a distinct role. Each module folds into a compact domain and thus expressing the domain itself is a useful tool to probe the structural and functional properties of a particular domain. The same module may exist multiple times in the same protein, or exist in other proteins. This multiple occurrence of modules likely evolved from exon shuffling and is an efficient way to make use of functional components (Liu and Grigoriev, 2004; Patthy, 2003; Roy, 2003).

1.3.1 Non-protein components of the Extracellular Matrix

Non-protein components that play a key role in extracellular matrix function include the phospholipids from the plasma membrane and also carbohydrates (Hakomori, 1990; Hileman et al., 1998; Hricovini, 2004). The main extracellular lipids of the outer leaflet of plasma membranes are the zwitterionic lipids phosphatidylcholine, phosphatidylethanolamine and sphingomyelin (Buckland and Wilton, 2000). Carbohydrates can also be attached to lipids as glycolipids. Perhaps more commonly, carbohydrates are found attached to proteins as glycoproteins or proteoglycans, or exist by themselves as in the case of hyaluronan. The ionic composition of the extracellular matrix is also different from that inside cells, as divalent ions such as calcium are often present at relatively high levels (Riccardi,

2000). Calcium is an important, and often necessary, component of signal transduction cascades and cell adhesion.

1.3.2 Collagens

Collagen, the most abundant protein in the animal kingdom, is found ubiquitously in the extracellular matrix and its main role is to provide structure to the organism (Haralson and Hassell, 1995). To date, more than 25 vertebrate collagens have been identified (Gelse et al., 2003; Myllyharju and Kivirikko, 2004). The hallmark of the collagen structure is a coiled coil triple helix formed from three separate polypeptides chains. Each polypeptide contains a repetitive Glycine-X-Y motif, where X and Y are other amino acids but often proline or hydroxyproline. Glycine, the smallest amino acid, is required at every third amino acid in order for the triple helix to form properly. Post-translational modifications on collagen consist of hydroxylation of prolines and lysines. Hydroxyprolines are critical for the stability of the triple helix, while hydroxylysines mediate covalent crosslinking of collagen subunits. In addition, hydroxylysines allow for the attachment of carbohydrates to collagen.

Several classes of collagens exist, classified mainly by differences in their structure (Gelse et al., 2003; Haralson and Hassell, 1995; Myllyharju and Kivirikko, 2004; Olsen and Ninomiya, 1999). These include fibrillar collagens, FACIT collagens, short chain collagens, collagens of the basement membranes, multiplexins, MACIT collagens, and ungrouped collagens. Fibrillar collagens form long, uninterrupted triple helices of about 300nm in length. Fibrillar collagens are comprised of types I, II, III, V, XI, XXIV, and XXVII. FACIT (Fibril Associated

Collagens with Interrupted Triple helices) collagens act as bridges between fibrillar collagens and other components of the extracellular matrix. These collagens include types IX, XII, XIV, XVI, XIX, XX, XXI, XXII, and XXVI. Short chain collagens include types VIII and X, and have short subunits of only about 60kDa. Type IV collagen is the major basement membrane component, forming a network-like structure with other components such as laminin, nidogen, and heparan sulfate proteoglycan. Multiplexins, comprised of collagen types XV and XVIII, have short triple-helical domains, separated and flanked by non-triple-helical regions. They are termed multiplexins because they have multiple triple helix domains with interruptions. There are also collagens with transmembrane domains, known as MACITs (Membrane-Associated Collagens with Interrupted Triple helices). Types XIII, XVII, XXIII, and XXV belong to the MACITs. Finally, collagens not belonging to any of the above families are types VI and VII. Type VI collagen is a heterotrimer that is further linked together to form disulfide-linked dimers and tetramers, and tetramers associate end-to-end to generate microfibrils. Type VII collagen is a homotrimer with a triple-helical domain about 50 percent longer than the triple helix of fibrillar collagens. In addition, it contains N- and C- terminal flanking regions of non-triple-helical domains. The C-terminal domain is cleaved, allowing for the formation of antiparallel dimers through a C-terminal overlap region.

Elastin has a similar, but non-identical amino acid content to collagen – 33% glycine, 10-13% proline, and 24% alanine, but does not contain hydroxylysine or methionine (Haralson and Hassell, 1995). In its mature form, elastin is the most insoluble protein in the body (Davidson et al., 1995). The role of elastin is to confer

flexibility to tissues.

1.3.3 Other Structural Glycoproteins

Many other structural glycoproteins serve to maintain the adhesiveness and engage in signaling mechanisms of the extracellular matrix. The following will briefly describe fibronectin, laminin, and tenascin.

Fibronectin is present in both the extracellular matrix and plasma (Haralson and Hassell, 1995; Hynes, 1999). Each subunit of fibronectin is about 250 kDa, and they are disulfide-linked together near their C terminus. Fibronectin is initially secreted as a disulfide-linked dimer, but is then further disulfide-linked into higher order polymers. Various spliced forms of fibronectin exist. Located throughout each fibronectin subunit are three types of fibronectin modules termed the type I, type II, and type III fibronectin repeats. The fibronectin type III repeat is abundantly found in other extracellular proteins. Fibronectin, which contains the RGD sequence, was the first RGD-containing protein shown to bind integrins (Pierschbacher and Ruoslahti, 1984).

Laminin, an important component of basement membranes, separates epithelial, endothelial, muscle, and nerve cells from the stromal matrix (Aumailley and Smyth, 1998; Quondamatteo, 2002). It is involved in cell adhesion and migration, differentiation, gene expression, and cell fate. Each laminin molecule, which ranges from about 400 to 1000 kDa, is composed of a trimer of α, β, and γ subunits (Colognato and Yurchenco, 2000; Miner et al., 1997; Sasaki and Timpl, 1999). There are currently 12 known laminins based on five α chains, three β chains, and three γ chains. All of the chains contain a region with about 80 heptad-

sequence repeats at or close to their C-terminus. This region is crucial for the formation of a coiled coil domain that allows for heterotrimeric assembly of laminin. Electron microscopy of laminin generally shows a cross-shaped structure consisting of a long arm (80nm) and two or three short arms (25-40nm), where the long arm is comprised of the coiled-coil domain formed from the three chains.

Tenascins are a group of proteins built from modules such as heptad repeats, EGF-like repeats, fibronectin type IIII domains, and a C-terminal globular domain shared with fibrinogens (Chiquet-Ehrismann, 2004; Joester and Faissner, 2001). They have a TA domain that allows them to form trimers, and in the case of TN-C, hexamers. Cell surface receptors for tenascins include integrins, cell adhesion molecules of the Ig superfamily, phosphacan and annexin II. TN-C also interacts with extracellular proteins such as fibronectin and lecticans. Tenascins have complex patterns of expression. In embryogenesis, for example, the rate of tenascin synthesis changes significantly. In normal adult tissues, tenascins are not expressed, but they are present in pathological situations. For example, TN-C is expressed during wound healing and in other processes involving neovascularization such as tumour growth.

1.3.4 Proteoglycans

Proteoglycans are so named because they contain a central protein core, and long branched chains of carbohydrates, called glycosaminoglycans, emanating from the protein core (Haralson and Hassell, 1995; Hricovini, 2004; Iozzo, 1998). Proteoglycans can have one of four different types of glycosaminoglycans attached to the protein core: heparan sulfate, chondroitin sulfate, keratin sulfate, or dermatan

sulfate. The sugars of the glycosaminoglycan chains consist of a repeat disaccharide unit consisting of a uronic acid, such as glucuronic acid or iduronic acid, and a hexosamine, such as aminodeoxyglucose or aminodeoxygalactose. These sugars contain varying amounts of negatively-charged sulfate groups found on each carbohydrate chain. The long and negatively-charged sugar chains of proteoglycans allow them to absorb a lot of water (Prydz and Dalen, 2000). As such, the function of proteoglycans include cushioning tissues, in addition to other cellular processes such as differentiation, cell division, and cell motility (Kresse and Schonherr, 2001). Proteoglycans can either be secreted or bound to the membrane. Examples of proteoglycans include the adhesion receptors syndecans, heparan sulfate proteoglycan, and agrin.

1.3.5 Glycan-binding proteins

Many proteins of the extracellular matrix also bind carbohydrates (Varki et al., 2000). The common features of these protein-glycan complexes are that the glycan-binding sites are small (about 2.5 sugar residues on average), and interactions with proteins involve hydrogen bonding to hydroxyl groups and also involve hydrophobic interactions. Two main types of glycan-binding proteins exist in the extracellular matrix: the glycosaminoglycan (GAG)-binding proteins and the lectins. GAG-binding proteins bind to glycosaminoglycan carbohydrate polymers, while lectins bind to more discrete sugar entities.

As there are five main types of glycosaminoglycans, there are also five types of GAG-binding proteins: those that bind 1) hyaluronan; 2) heparin or heparan sulfate proteoglycans, 3) chondroitin sulfate proteoglycans, 4) dermatan sulfate

proteoglycans, or 5) keratan sulfate proteoglycans (Hileman et al., 1998; Varki et al., 2000). As glycosaminoglycan chains contain many negatively-charged sulfate groups, ionic interactions typically involving positively-charged arginines, are thus a key component of binding to these carbohydrates. Examples of GAG-binding proteins include aggrecan, which binds hyaluronan; and thrombospondin, which binds heparin, heparan sulfate, or chondroitin sulfate.

Lectins are non-immunoglobulin proteins that bind sugars other than glycosaminoglycans, although some consider GAG-binding proteins to be lectins too (Sharon and Lis, 2003). The ability of lectins to bind carbohydrates often works by having one primary binding site with a low binding affinity. Additional subsites on lectins then stabilize that binding, increasing the affinity constant by two to fifty fold (Loris, 2002). Lectins are derived from both plants and animals. Examples include concanavalin A from plants (the jack bean), in addition to the galectins and the calcium-dependent C-type lectins from animals. The adhesion molecules selectins are examples of C-type lectins. Interestingly, the structures of many of these lectins show a similar structural fold in both animals and plants despite differences in sequences. This is a striking example of convergent evolution. A puzzling feature of some lectins is they can also bind proteins, lipids, or nucleic acids as well as carbohydrates (Kilpatrick, 2002). The binding site in lectins to these other molecules may overlap with that of their carbohydrate recognition domain.

1.3.6 Other Adhesion Proteins

Transmembrane receptors provide key adhesion points. These include the integrins, cadherins, and members of the immunoglobulin superfamily. They provide

anchor points for the extracellular matrix and for cell-cell contacts.

There are 24 different types of integrins formed from the combination of 18 α and 8 β subunits. Integrins are ubiquitously expressed and are often involved in signal transduction cascades at focal adhesion complexes (Dedhar, 1999; Humphries, 2002). The crystal structure of the extracellular domain of the $\alpha_v\beta_3$ integrin revealed that it consists of the two subunits joining together to form a "head" that sits on two "legs" flexed at the "knees" (Xiong et al., 2001). Extracellularly, integrins bind a wide variety of ligands, but the common theme is having an exposed aspartate or glutamate in the ligand, such as in the RGD motif (Arnaout et al., 2002). The ligand-binding ability of integrins is generally possible for a wide range of magnesium and manganese ion concentrations. For calcium, however, binding is aided at micromolar calcium concentrations, but inhibited at millimolar concentrations. This may indicate the dynamic properties of integrins and may help dissociate their ligands from binding.

The cadherins are another important class of transmembrane adhesion molecules. Cadherins have been generally thought to mediate homotypic adhesion with the same type of cadherin, a process key for the sorting of cells into tissues (Takeichi et al., 1989). However, they have recently been found to also mediate heterotypic adhesion with other types of cadherins or with integrins (Karecla et al., 1996; Shan et al., 2000; Whittard et al., 2002). Different members of the cadherin family have a variable number of extracellular cadherin (EC) domains (Koch et al., 2004). The best-characterized members of the cadherin family, the classical cadherins, interact at their cytosolic surfaces with catenins, which help link cadherins

to cytoskeletal proteins and regulate adhesive interactions. Structural elucidation of the extracellular EC domains in classical cadherins has also provided insights into how cadherins mediate homotypic adhesion. These studies indicate that Trp2 near the N-terminus of cadherins is a key residue involved in their homotypic binding (Boggon et al., 2002; Nagar et al., 1996; Pertz et al., 1999; Shapiro et al., 1995). However, there is still much controversy with respect to the number of EC domains that are required to mediate adhesion and the mechanism of adhesion (Harrison et al., 2005; Koch et al., 2004; Perret et al., 2004; Shan et al., 2004).

The immunoglobulin superfamily also consists of proteins that are key to adhesion (Barclay, 2003; Isacke and Horton, 2000). This family is so named because of its similarity to the immunoglobulin fold, consisting of a sandwich of β sheets containing antiparallel strands. Members of this family generally have low sequence identity with each other, but key characteristics usually present include a pair of disulfide-linked cysteines separated by about 55-75 amino acids, and a tryptophan located 10 to 15 amino acids carboxyl to the first cysteine. In addition, the β strands are often composed of alternating hydrophobic amino acids. Interestingly, despite lack of sequence similarity, the immunoglobulin fold also resembles that of the cadherin EC domain and that of the fibronectin type IIII domain. Immunoglobulin superfamily domains bind a wide variety of ligands, including other immunoglobulin superfamily members, integrins, laminins, and carbohydrates. Members of the immunoglobulin superfamily include molecules such as contactin, NCAM, and CD33. Although most members are transmembrane proteins, there are also secreted and cytosolic members in the family.

Within the cell, many cytoskeletal proteins and cytoskeletal-associated proteins link the inside of the cell to components of the plasma membrane and extracellular matrix (Zamir and Geiger, 2001). Therefore, these cytosolic proteins also constitute key maintainers and regulators of cellular adhesion. Additionally, they help carry out the signal transduction cascades that let the cell respond to its extracellular environment, and transduce signals from within the cell to the extracellular environment. This latter case is an example of what integrins can do, and has been referred to as "inside-out" signaling (Hynes, 2002).

1.3.7 Extracellular Proteases

Extracellular proteases constitute an important part of the extracellular matrix since they allow for the turnover of extracellular proteins, and regulation of various cellular functions (Puente et al., 2003; Sternlicht and Werb, 1999). Proteases are either exopeptidases or endopeptidases. Exopeptidases hydrolyze peptide bonds at the amino or carboxyl terminus of proteins. Endopeptidases are comprised of three main classes: serine, cysteine, and metalloproteinases. Serine proteases have a His-Asp-Ser catalytic triad and include enzymes such as trypsin, chymotrypsin, tissue kallikreins, and mast cell chymases. Cysteine proteinases that can hydrolyze extracellular matrix proteins include the lysosomal cathepsins B, K, L, and S. These enzymes have acidic pH optima.

There are five superfamilies of metalloproteinases (Sternlicht and Werb, 1999). One superfamily is the metzincins, which has a consensus motif of HEBXHXBGBXHZ, where H is histidine, E is glutamate, G is glycine, B is a bulky hydrophobic residue, and X is a variable amino acid. Z distinguishes the family. Z is

serine or occasionally threonine or valine in the case of matrix metalloproteinases, proline in serralysins, glutamate in astacins, and aspartate in adamalysins. The three histidines of the consensus motif bind zinc at the catalytic site. In addition, metzincins have a conserved Met-turn motif, which also contains family-specific amino acids, that sits below the active site.

One of the most highly studied and important classes of extracellular matrix proteases are the matrix metalloproteinases, which belong to the metzincin superfamily (Lee and Murphy, 2004; Mott and Werb, 2004; Overall, 2001; Sternlicht and Werb, 1999). More than 20 mammalian matrix metalloproteinases are known, and together, they may cleave virtually all extracellular matrix proteins. Inhibitors of matrix metalloproteinases include zinc ion chelators and tissue inhibitors of metalloproteinases. Matrix metalloproteinases contain a signal sequence, followed by a pro-domain that maintains their inactive zymogen status, and a catalytic domain with a zinc-binding active site consensus sequence. Most matrix metalloproteinases also possess a hemopexin C-terminal domain linked to the catalytic domain by a potentially flexible proline-rich linker. Besides their active catalytic domain, matrix metalloproteinases may possess additional exosites to regulate their activity.

1.4 X-linked Retinoschisis

1.4.1 Clinical Features and Diagnostic Tests

X-linked retinoschisis is a recessive hereditary retinal degeneration and one of the most common causes of juvenile macular degeneration in males (Consortium, 1998). It is characterized by the presence of cystic cavities in the macula. Cystic

cavities result from a splitting of the inner retinal layers as viewed by optical coherence tomography, a technique that it uses infrared light to detect the image (Apushkin et al., 2005; Azzolini et al., 1997; Eriksson et al., 2004; Hrynchak and Simpson, 2000). Figure 1.3A shows cleavage in the foveal region by optical coherence tomography. When viewed with an ophthalmoscope (Fig. 1.3B), cleavage from retinoschisis resembles spokes radiating from a wheel in the macula (George et al., 1995b). However, these spokes are often subtle and difficult to detect by ophthalmoscopy.

Although all patients display foveal schisis, only about half of the patients have peripheral schisis (George et al., 1995b). In addition, decrease in visual acuity is the most common symptom, but the rate and extent of decline in acuity is variable (Ewing and Ives, 1970; Forsius et al., 1973; Kellner et al., 1990). In some patients visual acuity is stable, while in others, it rapidly declines. Due to this diversity of macular and peripheral changes present and the subtlety when viewing the schisis with an ophthalmoscope, the disease may be mis-diagnosed or remain undiagnosed for a long period (George et al., 1995b).

Another diagnostic feature of X-linked retinoschisis is the electroretinogram. Electroretinograms in X-linked retinoschisis patients generally show reduced b-waves (Kellner et al., 1990; Peachey et al., 1987). The b-wave is thought to reflect the electrophysiological properties of bipolar cells, so reduced b-waves may indicate functional or structural defects in these cells or at the photoreceptor-bipolar synapse (Friedburg et al., 2004; Knapp and Schiller, 1984). However, there have been patients whose b-wave is preserved or whose a-wave, which signifies photoreceptor

A
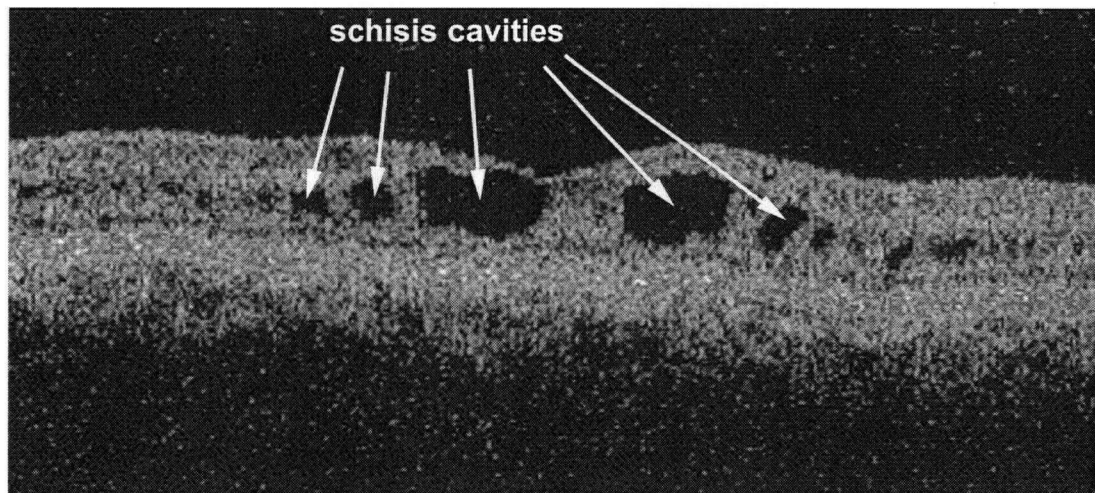
B
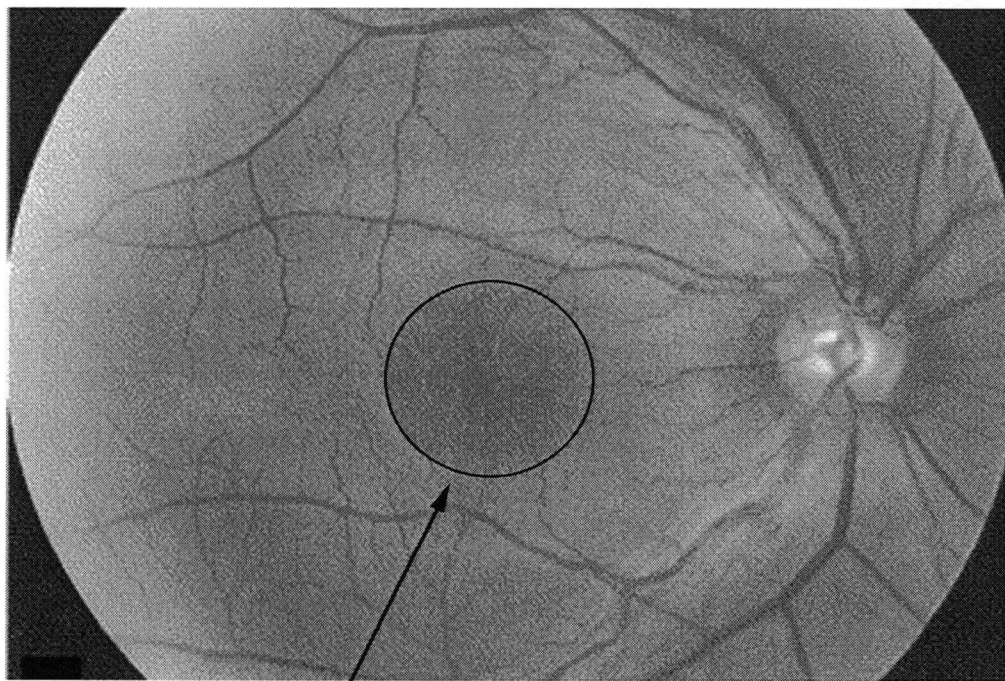
foveal schisis

Figure 1.3. Splitting of the retinal layers of the fovea in X-linked retinoschisis.
(A) Optical coherence tomography image showing schisis cavities, or holes, in the layers of the retina. **(B)** Ophthalmoscope image showing an abnormal fovea with splitting, which resembles spokes radiating from a wheel. Modified from Apushkin et al., 2005.

functioning, is affected (Bradshaw et al., 1999; Sieving et al., 1999). Since there is

heterogeneity also with the electroretinogram, it should be used in conjunction with

other tests when diagnosing X-linked retinoschisis. Besides ophthalmoscopy,

electrophysiology and optical coherence tomography, the recent positional cloning of

the candidate X-linked retinoschisis gene (see below) allows for molecular diagnosis

of patients with the disease.

1.4.2 Genetics and Pathophysiology

The prevalence of X-linked retinoschisis is estimated to range from 1:5000 to

1:25000 (Consortium, 1998). The disease is completely penetrant, as all males who

inherit the defective gene will be affected (Forsius et al., 1973). Carrier females are

rarely affected (George et al., 1995b), but females have been found to possess the

retinoschisis pathology due to mutations in the retinoschisis gene on both their X

chromosomes from consanguineous marriage (Ali et al., 2003; Mendoza-Londono et

al., 1999).

The gene linked to retinoschisis, *RS1*, was found by positional cloning in 1997

(Sauer et al., 1997). Since then, several collaborating groups have established a

database to record mutations, mainly missense, found in the gene

(http://www.dmd.nl/rs/; Consortium, 1998). Many of these missense disease

mutations contain mutated cysteine residues or residues mutated into cysteines,

suggesting that in some cases, the mutation may be affecting the folding of the

protein due to improper disulfide bond formation. The most common missense

mutation is the E72K mutation, found in about 15% of all retinoschisis patients with

missense mutations. Unfortunately, genotype-phenotype correlations have been particularly difficult because even patients with the same mutation can have different phenotypes (Eksandh et al., 2000; Park et al., 2000; Shinoda et al., 2000).

Recent studies with *RS1* knockout mice have revealed that deletion of the gene results in disrupted retinal layers and synapses (Weber et al., 2002). The retinal splitting in these mice occurs mainly in the outer plexiform and inner nuclear layers. Therefore, *RS1* knockout mice display a phenotype similar to patients with X-linked retinoschisis.

1.4.3 Clinical Management

In general, a conservative approach is indicated in treating X-linked retinoschisis, as many of the clinical features seen in retinoschisis will revert to normal. For example, even large bullous peripheral schisis cavities in infants and young children will often disappear (George et al., 1995a; Kawano et al., 1981). The most serious threats to sight in retinoschisis patients with advanced stages of this disease are complications such as vitreous haemorrhage and retinal detachment (Tantri et al., 2004). Therefore, the only conditions perhaps requiring surgery are when there are complications that cause the macula to be affected and that cause patients to have difficulty seeing (Regillo et al., 1993). There is currently no treatment for the foveal schisis that causes reduced visual acuity (Sieving, 1998). However, the future holds promise, as the identification of the gene involved in retinoschisis and the availability of a knockout mouse provide the ability to test gene therapy regimes, which will hopefully be introduced into humans for possibilities of therapy.

1.5 RS1 (Retinoschisin)

The most striking feature of the primary amino acid sequence of RS1 is that it contains a discoidin domain (Sauer et al., 1997), also known as the F5/8 type C domain. The discoidin domain has been found in a wide variety of proteins that function in cell and matrix adhesive processes and signal transduction (Fig. 1.4).

1.5.1 Structural and Functional Features of Discoidin Family Members

The prototypical member of the discoidin protein family, discoidin I, is a tetrameric carbohydrate-binding protein found in the slime mold *Dictyostelium discoideum* (Rosen et al., 1973; Simpson et al., 1974). Discoidin I is produced and secreted during cell aggregation when these amoebas differentiate into a multicellular organism. Discoidin I can bind galactose, as well as an unknown cell adhesion protein (Gabius et al., 1985; Rosen et al., 1973; Springer et al., 1984). It is the only discoidin family member to possess the RGD sequence, which is likely important for its attachment to cells.

The blood coagulation Factors V and VIII were the first members of the discoidin domain family found to possess homology to the sequence of discoidin I (Jenny et al., 1987; Kane and Davie, 1986; Poole et al., 1981; Wood et al., 1984). Factors V and VIII are multi-domain proteins, each containing two discoidin domains in tandem termed the C1 and C2 domains. The C2 domain is thought to bind negatively-charged phospholipids such as phosphatidylserine at the surface of platelets (Arai et al., 1989; Foster et al., 1990; Ortel et al., 1992). However, it has recently been demonstrated that their C1 domain may also contribute to phospholipid binding (Saleh et al., 2004). Mutations in Factor VIII result in
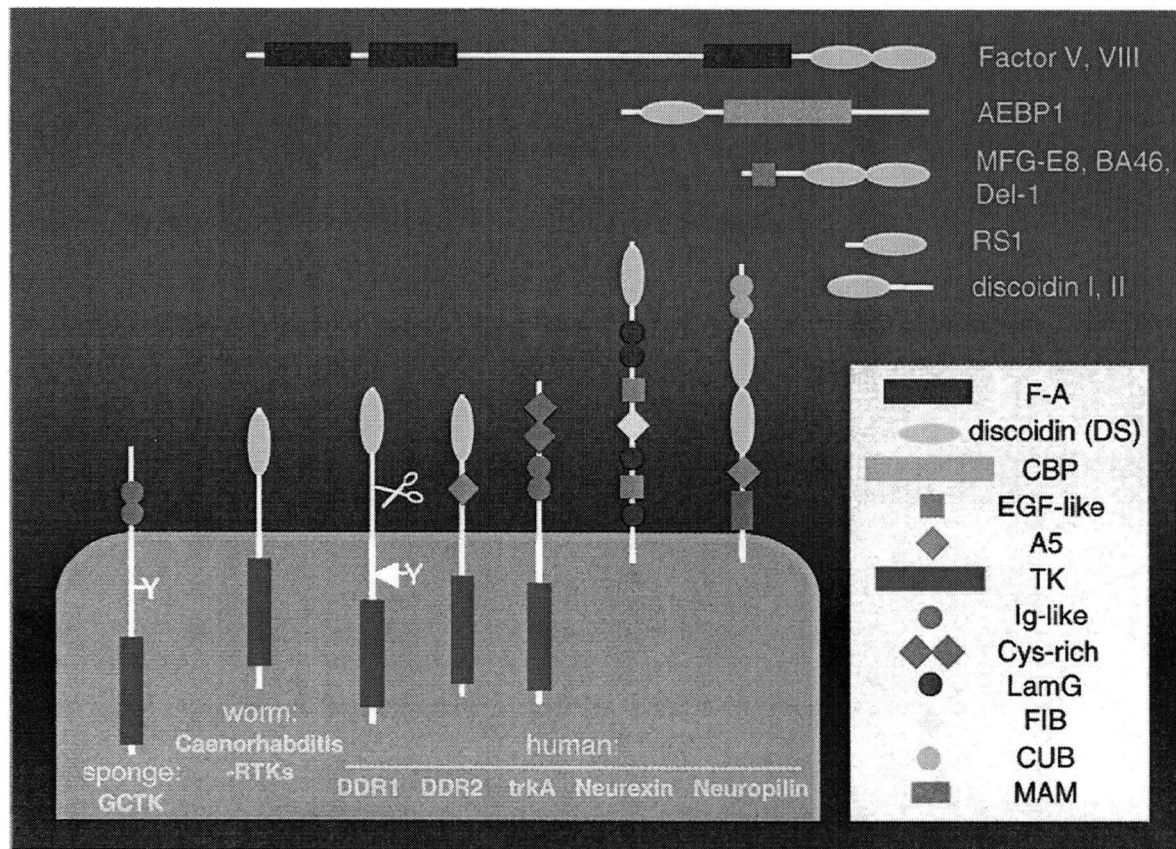
Figure 1.4. Schematic representation of selected discoidin domain family proteins. There are both transmembrane and secreted members of the discoidin domain family. They span many species from the slime mold, sponge, and nematode to humans. Some members of the family possess the discoidin domain in tandem. The discoid shape (*yellow*) represents the discoidin domain. The other shapes represent other domains present in these proteins. Modified from Vogel, 1999.

hemophilia A, an X-linked recessive disorder occurring in about 1:5000 males (Antonarakis et al., 1995; Kemball-Cook et al., 1998). Many of these mutations reside in the C2 discoidin domain of Factor VIII. Factor V mutations are associated with parahemophilia, an autosomal recessive disorder occurring in about one in one million individuals (van Wijk et al., 2001). The rare nature of parahemophilia is probably because Factor V occurs later in the blood coagulation cascade than Factor VIII. Perturbations in its function would thus have a less negative effect than in a molecule involved at an earlier step due to the cascade's exponential nature. (Fuentes-Prior et al., 2002).

A subset of tyrosine kinase receptors, termed discoidin domain receptors 1 and 2, also possesses the discoidin domain. Collagen can interact *in vitro* with discoidin domain receptors and activate their tyrosine receptor kinase activity (Vogel et al., 1997). This contributes to a variety of signaling processes (Dejmek et al., 2003; Ikeda et al., 2002; Matsuyama et al., 2004; Ongusaha et al., 2003). Lack of expression or overexpression of these discoidin domain receptors are correlated with diseases such as cancer metastasis, kidney disease and certain forms of arthritis (Gross et al., 2004; Heinzelmann-Schwarz et al., 2004; Xu et al., 2005).

The neuropilins are also examples of vertebrate proteins that contain the discoidin domain. Neuropilins 1 and 2 mediate axonal guidance in the nervous system (Baumgartner et al., 1998; Fuentes-Prior et al., 2002; Vogel et al., 1997). Neuropilin 1 was originally shown to bind semaphorin 3, a key protein involved in neuronal axon modeling and regeneration (He and Tessier-Lavigne, 1997; Kolodkin et al., 1997). Subsequently, it was reported that neuropilin 1 can bind $VEGF_{165}$,

placenta growth factor-2 (another VEGF member), and heparin (Mamluk et al., 2002; Migdal et al., 1998; Soker et al., 1998). All these interactions are physiologically relevant (Nakamura et al., 1998; Soker et al., 1998).

Further studies have given more details about these binding interactions. Neuropilin 1 binds $VEGF_{165}$, placenta growth factor-2, and heparin via its b1b2 tandem discoidin domains (Mamluk et al., 2002). Both the b1 and b2 discoidin domains are required for binding. The positively-charged basic tail of semaphorins is thought to bind to negatively-charged residues on the b1b2 discoidin domains of neuropilin (Lee et al., 2003). Strangely, the presence of heparin, which is negatively charged, enhances the binding of neuropilin 1 to semaphorins, $VEGF_{165}$, and placenta growth factor-2 (De Wit et al., 2005; Mamluk et al., 2002). Binding to neuropilin is also competed by semaphorins and VEGFs, indicating that they bind to the same site on neuropilin (Miao et al., 1999).

More recently, neuropilin 1 has been reported to bind *in vitro* to a wide variety of heparin-binding proteins (West et al., 2005). This variety of ligands for neuropilin indicates that it is a versatile discoidin domain family member. The basic residues of neuropilin likely allow it to bind heparin, while its acidic residues enable it to bind heparin-binding proteins or positively-charged residues on other proteins. Whether all these heparin-binding proteins are physiologically relevant and in what context remains to be determined.

Still other members of the discoidin family are involved in physiological processes in vertebrates ranging from vascular smooth muscle differentiation and axoglial junction stability to milk lactation and sperm motility (Ensslin and Shur,

2003; Larocca et al., 1991; Layne et al., 1998; Peles et al., 1997). In invertebrates, discoidin proteins are important in immunity and metamorphosis in the silkworm, and in extracellular matrix formation in the sea urchin zygote (Matese et al., 1997; Yamakawa and Tanaka, 1999). A number of proteins of unknown function also contain the discoidin domain.

The discoidin domain often occurs more than once in the same protein. For example, besides the coagulation factors and neuropilin mentioned above, milk fat globule protein also contains the discoidin domain occurring in tandem (Vogel, 1999). Similarly, echinonectin from the sea urchin occurs as a disulfide-linked homo-dimer (Alliegro and Alliegro, 1991). Discoidin domain receptors 1 and 2, being tyrosine receptor kinases, require dimerization for activation (Leitinger, 2003). Discoidin I and RS1 are the only discoidin family members existing as homo-oligomers comprised predominantly of discoidin domains (Madley et al., 1982; Molday et al., 2001).

The crystal structures of three members of the discoidin family, Factors V and VIII and neuropilin 1, have been solved (Lee et al., 2003; Macedo-Ribeiro et al., 1999; Pratt et al., 1999). All the structures—the C2 domains of Factors V and VIII, as well as the b1 domain of neuropilin 1—consist of an eight-stranded anti-parallel β barrel clamped together at the N- and C- termini by a disulfide bond from a pair of cysteines that mark the beginning and the end of the discoidin domain. A sensitive multiple sequence alignment technique and structural studies indicate that the discoidin domain is distantly related to the structural fold of galactose oxidase (Baumgartner et al., 1998). However, the main difference between their structures is

the high degree of sequence divergence in the barrel's "spike" regions, stretches of amino acids projecting from one end of the barrel (Fuentes-Prior et al., 2002). These spikes have also been suggested to mediate the contacts of discoidin proteins with their ligands. Experiments performed with the coagulation factors, neuropilin 1, and discoidin domain receptors support this claim (Abdulhussein et al., 2004; Gilbert et al., 2002; Kim et al., 2000; Leitinger, 2003; Shimizu et al., 2000; Srivastava et al., 2001).

1.5.2 The RS1 Protein

The protein associated with X-linked retinoschisis is termed RS1 (also called retinoschisin). It is normally found as a large disulfide-linked oligomeric complex, and when disulfide reduced, migrates as a 25 kDa protein by SDS-PAGE (Molday et al., 2001).

Screening with Northern blots have shown that *RS1* mRNA is specific to the retina (Molday et al., 2001; Reid et al., 1999; Sauer et al., 1997). However, RS1 transcripts have also been detected in the human uterus, and it has been suggested that RS1 may be necessary for embryonic implantation or survival (Huopaniemi et al., 1999). In the retina, RS1 is expressed by photoreceptors and bipolar cells (Molday et al., 2001). It is secreted as a multimeric complex that binds to the surfaces of these cells and the synaptic regions of the retina (Fig. 1.5) (Molday et al., 2001;Weber et al., 2002). RS1 is also secreted from Weri-Rb1 retinoblastoma cells (Grayson et al., 2000). Biochemical studies indicate that RS1 is present in the membrane fraction of retinal tissue homogenates and transfected COS-1 cells (Molday et al., 2001).

retinal pigment epithelium (RPE)
outer segment (rods & cones)

inner segment (rods & cones)

outer nuclear layer
(rods & cones)

outer plexiform layer
inner nuclear layer

inner plexiform layer

ganglion cells
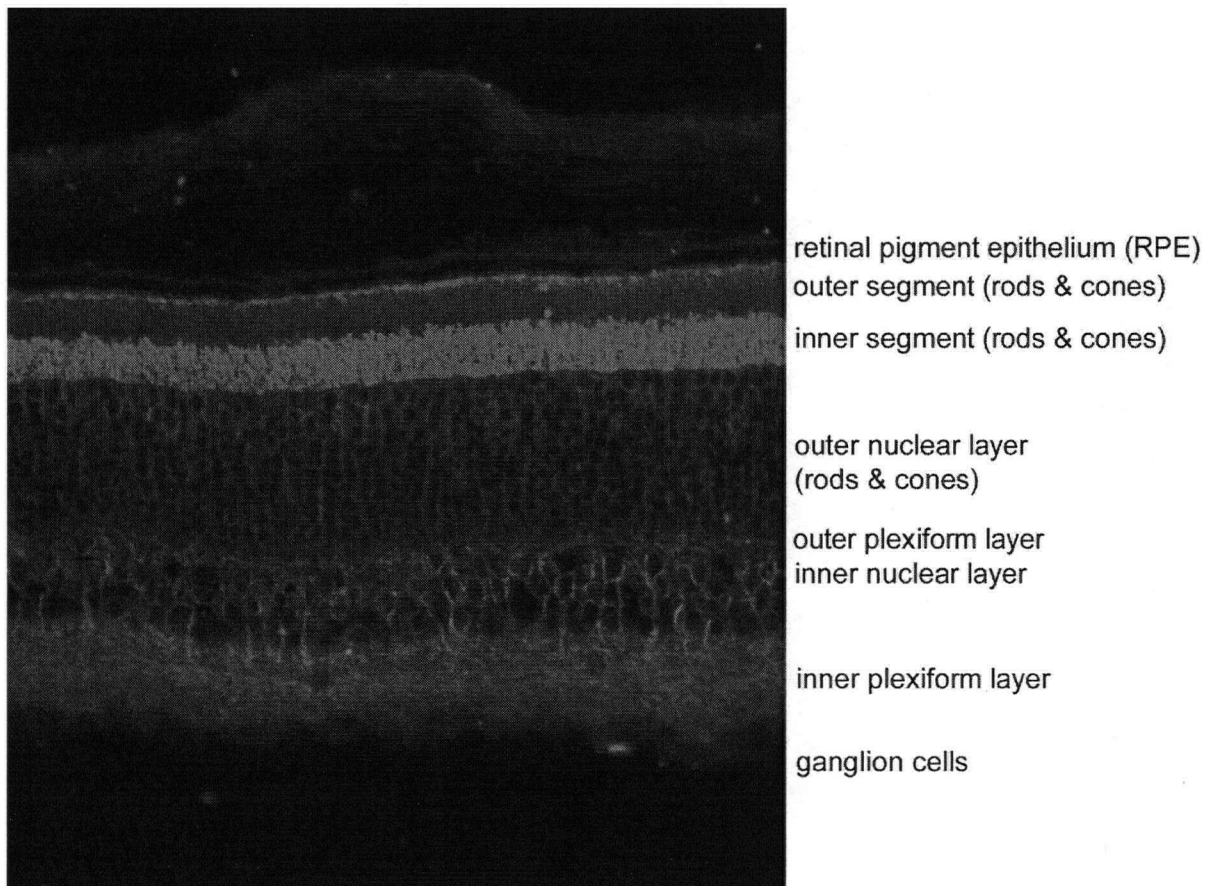
Figure 1.5. Localization of RS1 in murine retina. Immunofluorescence microscopy of RS1 in the retina labelled with an RS1 monoclonal antibody. RS1 (*red*) is found throughout the retina, but predominantly in the photoreceptor inner segments, bipolar cells of the inner nuclear layer, and synapses at the outer and inner plexiform layers. Modified from Weber et al., 2002.

Human RS1 contains 224 amino acids in each unprocessed subunit (Fig. 1.6) (Sauer et al., 1997). Ten of these are cysteine residues, which may be important in forming disulfide bonds to stabilize protein structure and to link its subunits together. The discoidin domain of RS1 starts at C63 and ends at C219. In addition, sequence analysis suggests that RS1 has a 23-amino acid N-terminal leader sequence important for its secretion from cells.

The sequences of murine and fugu RS1 have also been determined. Murine RS1 is 224 amino acids long, and shares 96% homology with the human orthologue (Gehrig et al., 1999b). Fugu RS1 is longer, being composed of 280 amino acids (Brunner et al., 1999). The discoidin domain of fugu RS1, however, is 76% identical in sequence to that of the human RS1, with most of the differences being conservative amino acid replacements. The amino acid alignment of RS1 from several species is shown in Figure 1.6B.

1.6 Thesis Investigation

Although the gene for RS1 was cloned in 1997 (Sauer et al., 1997), little was known about the protein when this project was started in 2000. A monoclonal antibody had been generated (Molday et al., 2001), and could be used as a key tool to probe the structure and function of RS1 and its role in X-linked retinoschisis.

Chapter 2 describes the structural properties of RS1. As RS1 contains ten cysteine residues, and exists as an oligomeric protein under nonreducing conditions, the goals of these studies were to determine the intermolecular and intramolecular

A

B

```
human    MSRKIEGFLLLLL----FG----------------YEATLGLSSTEDEG--------- 29
mouse    MPHKIEGFFLLLL----FG----------------YEATLGLSSTEDEG--------- 29
bovine   MPRKIENFLFLLL----FG----------------YEATLGLSSTEDEG--------- 29
fugu     MHLPREAFLLALAGAFIFPSSQQEKRTQRDLRVVCFYQKDFRNGTKAEQWGKKTPTQIW 59
         *       * *:: *       *                *:   :   .:. ::

human    ------------------EDPWYQKACKCDCQGGPN-------ALWSAGATSLDCIPE 62
mouse    ------------------EDPWYQKACKCDCQVGAN-------ALWSAGATSLDCIPE 62
bovine   ------------------EDPWYHKACKCDCQGGAN-------ALWSAGPTPLDCIPE 62
fugu     RGCMSVCNAIVVCLFELGVSETWNSKSCKCDCEGGESPTEFPSIRTGSSMVRGVDCMPE 118
                         .:.*   *:*****: *  .          *:     :**:**

human    CPYHKPLGFESGEVTPDQITCSNPEQYVGWYSSWTANKARLNSQGFGCAWLSKFQDSSQWL 123
mouse    CPYHKPLGFESGEVTPDQITCSNPEQYVGWYSSWTANKARLNSQGFGCAWLSKYQDSSQWL 123
bovine   CPYHKPLGFESGEVTPDQITCSNVEQYVGWYSSWTANKARLNSQGFGCAWLSKFQDSSQWL 123
fugu     CPYHRPLGFEAGSISPDQITCSNQDQYTAWFSSWLPSKARLNTQGFGCAWLSKFQDNTQWL 179
         ****:*****:*.::********* :**..*:*** ..*****:**********:**..:***

human    QIDLKEIKVISGILTQGRCDIDEWMTKYSVQYRTDERLNWIYYKDQTGNNRVFYGNSDRTS 184
mouse    QIDLKEIKVISGILTQGRCDIDEWVTKYSVQYRTDERLNWIYYKDQTGNNRVFYGNSDRSS 184
bovine   QIDLKEVKVISGILTQGRCDIDEWMTKYSVQYRTDESLNWIYYKDQTGNNRVFYGNSDRTS 184
fugu     QIDLIDAKVVSGILTQGRCDADEWITKYSLQYRTDEKLNWIYYKDQTGNNRVFYGNSDRSS 240
         ****  :  **:********** ***:****:****** ********************:*

human    TVQNLLRPPIISRFIRLIPLGWHVRIAIRMELLECVSKCA 224
mouse    TVQNLLRPPIISRFIRLIPLGWHVRIAIRMELLECASKCA 224
bovine   TVQNLLRPPIISRFIRLIPLGWHVRIAIRMELLECVSKCA 224
fugu     SVQNLLRPPIVARYIRILPLGWHTRIALRLELLLCMNKCS 280
         :*********::*:**:.*****.***:*:*** *  .**:
```

Figure 1.6. Schematic and sequence of the RS1 protein. **(A)** Schematic of the various regions in human RS1. Each subunit of unprocessed RS1 is 224 amino acids in length. LS denotes the leader sequence, and Rs1 denotes the Rs1 domain. The discoidin domain starts at C63 and ends at C219. **(B)** Alignment of the RS1 protein sequence from various species. The discoidin domain of each species is highlighted in black. Asterisks indicate residues conserved among all four species. The accession numbers of the sequences used are as follows: NP_000321 (human), NP_035432 (mouse), and AAD28797 (fugu). The bovine sequence is a personal communication from Weber, BHF. Alignments were performed with CLUSTAL W (Thompson et al., 1994).

disulfide bonding patterns, and to determine the oligomerization state of RS1. In addition, the site of leader sequence cleavage was determined experimentally. The relationship of these structural properties to the role of RS1 in retinal adhesion is discussed. This work has been published (Wu and Molday, 2003; Wu et al., 2005). All experimental work except the MS/MS sequencing was performed by the author.

Chapter 3 delves into the molecular basis for X-linked retinoschisis. As mentioned, the worldwide Retinoschisis Consortium had established a database of retinoschisis mutations. Therefore, cysteine disease mutations and other selected disease mutations were constructed and expressed in HEK 293 cells to examine the effect of these mutations on the expression, localization, folding, secretion, and oligomeric assembly of RS1. Most of these studies have been published (Wu and Molday, 2003).

Chapter 4 recounts the ability of RS1 to bind galactose. Because other members of the discoidin protein family are known to bind various ligands, the ability of RS1 to bind to these ligands was tested. Results showed that RS1, unlike Factors V or VIII, did not bind phospholipids. In addition, unlike neuropilin, RS1 did not bind heparin. However, similar to discoidin I, RS1 did bind galactose. In fact, only the octameric form of RS1 bound strongly to galactose, indicating its lectin-like properties. The ability to elute RS1 from a galactose column and extract it from retinal membranes with IPTG is also discussed. On the basis of these properties, a method to purify RS1 has been developed. This work has been presented at the Synaptic Function and Plasticity Conference in July, 2005 (Wu and Molday, 2005).

CHAPTER 2: STRUCTURAL CHARACTERIZATION OF RS1 [1]

2.1 Introduction

X-linked retinoschisis is a relatively common, inherited macular degeneration that affects males early in life (George et al., 1995b; Sieving, 1998; Tantri et al., 2004). The gene responsible for X-linked retinoschisis encodes the retinal-specific protein, RS1 (Sauer et al., 1997). RS1 is expressed and secreted from photoreceptor cells of the outer retina and bipolar cells of the inner retina as a multisubunit protein (Grayson et al., 2000; Molday et al., 2001; Reid et al., 1999; Reid et al., 2003). RS1 is believed to function as a retinal cell adhesion protein because mice deficient in RS1 have a disorganized retina with displacement of bipolar cells into the outer retinal layer, gaps between bipolar cells within the inner retina, disruption of the photoreceptor-bipolar synapse, and degeneration of rod and cone photoreceptors (Weber et al., 2002).

The dominant structural feature of the RS1 polypeptide is the 157-amino acid discoidin domain, which comprises more than 75% of the processed polypeptide chain (Sauer et al., 1997). In addition to its discoidin domain, RS1 contains a putative 23-amino acid leader or signal sequence, followed by a 39-amino acid segment known as the Rs1 domain. Discoidin domains are present in a wide range of membrane and extracellular proteins where they mediate a variety of cell

---

[1] A version of this chapter has been published.

Wu, WWH, Wong, JP, Kast, J, and Molday, RS. (2005). RS1, a discoidin domain-containing retinal cell adhesion protein associated with X-linked retinoschisis, exists as a novel disulfide-linked octamer. J Biol Chem *280*, 10721-10730.

Wu, WWH and Molday, RS. (2003). Defective discoidin domain structure, subunit assembly, and endoplasmic reticulum processing of retinoschisin are primary mechanisms responsible for X-linked retinoschisis. J Biol Chem *278*, 28139-28146.

adhesion and signal transduction cascades (Baumgartner et al., 1998; Vogel, 1999). Some proteins that contain discoidin domains are Factors V and VIII involved in blood coagulation; neuropilins 1 and 2, which mediate nervous system regeneration and degeneration; discoidin domain receptors implicated in cancer metastasis, and discoidin I involved in cellular adhesion during slime mold differentiation and development (Baumgartner et al., 1998; Fuentes-Prior et al., 2002; Lee et al., 2003; Vogel, 1999).

The high resolution structures of the C2 discoidin domains of Factors V and VIII and the b1 discoidin domain of neuropilin 1 have been determined (Lee et al., 2003; Macedo-Ribeiro et al., 1999; Pratt et al., 1999). These domains consist of eight antiparallel β-strands arranged in a barrel-like structure with several loops, or "spikes," projecting from one end of the core structure. These spikes are likely involved in mediating interactions with target ligands (Fuentes-Prior et al., 2002).

Although it has previously been shown that RS1 exists as a disulfide-linked oligomeric protein (Molday et al., 2001), the number and arrangement of these subunits in the native complex and the role of intramolecular and intermolecular disulfide bonds and noncovalent interactions in the assembly and stabilization of the RS1 complex have not been investigated. In this study, site-directed mutagenesis, exogenous expression, velocity sedimentation, and peptide mapping by mass spectrometry have been used to gain insight into the tertiary and quaternary structures RS1. Both retinal and recombinant RS1 have been examined under native and denaturing conditions. Results from this study show that native RS1 has an unusual oligomeric structure consisting of disulfide-linked dimers within a

disulfide-linked homo-octameric complex. Cysteines involved in the formation of key intramolecular and intermolecular disulfide bridges are also identified. Furthermore, the site of leader peptide cleavage is experimentally determined.

2.2 Methods

2.2.1 Site-directed mutagenesis and RS1 monoclonal antibody

Human *RS1* cDNA was subcloned into the pCEP4 vector (Invitrogen, Carlsbad, CA) using the *Hind*III and *Xho*I restriction sites. The QuikChange site-directed mutagenesis kit (Stratagene, La Jolla, CA) was used to introduce the following cysteine mutations: 10 single cysteine mutants (C38S, C40S, C42S, C59S, C63S, C83S, C110S, C142S, C219S, C223S); 5 double mutants (C59S/C219S, C63S/C219S, C59S/C223S, C63S/C223S, C110S/C142S; 5 triple mutants (C59S/C223S/C38S, C59S/C223S/C40S, C59S/C223S/ C42S, C59S/C223S/C83S, and C38S/C40S/C42S); and the quadruple cysteine mutant, termed Δ4Cys, C38S/C40S/C42S/C83S. All constructs were sequenced to verify the presence of the desired mutation(s) and absence of random mutations. The RS1 3R10 monoclonal antibody (Molday et al., 2001) was purified and coupled to cyanogen bromide-activated Sepharose 2B as previously described (Molday et al., 1990).

2.2.2 Transfections

A version of HEK 293 cells known as EBNA HEK 293 cells (Invitrogen) were transfected with WT or mutant *RS1* cDNA. Each transfection was performed in one

10-cm dish with 20 µg of cDNA using the calcium phosphate transfection procedure (Chen and Okayama, 1987). Briefly, 62 µl of a 1M calcium chloride solution was added to a 188 µl solution of cDNA, prior to the addition of 250 µl of BBS (N,N-bis(2-hydroxyethyl)-2-aminoethane-buffered saline), pH 6.95. The HEK 293 cells were resuspended in this cDNA transfection mixture and added to a 10-cm dish containing DMEM media supplemented with 10% fetal calf serum. This media, which contained the transfection solution, was replaced with regular media without the transfection solution on day 2, and the cells were harvested on day 4.

2.2.3 Harvesting the cellular and secreted fractions

The cellular fraction of RS1 protein was obtained by washing the transfected HEK 293 cells twice in PBS (137 mM NaCl, 2.7 mM KCl, 10 mM Na_2HPO_4, 1.8 mM KH_2PO_4) by low speed centrifugation. The final pellet was resuspended in 200 µl of PBS containing 20 mM NEM (Calbiochem, Darmstadt, Germany) and added to an equal volume of PBS containing 2% Triton X-100, 20 mM NEM, and Complete Protease Inhibitor (Roche Applied Science, Basel, Switzerland). After stirring for 20 min at 4°C, the solution was centrifuged at 100,000 x g in a TLA-100.4 rotor (Beckman, Fullerton, CA) for 20 min, and the supernatant was retained for SDS gel electrophoresis. The secreted fraction of the protein was obtained by centrifuging 10 ml of the media at 300,000 x g in a TLA-75 rotor (Beckman) at 4°C for 20 min to remove any insoluble membrane material. The samples were then incubated for 2 h with the RS1 3R10-Sepharose 2B immunoaffinity matrix. After washing with column buffer (20 mM Tris, pH 7.4, 0.2% Triton X-100, and 20 mM NEM), bound protein was eluted with 1% SDS in column buffer.

2.2.4 SDS-PAGE and Western blotting

Proteins were denatured in a denaturing solution in the absence or presence of 4% β-mercaptoethanol, and separated on 6.5% or 10% polyacrylamide SDS gels, or gradient polyacrylamide SDS gels as indicated in the results. For the 6.5% or 10% polyacrylamide SDS gels, running buffer containing 25 mM Tris, 192 mM glycine, and 1% SDS was used. A denaturing mixture of 10 mM Tris, pH 6.8, 1% SDS, and 10% glycerol was used to denature the proteins that were run on the 6.5% or 10% polyacrylamide gels (Laemmli, 1970). These gels were transferred to Immobilon P membranes (Millipore, Billerica, MA) for 20 min in transfer buffer (25mM Tris, 192 mM glycine) containing 12% methanol for the 6.5% polyacrylamide gels, and 20% methanol for the 10% polyacrylamide gels (Towbin et al., 1979).

Gradient gels were used on several occasions. In these cases, nonreduced or reduced samples were run on 4–12% NuPAGE gradient gels (Invitrogen) using 50 mM MOPS, 50 mM Tris, 2% SDS, and 1 mM EDTA as the running buffer. 3–8% NuPAGE denaturing gradient gels were also used for analysis of nonreducing samples, and running buffer containing 50 mM tricine, 50 mM Tris, and 2% SDS was used. The denaturing mixture used for the gradient gels was the same as the one used above for the 6.5% and 10% polyacrylamide gels, except 1% SDS was replaced with 2% lithium dodecyl sulfate, and 2 mM EDTA was also included. NuPAGE gradient gels were transferred using transfer buffer containing 25 mM bicine, 25 mM Bis-Tris, 1 mM EDTA, and 10% methanol.

Western blots were viewed with either enhanced chemiluminescence or by infrared detection. For enhanced chemiluminescence, blots were blocked with 1%

skim milk in PBS and labelled with the RS1 3R10 monoclonal antibody for 1 h and goat anti-mouse Ig-peroxidase (Sigma, St. Louis, MO) in PBS for 30 min for detection by ECL (Amersham, Buckinghamshire, UK). For infrared detection, blots were blocked with 0.5% skim milk in PBS and labelled with the RS1 3R10 antibody containing 0.5% skim milk in PBS with 0.1% Tween 20 for 1 h, and goat anti-mouse Ig conjugated to the CW800 dye (Licor, Lincoln, NE) containing 0.5% skim milk in PBS with 0.2% SDS for 30 min for detection with the Odyssey Infrared Imaging System (Licor).

2.2.5 Molecular modeling

The discoidin domain of RS1 was modeled from the crystal structures of the C2 discoidin domains of coagulation Factor V (40% sequence identity) and Factor VIII (33% identity) using SWISS-MODEL (Guex and Peitsch, 1997; Macedo-Ribeiro et al., 1999; Pratt et al., 1999). The structure was further refined to account for intramolecular disulfide bonds using the Crystallography and NMR software system (Brunger et al., 1998).

2.2.6 Immunoprecipitation of RS1 from bovine retina

RS1 was immunoprecipitated from bovine retina on an RS1 3R10-Sepharose column as follows. Frozen bovine retinas were thawed, and then washed twice in low salt containing 10 mM Tris, pH 7.4, by centrifugation at 14,000 x g in an SS-34 Sorvall rotor (Kendro Laboratory Products, Asheville, NC). The retinal cells were then disrupted as follows: the pellet of cells was resuspended in lysis buffer consisting of 10 mM Tris, pH 7.4, 10 mM NEM, and Complete Protease Inhibitor and

incubated for 10 min on ice, followed by several passages through a 26-gauge needle attached to a syringe. To obtain the membrane fraction, the lysed cells were applied to the top of a 60% sucrose solution containing 10mM Tris, pH 7.4, and centrifuged for 30 min at 38,000 x g in a TLS 55 rotor (Beckman). The membranes were collected from the top of the 60% sucrose, and washed with 10 mM Tris, pH 7.4, by centrifugation at 100,000 x g for 10 min in a TLA 100.4 rotor.

The retinal membranes obtained were then solubilized in buffer containing 18 mM CHAPS, 20 mM Tris, pH 7.4, 0.15 M NaCl, 10 mM NEM, and Complete Protease Inhibitor for 20 min at 4°C and subsequently centrifuged at 100,000 x g for 10 min to remove insoluble material. The supernatant was immunoaffinity-purified by incubating with it the RS1 3R10-Sepharose beads for 1 h at 4°C and washed in column buffer consisting of 0.15 M NaCl, 20 mM Tris, pH 7.4, and 2 mM CHAPS. After elution with column buffer containing 4% SDS, the purified bovine retinal RS1 sample was run under reduced or nonreduced conditions on SDS-PAGE.

2.2.7 N-terminal sequencing

For N-terminal sequencing, RS1 was isolated from bovine retina on an RS1 3R10 monoclonal antibody-Sepharose matrix as described above in Section 2.2.6, run on a 10% SDS gel under reducing conditions, and electrophoretically transferred to an Immobilon-P membrane. The N-terminal sequence was determined by the University of British Columbia Nucleic Acid Protein Service Unit using the Edman degradation procedure.

2.2.8 In-gel trypsinization and mass spectrometry

RS1 from bovine retina was immunoaffinity-purified as described above in Section 2.2.6, applied to a 10% polyacrylamide gel, and run under reducing or nonreducing conditions. In-gel digestion of the purified RS1 was performed by punching out the Coomassie blue-stained RS1 bands with a glass Pasteur pipette. The gel pieces were washed with water several times to remove acetic acid. They were then destained in a 1:1 mixture of 100 mM ammonium bicarbonate and 100% acetonitrile several times. After shrinking and drying the gels with 100% acetonitrile, the gels were incubated with either 50 mM NEM for nonreducing samples, or 10 mM DTT (Sigma) followed by 50 mM IAM (Sigma) for reducing samples. After incubations, samples were washed with ammonium bicarbonate, and dried from 100% acetonitrile. The gel pieces containing the samples were then incubated with proteases (see below) at 12 ng/μl for 30 min on ice. The protease solution was removed, and the gel pieces were overlaid with 50 mM ammonium bicarbonate and 5 mM calcium chloride. Nonreduced samples also contained 0.6 M urea. The samples were then digested for 18 h at 37°C. The solution containing the digested RS1 peptides was collected in a tube and gel pieces were re-extracted with 50 mM ammonium bicarbonate/66% acetonitrile (basic extraction) and with 5% formic acid/66% acetonitrile (acidic extraction). The samples from the overnight digestion and morning extraction were pooled, dried in a Savant SpeedVac (Thermo Electron, Waltham, MA) and resuspended in 10 μl of 50 mM ammonium bicarbonate.

For analysis with MALDI-TOF mass spectrometry, the protease-digested RS1 solution (2 μl) was applied to an H4 chip (Ciphergen, Fremont, CA). The sample

was dried and washed with two quick rinses of water before applying a 20%-saturated solution of α-cyanohydroxycinnamic acid matrix in a solvent with 50% acetonitrile and 0.1% trifluoroacetic acid. Samples were analyzed on a surface-enhanced laser desorption ionization-time of flight mass spectrometer (Ciphergen). Masses obtained were average masses.

A QSTAR XL LC/MS/MS (Applied Biosystems, Foster City, CA) was used for MS/MS sequencing of the RS1 peptides. Trypsinized samples were obtained as above, lyophilized, and reconstituted in formic acid. A PepMap C18 column, with a 3-μm particle size and 100-Å pore size column from LC Packings (Amsterdam, Netherlands) was used for peptide separation. Solvents B and A contained 20% and 5% acetonitrile in water, respectively. LC conditions started at 2% solvent B, with a gradient to 60% B over 60 min, to 95% B at 93 min, and held for 3 min before returning to 2% B. Masses obtained were monoisotopic masses.

The proteases used for the digestion of RS1 were trypsin (Promega, Madison WI), endo-LysC (Roche Applied Science), and endo-AspN (Roche Applied Science). Background control enzyme digestions of blank gel pieces were also performed to subtract out peaks due to autoproteolysis and other contaminating peptides.

2.2.9 Ammonium sulfate precipitation of recombinant RS1 and extraction of retinal RS1

Human recombinant WT RS1 and the C59S/C223S mutant were transfected as described above in Section 2.2.2 on a larger scale. For these larger-scale transfections, six times the original amount of reagents was used, and T150 flasks were used to grow the cells. The media containing 10% fetal calf serum was

replaced the following day after transfection with fresh media. One week later, it was replaced with media containing 2% fetal calf serum. The media containing 2% fetal calf serum was harvested once a week for 2 or 3 weeks. The secreted RS1 protein was concentrated by precipitation with 40% ammonium sulfate at 4°C and resuspended in 1/40th the volume of the cell culture media. The protein solution was dialyzed overnight against 20mM Tris, pH 7.4 and 0.1 M NaCl, and then centrifuged the next day at 100,000 x g to remove any insoluble material.

Bovine retinal membranes were obtained as described above in Section 2.2.6. To wash the membranes and remove as many contaminating proteins as possible, the membranes were resuspended in 2 M urea, incubated for 10 min, and centrifuged at 100,000 x g for 10 min. This washing procedure with 2 M urea was repeated, and retinal RS1 was subsequently extracted with buffer containing 6 M urea, 10 mM CHAPS, and 0.5 M NaCl. The extract containing RS1 was centrifuged at 100,000 x g for 10 min, and the supernatant was dialyzed overnight against 20 mM Tris, pH 7.4, and 0.1 M NaCl to remove the urea and CHAPS. The next day, the sample was centrifuged again at 100,000 x g for 10 min, and the supernatant was retained for further analysis.

2.2.10 Sedimentation velocity

Bovine retinal RS1, recombinant WT RS1 (rWT), and RS1 with the C59S/C223S mutation were sedimented through a 5–20% (w/w) linear sucrose gradient containing PBS at 4°C for 17 h and 72,449 x g in a Beckman TLS-55 rotor. Bovine retinal RS1 was obtained by urea and CHAPS extraction as described above in Section 2.2.9. The secreted fraction of transfected WT and C59S/C223S RS1

was concentrated by ammonium sulfate precipitation as described above before subjecting to velocity sedimentation. Mouse IgG having a molecular mass of 160 kDa was run as a standard. All samples were incubated with 10mM NEM for 10 min at 4°C. They were then centrifuged for 20 min at 100,000 x g in a Beckman TLA 100.4 rotor prior to loading onto the sucrose gradient to remove any insoluble material. Three-drop fractions were collected, run on reducing gels, and blotted with the RS1 3R10 antibody. The intensity of the labelled bands was quantified with the Odyssey Infrared Imaging System. Sucrose concentration in each fraction was determined by refractometry to plot the percentage of each protein species versus the percentage of sucrose.

2.3 Results

2.3.1 Analysis of single cysteine-to-serine mutants

RS1 contains a 157-amino acid discoidin domain, which is flanked on the N-terminal side by a 39-amino acid Rs1 domain, not found in other proteins, and on the C-terminal side by a 5-amino acid segment (Fig. 2.1A). Of the ten cysteines found in RS1, 5 are located in the discoidin domain, 4 in the Rs1 domain, and 1 in the C-terminal segment. To determine the importance of individual cysteines on structural properties of RS1, each cysteine was individually replaced with a serine. These single cysteine mutants were analyzed with respect to their protein expression and oligomerization state in the cellular and secreted fractions of HEK 293 cells under reducing and nonreducing conditions on SDS gels (Fig. 2.1B). These experiments were repeated in four to five separate transfections to ensure reproducibility.
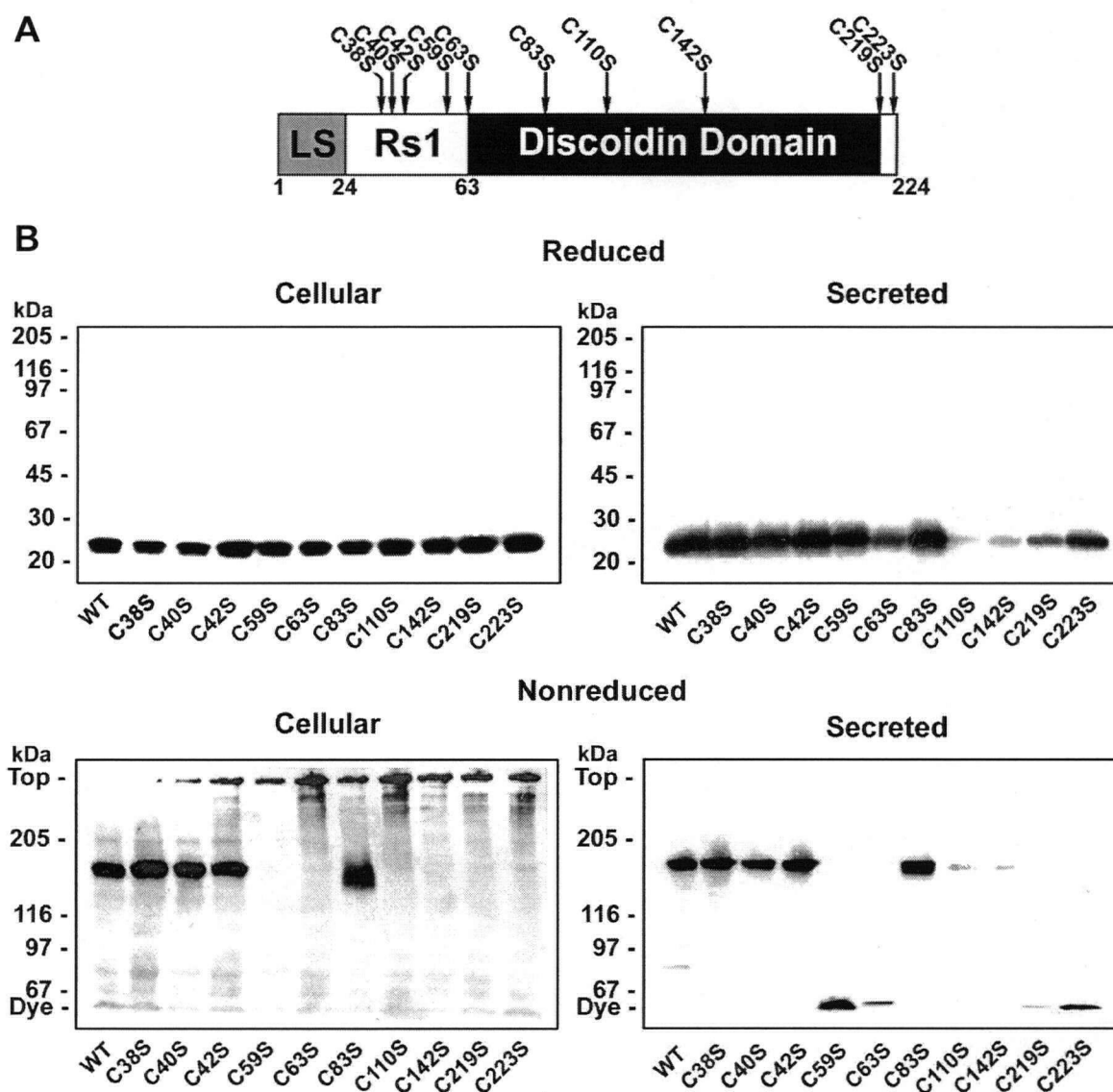
Figure 2.1. Expression and characterization of WT RS1 and single cysteine-to-serine mutants. (A) Domain schematic showing the relative locations of the cysteines in the RS1 polypeptide chain. **(B)** Cellular and secreted fractions of RS1 cysteine-to-serine mutants. Cells expressing WT or mutant RS1 were divided into the cellular (cells) and secreted (media) fractions. The expressed proteins were run on a 10% or 6.5% SDS-polyacrylamide gel under reducing or nonreducing conditions, respectively, and analyzed on Western blots labelled with the RS1 monoclonal antibody.

In the cellular fraction under disulfide-reducing conditions, WT RS1 and all cysteine-to-serine variants expressed at similar amounts, migrating as a 24-kDa monomer (Fig. 2.1B). Under nonreducing conditions, WT RS1 and 4 of the mutants (C38S, C40S, C42S, and C83S) migrated as a 180-kDa disulfide-linked oligomer. Of these 4 mutants, however, the C83S mutant was atypical in that it ran as a broader band. The remaining 6 cysteine mutants (C59S, C63S, C110S, C142S, C219S, and C223S) ran primarily as aggregates at the top of the gel, indicative of protein misfolding and aberrant disulfide bond formation.

In the secreted fraction, 5 mutants (C38S, C40S, C42S, C59S, and C83S) were secreted at a level comparable to that of WT RS1, 3 mutants (C63S, C219S, and C223S) showed moderate levels of secretion, and 2 mutants (C110S and C142S) displayed very limited secretion when analyzed under reducing conditions (Fig. 2.1B). The relative levels of secretion were consistent between experiments, indicating that the differences were not due to variations in transfection efficiency. Under nonreducing conditions, WT RS1 and 4 mutants (C38S, C40S, C42S, and C83S) secreted as 180-kDa oligomers. In contrast, C59S, which secreted at a high level, and 3 mutants (C63S, C219S, and C223S) that were secreted at moderate levels migrated at the dye front of a 6.5% gel. This suggests that selected cysteines in this subset participate in the disulfide-linked oligomerization of RS1.

2.3.2 C59 and C223 mediate homo-oligomeric formation

To further identify the residues responsible for disulfide-linked oligomerization, 4 cysteine-to-serine double mutants were characterized (Fig. 2.2).
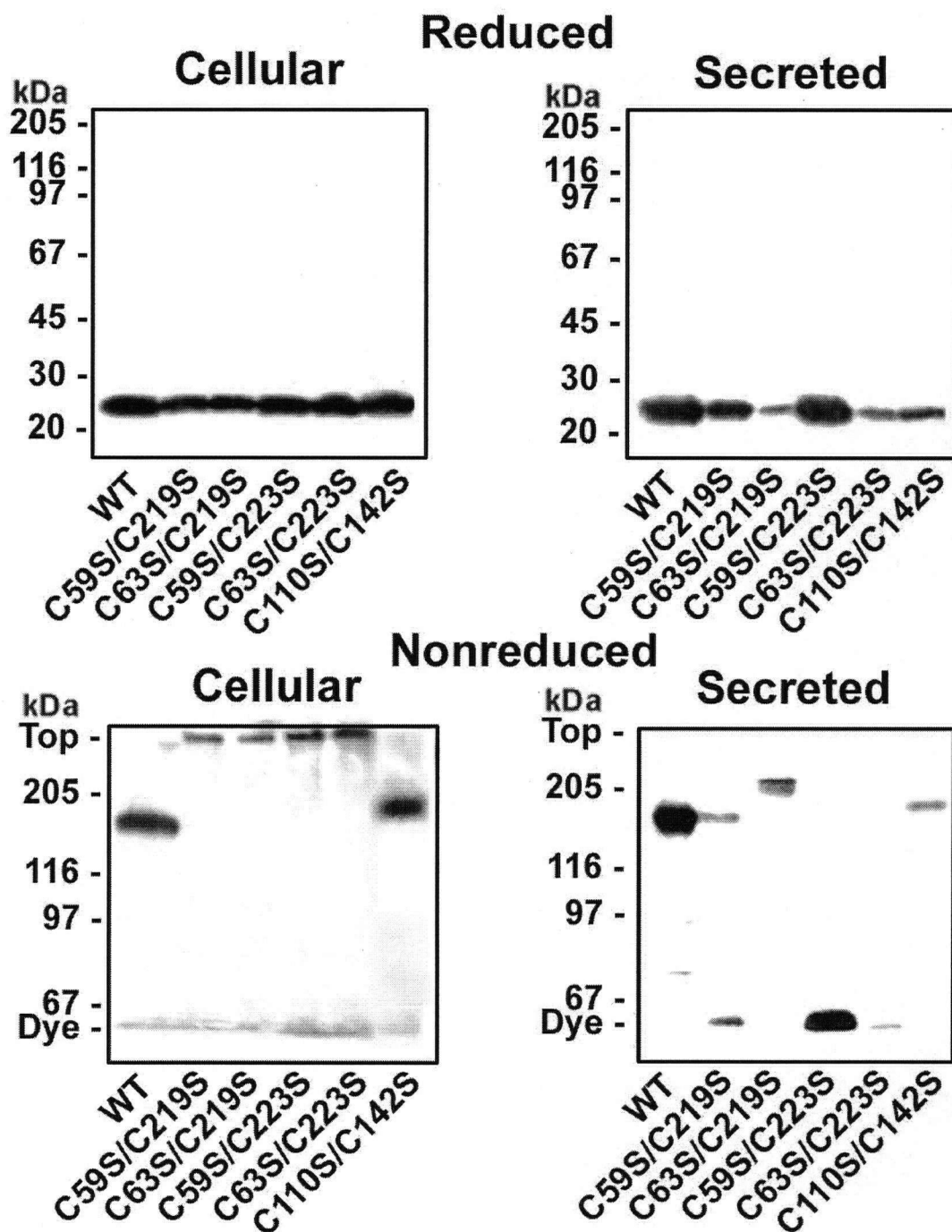
Figure 2.2. Expression and characterization of double cysteine-to-serine mutants. Cells expressing WT or mutant RS1 were divided into the cellular (cells) and secreted fractions (media). The expressed proteins were run on a 10% or 6.5% SDS-polyacrylamide gel under reducing or nonreducing conditions, respectively, and analyzed on Western blots labelled with the RS1 monoclonal antibody.

Only the C59S/C223S mutant secreted at a level comparable to that of WT

RS1 when analyzed under reducing conditions. When the secreted mutants were

analyzed under nonreducing conditions, the C59S/C223S mutant, unlike WT RS1,

migrated as a low molecular weight species at the dye front of a 6.5% gel. The

C63S/C223S mutant also migrated at the dye front on a 6.5% gel, but this variant

was present at extremely low levels. The C59S/C219S mutant was present as a

mixture of oligomers and low molecular weight components, and the C63S/C219S

variant migrated anomalously slowly.

The size of the secreted nonreduced C59S/C223S mutant was further

analyzed on a nonreducing 10% SDS-polyacrylamide gel. As shown in Figure 2.3,

the secreted C59S/C223S mutant migrated as a dimeric species. The results of

these single and double mutants indicate that the C59 and C223 residues are solely

responsible for the generation of the 180-kDa disulfide- linked multimeric RS1

complex.

2.3.3 C40 maintains dimeric assembly

When the C59S, C223S single or double mutants from the secreted fraction

were analyzed on higher percentage acrylamide gels, they migrated at a molecular

mass corresponding to a dimer. To determine which of the one or more cysteine

residues in RS1 are responsible for disulfide-mediated dimer formation, we

individually replaced each of four apparently benign cysteine residues (C38, C40,

C42, and C83) with a serine in a C59S/C223S oligomer-defective mutant, and

analyzed the cellular and secreted protein fractions from transfected HEK 293 cells

(Fig. 2.3). These four cysteines were selected because the studies on the single
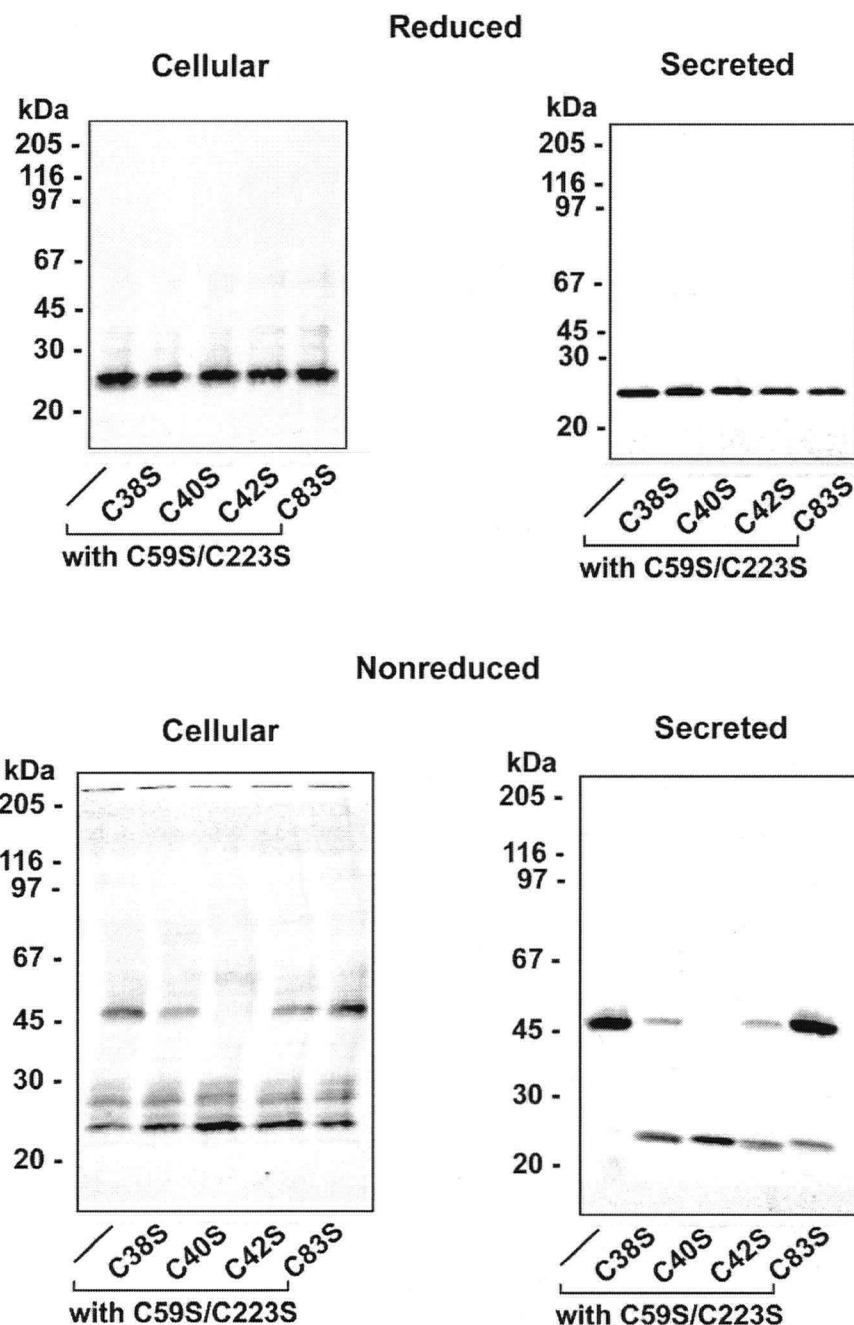
Figure 2.3. Analysis of cysteines responsible for RS1 dimer formation.
Dimeric C59S/C223S RS1 mutants containing an additional C38S, C40S, C42S, or
C83S mutation were expressed in HEK 293 cells, and the cellular and secreted
fractions were analyzed on 10% polyacrylamide gels for both reducing and
nonreducing conditions. Western blots were labelled with the RS1 monoclonal
antibody. Although some loss in dimer formation was observed for the C38S, C42S,
and C83S mutants, only the C40S mutant showed complete absence of dimers.
The first lane in each gel is the control containing only the background C59S/C223S
mutation.

cysteine mutants suggested that the remaining cysteines (C63, C110, C142, and C219) contribute to protein folding and are involved in intramolecular disulfide bonds within the discoidin domain (see below).

Under disulfide-reducing conditions, all four triple mutants exhibited similar levels of cellular expression and secretion on SDS gels and migrated as 24-kDa monomers (Fig. 2.3). Under nonreducing conditions, the parent C59S/C223S mutant from the secreted fraction ran solely as a 47-kDa dimer, whereas three C59S/C223S mutants containing an additional C38S, C42S, or C83S mutation migrated as a mixture of dimers and monomers. Only the C59S/C223S mutant containing a C40S mutation ran as the monomer under nonreducing conditions in both the cellular and secreted fractions without detectable dimer.

These studies suggest that C40 residues of individual RS1 subunits are directly involved in dimer formation. There was also partial loss of dimer formation in the C38S and C42S mutants, and to a lesser extent, the C83S mutant. This most likely resulted from structural perturbations, which partially restricted the formation of C40-mediated intermolecular disulfide bonds required for dimeric assembly.

All of these cysteine mutants exhibit an additional protein band just above the 24-kDa monomer in the cellular fraction of nonreduced gels (Fig. 2.3, lower left). This upper band, not found in the secreted fraction, most likely corresponds to a misfolded monomer that migrates anomalously on nonreducing SDS gels due to the presence of abnormal intramolecular disulfide bonds. This species is most likely recognized by the quality control system of the ER as a misfolded protein and therefore is not secreted from the cell. Alternatively, this band may reflect the

protein in its initial unfolded state and prior to the formation of any intramolecular disulfide bonds.

2.3.4 C110 and C142 form an intramolecular disulfide bond

As the single cysteine mutants showed that C110S and C142S behaved similarly (Fig. 2.1B), it suggested that C110 and C142 form an intramolecular disulfide bond within each RS1 subunit. Therefore, a C110S/C142S double mutant was also expressed (Fig. 2.2).

As shown in Fig. 2.2, the C110S/C142S variant was present at low levels in the secreted fraction and migrated more slowly than WT RS1 under nonreducing conditions. This suggests that replacement of both these cysteine leads to an alteration in the structure that causes a reduction in secretion of RS1 and anomalous migration behavior. The slower migration of the C110S/C142S double mutant may be due to the partial opening of the discoidin domain, which may increase its resistance and slow its migration as it moves through the polyacrylamide gel. To obtain more direct proof for the existence of the C110-C142 intramolecular disulfide bond within the discoidin domain of RS1, mass spectrometry studies were performed. The reduced 24-kDa monomer and nonreduced 180-kDa oligomer of RS1 from bovine retina were digested with trypsin, and the resulting peptides were analyzed by MALDI-TOF MS and LC/MS/MS. As listed in Table 2.1 and illustrated in Figures 2.4, 2.5, and 2.6, 14 tryptic peptides were identified from various regions of the reduced form of RS1. In addition to peptides identified in reduced RS1, a peak at m/z of 2548.8 was observed when RS1 was digested under nonreducing conditions (Fig. 2.5). This peak corresponded to a tryptic peptide (1410.6 Da)

Table 2.1 Tryptic peptides of RS1.

Bovine retinal RS1 was solubilized with CHAPS in the presence of NEM and purified on an RS1 3R10 immunoaffinity column. Samples were run on a nonreducing polyacrylamide gel. For electrospray LC/MS/MS, bands were excised, reduced with DTT, alkylated with IAM, and digested with trypsin. For MALDI-TOF MS, samples were reduced with DTT and alkylated with IAM after digestion. Control digestions without trypsin were performed for both electrospray and MALDI-TOF MS. For cysteine-containing peptides, the mass noted is the mass after alkylation with IAM. Cysteines in the sequence are in bold. See Fig. 2.4 for the locations of the peptides.

	Position	Sequence	Mis-cuts	Empirical mass, MALDI (Da)	Theoretical mass, average (Da)	Empirical mass, LC/MS/MS (Da)	Theoretical mass, mono-isotopic (Da)
A	24–36	STEDEGEDPWYHK	0	1592.89	1592.60		
B	103–115	LNSQGFG**C**AWLSK	0	1467.55	1467.66		
C	116–128	FQDSSQWLQIDLK	0	1607.68	1607.78		
D	132–141	VISGILTQGR	0	1043.22	1043.23		
E	142–150	**C**DIDEWMTK	0			1196.43	1196.48
F	142–150	(Met oxidized)	0			1212.38	1212.48
G	151–156	DQTGNNR	0	814.97	814.90	814.32	814.40
H	157–167	TDESLNWIYYK	0	1431.45	1431.56		
I	175–182	VFYGNSDR	0	957.05	957.01	956.37	956.44
J	183–197	TSTVQNLLRPPIISR	0	1695.08	1695.00	1693.86	1693.98
K	201–209	LIPLGWHVR	0	1090.15	1090.34		
L	214–222	MELLE**C**VSK	0			1107.44	1107.53
M	214–222	(Met oxidized)	0			1123.42	1123.53
N	157–174	TDESLNWIYYKDQTGNNR	1	2217.27	2217.34		
O	68–100	PLGFESGEVTPDQIT**C**SNVEQYVG WYSSWTANK [a]	0	3819.11	3819.12		
P	79–100	DQIT**C**SNVEQYVGWYSSWTANK [a]	0	2704.92	2704.91		

[a] Peptide O was generated from a double digest of Trypsin/LysC, and Peptide P was generated from a double digest of Trypsin/AspN. The mass noted corresponds to the NEM-alkylated peptide.

N-terminal tryptic peptide
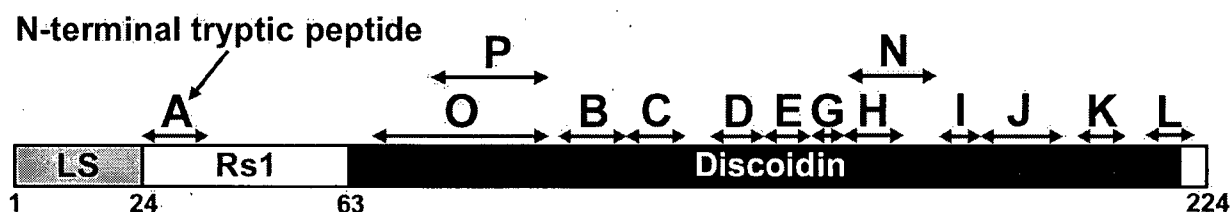
Figure 2.4. Locations of the peptides obtained from proteolytic digestion of RS1. Abbreviations used: LS, leader sequence; Rs1, Rs1 domain; Discoidin, discoidin domain.
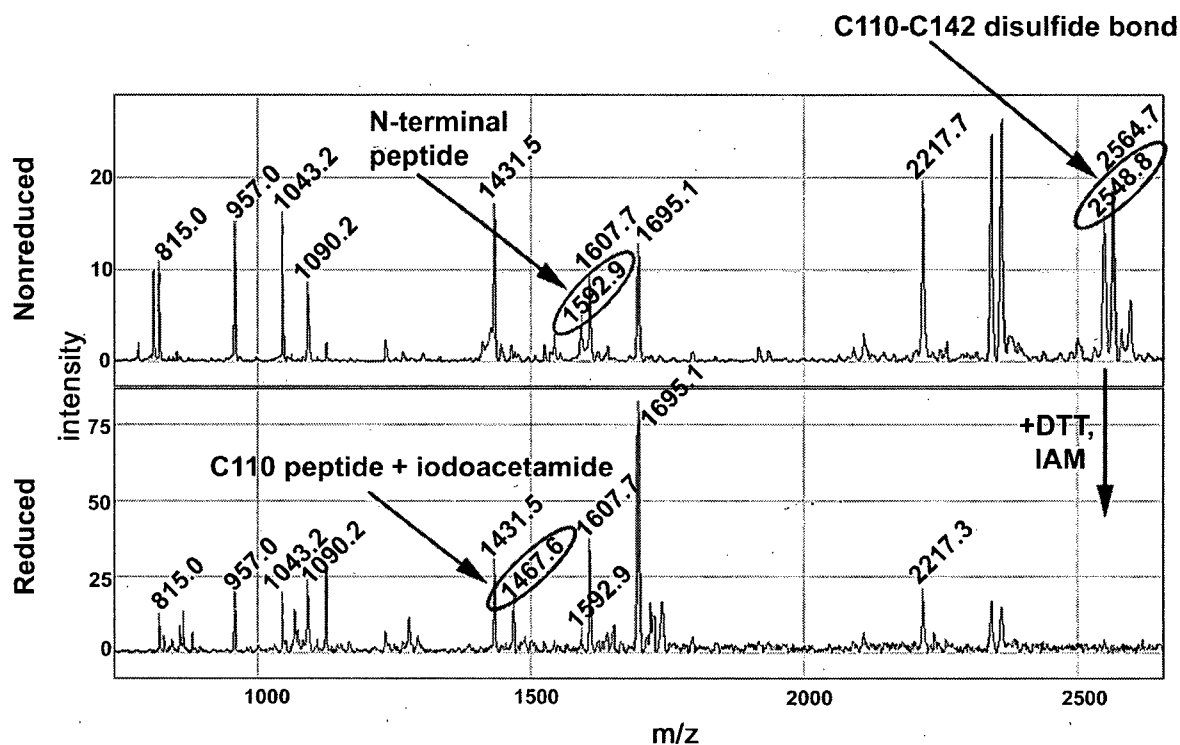
Figure 2.5. Mass spectrum of tryptic peptides from reduced and nonreduced RS1. Bovine retina was solubilized with 18 mM CHAPS in the presence of 10 mM NEM and purified on an RS1 3R10 immunoaffinity column. After elution with 4% SDS, nonreduced RS1 was run on SDS-PAGE. The RS1 band was excised, washed, and digested overnight with trypsin. A control digestion with trypsin only was also performed. Samples were analyzed by MALDI-TOF mass spectrometry in the nonreduced form, and subsequently in the reduced form after treatment with DTT and alkylation with IAM. Peaks corresponding to the RS1 N-terminal peptide, the C110-C142 disulfide-bonded peptide under nonreducing conditions, and the reduced, IAM-modified C110 peptide are *circled*.
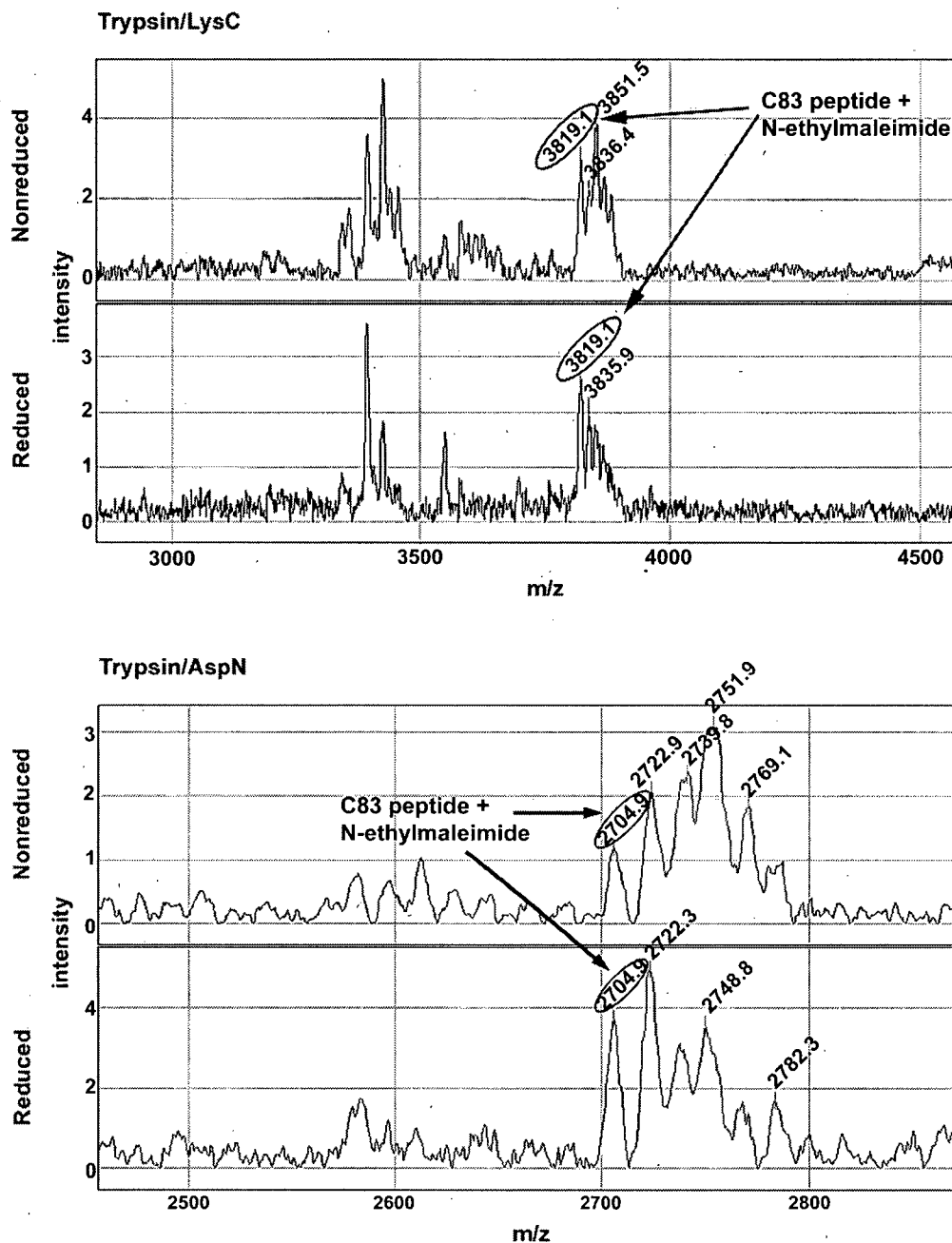
Figure 2.6. Mass spectrum of the C83-containing peptide from nonreduced and alkylated RS1. Detergent-solubilized bovine retinal RS1 was treated with NEM and purified on an RS1 3R10 immunoaffinity column. After elution with SDS, nonreduced RS1 was separated by SDS-gel electrophoresis. Bands were excised, washed, and doubly digested with trypsin/LysC or trypsin/AspN. Samples were analyzed by MALDI-TOF mass spectrometry in the nonreduced form, and subsequently in the reduced form after reduction with DTT and alkylation with IAM. Peaks corresponding to NEM-modified C83-containing peptides are indicated. Additional peaks differing by about 16 Da are likely oxidized forms of the peptide.

containing C110 that was disulfide bonded to a tryptic peptide (1140.3 Da) containing C142. (To calculate the theoretical mass of the nonreduced peptide, a mass of 2 Da was subtracted from the sum of the masses of these two cysteine-containing peptides due to removal of two hydrogens upon disulfide bond formation.) Another peak observed under nonreducing conditions at m/z of 2564.7 most likely corresponds to the same disulfide-linked peptide, but with the single methionine (located on the C142 peptide) existing in an oxidized state.

Next, it was necessary to ensure that these peptides at m/z of 2548.8 and 2564.7 obtained from digestion of nonreduced RS1 indeed contain a disulfide bond. Therefore, the sample was disulfide-reduced with DTT and the resulting free cysteines were alkylated with IAM. Under these conditions, the peaks at m/z of 2548.8 and 2564.7 disappeared and a new peak at 1467.6 appeared (Fig. 2.5). The mass of this new peptide is consistent with the tryptic peptide containing an IAM-modified C110 residue. The tryptic peptide containing the alkylated C142 residue was not observed by MALDI-TOF mass spectrometry, but was detected by LC/MS/MS (Table 2.1).

2.3.5 C63 and C219 mediate a second intramolecular disulfide bond

To date, it has been determined experimentally from four members of the discoidin domain family that a disulfide bridge exists between the first and the last cysteine residues that mark the beginning and end of the discoidin domain. This result comes from the three solved crystal structures of discoidin domains of Factor V, Factor VIII, and neuropilin 1, and from mass spectrometry of the discoidin domain of milk fat globule protein, PAS-6/7 (Hvarregaard et al., 1996; Lee et al., 2003;

Macedo-Ribeiro et al., 1999; Pratt et al., 1999). In addition, all discoidin domain family members contain both of these starting and ending cysteines (Consortium, 1998). This implicates a disulfide bond for all family members, and is one of the hallmarks of the discoidin domain fold. Thus, RS1 most likely also possesses an analogous disulfide bond between C63 at the beginning and C219 at the end of its discoidin domain.

Results obtained here support this. The C63S/C219S double mutant migrates much more slowly than WT on nonreducing SDS gels, suggesting that similar to the C110S/C142S mutant, the protein has an altered conformation that causes it to migrate more slowly in the absence of that key disulfide bond (Fig. 2.2).

From these results and based on the crystal structures of the C2 discoidin domain of coagulation Factors V and VIII, a molecular model of the discoidin domain of RS1 was generated (Fig. 2.7). The model incorporates intramolecular disulfide bonds C110-C142 and C63-C219.

2.3.6 C83 exists in its reduced state

To determine the redox state of C83, nonreduced RS1 from bovine retina was alkylated with NEM and double-digested with trypsin/LysC, or trypsin/AspN. The trypsin/LysC sample contained a peptide with an m/z of 3819.1, and the trypsin/AspN sample contained a peptide with an m/z of 2704.9 (Fig. 2.6 and Table 2.1). These masses correspond to peptides containing C83 that have been alkylated with NEM. This indicates that the C83 within the discoidin domain of RS1 exists in its reduced state. Additional peaks that have slightly higher masses appear to correspond to the same peptide containing one or more oxidized amino acids.

A

```
RS1 CPYHKPLGFESGEVTPDQITCSNPEQYVGWYSSWTANKARLNSQGFGCAWLSKFQ-DS-SQWLQIDLKEIKVISGILTQG
F5  CST--PLGMENGKIENKQITASSFKKS-WWGDYWEPFRARLNAQGRVNAWQAKAN-NN-KQWLEIDLLKIKKITAIITQG
F8  CSM--PLGMESKAISDAQITASSYF-TNMFA-TWSPSKARLHLQGRSNAWRP--QVNNPKEWLQVDFQKTMKVTGVTTQG
                β1       spike1            spike2              β2          β3

RS1 -RCDIDEWMTKYSVQYR-TDERLNWIYYKDQTG-NNRVFYGNSDRTSTVQNLLRPPIISRFIRLIPLGWHVRIAIRMELLEC
F5  CKSLSSE-MYVKSYTIHYSEQGVEWKPYRLKSSMVDKIFEGNTNTKGHVKNFFNPPIISRFIRVIPKTWNQSIALRLELFGC
F8  VKSLLTS-MYVKEFLISSSQDGHQWTLFFQN-GKV-KVFQGNQDSFTPVVNSLDPPLLTRYLRIHPQSWVHQIALRMEVLGC
      spike3      β4                   β5        β6          β7           β8
```

B
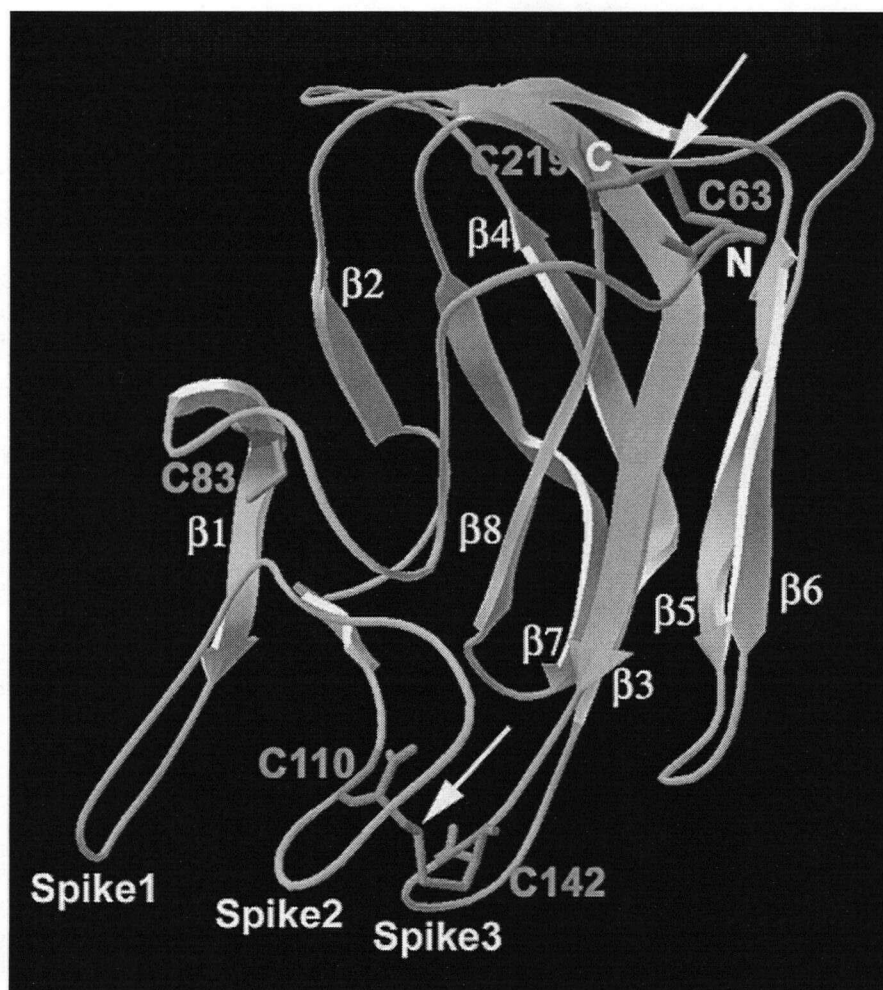
Figure 2.7. Sequence alignment and structural model of the RS1 discoidin domain. **(A)** Alignment of the discoidin domain of RS1 with the C2 discoidin domains of coagulation Factors V and VIII (F5 and F8). Conserved residues are highlighted in *yellow* and the two conserved cysteines (corresponding to C63 and C219 in RS1) are highlighted in *black*. The 8 core β strands and 3 spikes as initially described by Fuentes-Prior et al. (Fuentes-Prior et al., 2002) for Factors V and VIII are *underlined*. **(B)** Ribbon diagram of the RS1 discoidin domain modeled from the Factor V and VIII C2 discoidin domain crystal structures. The model shows the locations of the C63-C219 and C110-C142 intramolecular disulfide bonds (*arrows*), and C83.

2.3.7 Retinal RS1 is heterogeneous

To determine if RS1 from retinal tissue exhibits a similar disulfide-linked oligomeric structure as recombinant RS1, its migration behavior was compared with that of recombinant WT RS1 and the C59S/C223S mutant on denaturing polyacrylamide gradients gels under reducing and nonreducing conditions. RS1 obtained from retinal tissue was partially purified by extraction with CHAPS and urea as described in Section 2.2.9. The recombinant forms of RS1 (WT and C59S/C223S) were partially purified from the secreted fraction of EBNA HEK 293 cells transfected with those constructs, also as described in Section 2.2.9. As shown in Figure 2.8, a fraction of RS1 from the retina migrated as a 24-kDa monomer under reducing conditions and as a 180-kDa oligomer under nonreducing conditions similar to recombinant WT RS1. However, a significant fraction of retinal RS1 migrated more slowly.

Under reducing conditions, a portion of retinal RS1 migrated as a 47-kDa dimer and another fraction ran as a diffuse band between the monomer and dimer. Heating at 60°C or 95 °C for 5 min in the presence of reducing agent □-mercaptoethanol and SDS did not abolish these slowly migrating bands in the retinal RS1 sample. Under nonreducing conditions, a diffuse band was observed just above the 180-kDa oligomer. A similar diffuse RS1-labelled band has been reported for mouse retinal extracts under nonreducing conditions (Reid et al., 1999). These additional diffuse species were not observed for the recombinant WT or C59S/C223S mutant protein expressed in HEK 293 cells (Fig. 2.8), and nor were they seen in RS1 derived from Weri-Rb1 retinoblastoma cells (data not shown). The

Reduced   **Nonreduced**
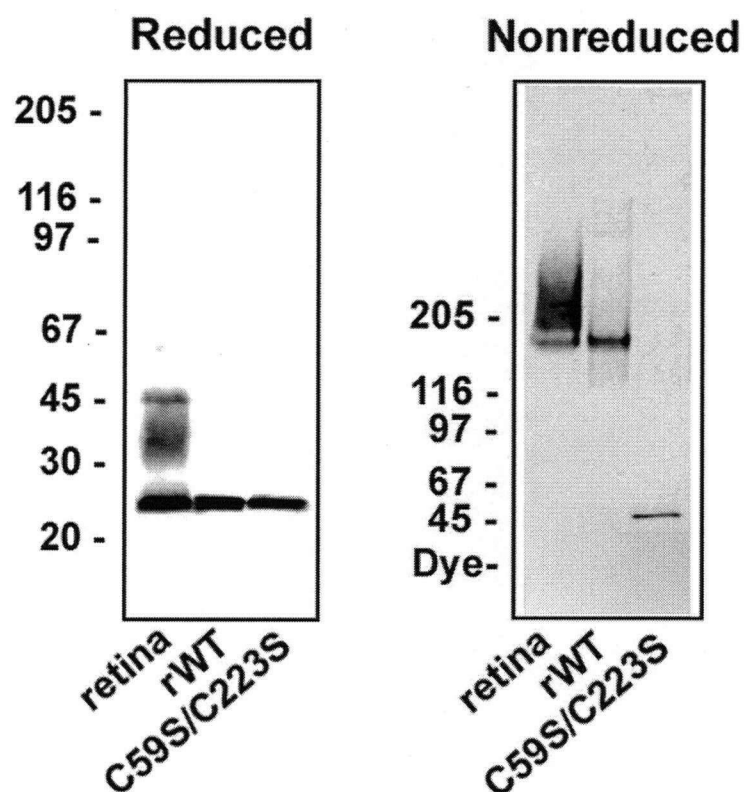
Figure 2.8. Comparison of retinal RS1 with WT and C59S/C223S recombinant RS1 by SDS gel electrophoresis. RS1 was isolated from bovine retina or from HEK 293 cells secreting recombinant WT (*rWT*) or C59S/C223S mutant RS1. Protein samples under reducing conditions (plus □-mercaptoethanol) were separated on a 4–12% NuPAGE polyacrylamide gradient denaturing gel, and samples under nonreducing conditions (minus □ -mercaptoethanol) were separated on a 3–8% NuPAGE gradient gel. Western blots were labelled with the RS1 3R10 antibody.

banding pattern reflecting the heterogeneity of nonreduced and reduced RS1 from frozen bovine retina was also observed for freshly dissected bovine and mouse retinal tissue (data not shown). This indicates that the diffuse bands observed in the retina sample are not due to artifacts generated from aged tissue or from species-specific tissue. These data suggest that a portion of RS1 expressed in photoreceptor and/or bipolar cells undergoes a heterogeneous type of post-translational modification. It is quite possible that this post-translational modification represents glycosylation, since heavily glycosylated proteins often show a high degree of heterogeneity due to variations in the size of the carbohydrate chains. However, experiments performed from purified RS1 using periodic acid oxidation and subsequent labeling of putative oxidized carbohydrates were unable to detect any glycosylation compared to the positive control that did show glycosylation.

2.3.8 RS1 forms a single disulfide-linked homo-octamer in the absence of dimer formation

As mentioned above, RS1 migrates on SDS gels as a high molecular weight oligomer under nonreducing conditions. To determine the size of the RS1 oligomer, a C38S/C40S/C42S triple mutant displaying partial disruption of the oligomeric complex was expressed, secreted from HEK 293 cells, and analyzed on nonreducing SDS-polyacrylamide gradient gels. As shown in Fig. 2.9A, the secreted triple mutant showed a ladder of eight distinct bands ranging from the 24-kDa monomer to the prominent 180-kDa octameric protein.
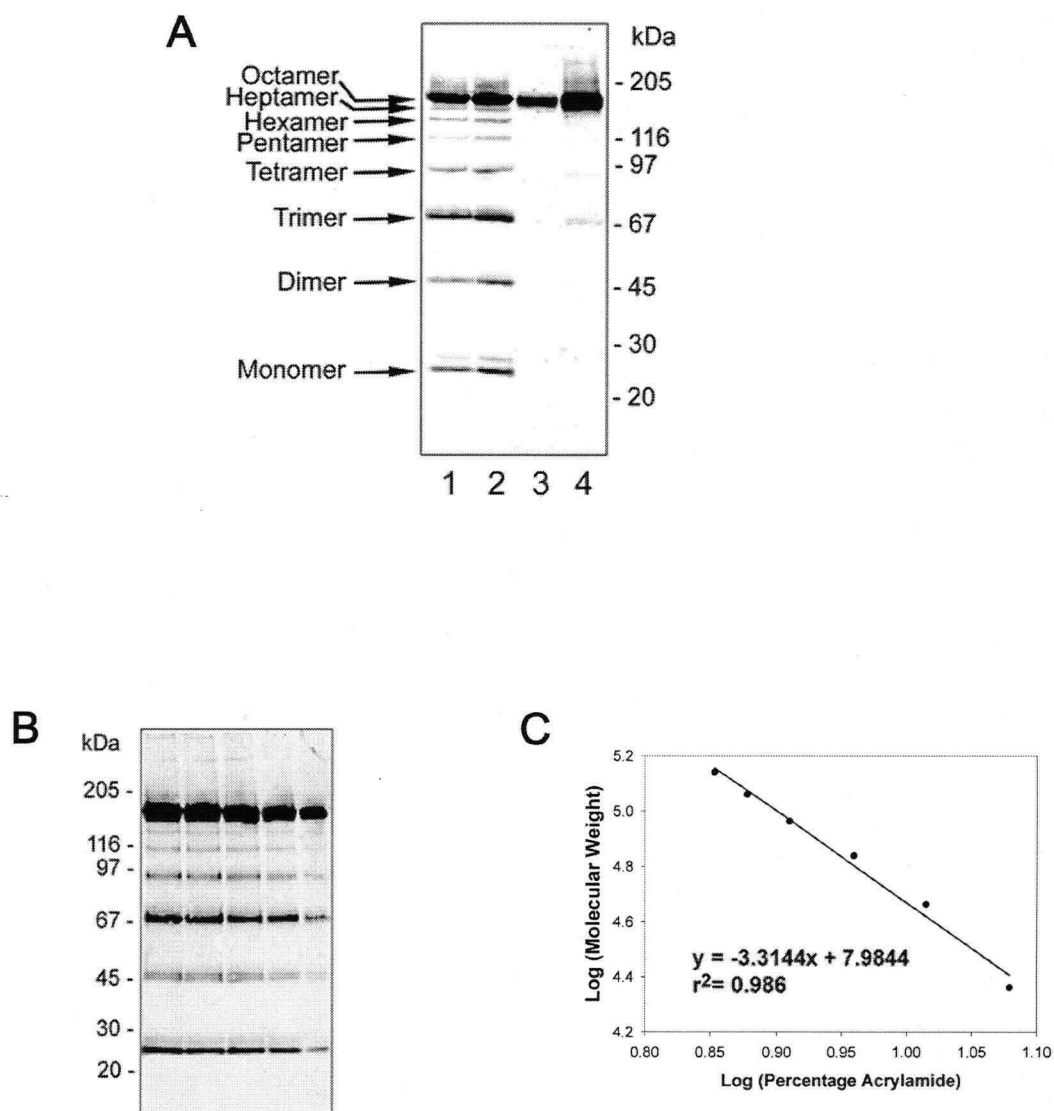
Figure 2.9. Analysis of disulfide-linked RS1 oligomers on nonreducing SDS gels. WT and the triple mutant, C38S/C40S/C42S RS1, were expressed in HEK 293 cells, purified from the secreted fraction on an RS1 immunoaffinity column, and analyzed on a nonreducing, denaturing 4–12% NuPAGE polyacrylamide gradient gel. The ladder of oligomeric species was detected on Western blots labelled with the RS1 3R10 monoclonal antibody. **(A)** The C38S/C40S/C42S mutant (*lanes 1* and *2*) and WT (*lanes 3* and *4*) at two different concentrations. Positions of the oligomeric species are indicated. **(B)** Serial dilutions of WT RS1 were run on nonreducing gels to determine the migration distance of the various oligomers. **(C)** Data from (B) was used to plot the logarithm of the molecular weight of the six lower bands *versus* logarithm of the percentage acrylamide. The line-of-best-fit equation was determined using SigmaPlot. The number of subunits for the 180-kDa WT RS1 protein (top prominent band) was calculated to be 7.7.

To confirm that WT RS1 is also an octamer, the secreted fraction of HEK 293 cells expressing WT RS1 was analyzed by nonreducing SDS-PAGE. As shown in Fig. 2.9B, a ladder of bands was also evident for WT protein when Western blots were exposed for extended times, with the 180- kDa complex being the most prominent species. Unlike the C38S/C40S/C42S mutant, however, only seven bands were resolved for WT RS1, presumably due to the masking of the heptamer by the dominant octameric complex. This was confirmed by plotting the logarithm of the apparent molecular mass for the six lower bands against the logarithm of the acrylamide percentage at which these species migrated (See and Jackowski, 1989). From the linear relation (Fig. 2.9C), the number of subunits in the prominent top band of the WT complex was calculated to be 7.7. This suggests that WT RS1, like the C38S/C40S/C42S mutant, exists as a disulfide-linked octamer.

Velocity sedimentation studies were further carried out to determine whether RS1 exists as a single octamer or as a higher-ordered oligomeric structure under nondenaturing conditions. Figure 2.10 shows the sedimentation profiles for retinal and recombinant RS1 generated from Western blots of fractions collected from a 5–20% sucrose gradient. The WT recombinant protein (rWT) sedimented just ahead of retinal RS1 and mouse IgG (approximately 160 kDa) used as a standard. This indicates that both retinal and WT RS1 exist as a single disulfide-linked octamer under nondenaturing conditions, as well as under denaturing (nonreducing) conditions, and does not form higher-ordered oligomers through noncovalent interactions. Heterogeneous post-translational modification may account for the small decrease in sedimentation rate and broader peak profile observed for retinal
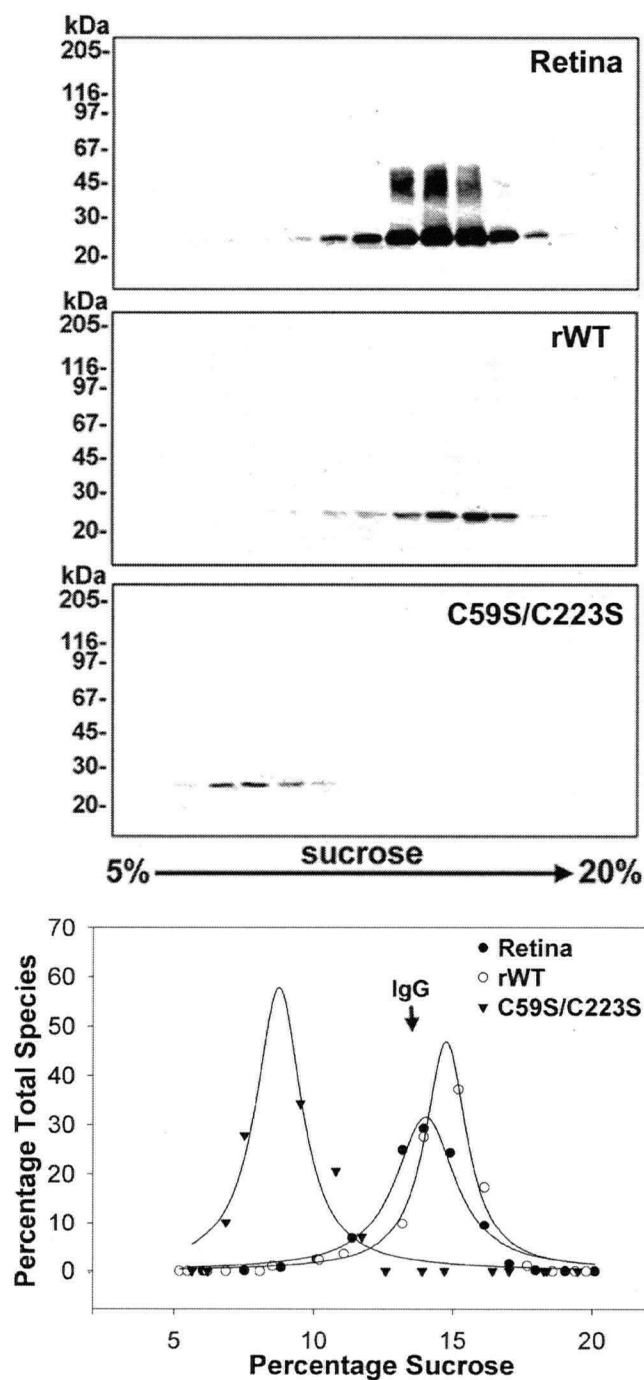
Figure 2.10. Velocity sedimentation analysis of retinal RS1 and recombinant WT (rWT) and C59S/C223S mutant RS1. Proteins were sedimented through a 5–20% sucrose gradient. Fractions were run on reducing gels containing 10% acrylamide and blotted with the RS1 3R10 antibody. The intensities of the labelled bands were quantified and displayed in the graph in the *lower panel*. Mouse immunoglobulin G (IgG) having a molecular mass of 160 kDa was run as a standard.

RS1 relative to the recombinant WT protein (Fig. 2.10). The octamer-defective C59S/C223S mutant migrated much more slowly, consistent with its smaller size, and presumably as a dimer as observed under nonreducing, denaturing conditions. This suggests that noncovalent interactions do not play a significant role in the octameric assembly or stabilization of RS1.

The arrangement of subunits within the octameric complex was explored. The finding that intermolecular disulfide bonds are formed between C59 and C223, and between individual C40 residues of different subunits, suggests two models. In one model (Fig. 2.11A left), the C59-C223 disulfide bonds are solely responsible for octamer formation, and additional C40 disulfide bonds form between two adjacent or opposing subunits within the octamer. In another model (Fig. 2.11A right), the C59-C223 intermolecular disulfide bonds result in the formation of tetramers. Two tetramers further link together in a head-to-head arrangement through C40 disulfide bonds to form the octamer. For the first model to hold true, one predicts that RS1 containing a C40S dimer-defective mutation should still form an octamer, whereas for the second model, this mutation should result in tetramers.

To distinguish between these models, a C38S/C40S/C42S/C83S quadruple mutant (termed Δ4Cys), which is completely defective in disulfide-linked dimer formation, was expressed and analyzed on reducing and nonreducing SDS gels. Even though only C40 was found to mediate dimer formation (Fig. 2.3), the three other cysteines (C38, C42, C83) may artificially mediate dimer formation within the octamer if C40 is mutated. Therefore, all four cysteines were mutated.
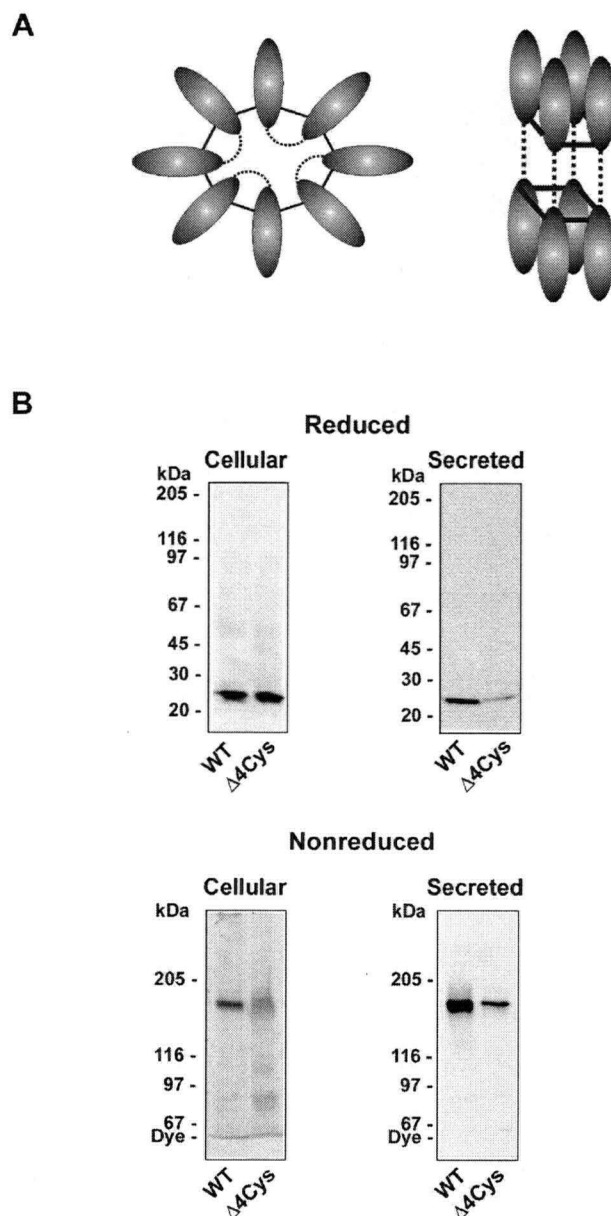
Figure 2.11. RS1 forms an octamer in the absence of dimer formation.
(A) Two possible models for the assembly of RS1 as dimers within an octameric
complex. In the first model (*left*), the C59-C223 disulfide bond is responsible for
octamer formation; within this complex the C40-C40 bond forms dimers between
adjacent subunits or opposite subunits (not shown). In the second model (*right*)
tetramers formed from C59-C223 bonds are linked via C40-C40 bonds in a head-to-
head arrangement. C59-C223 bonds are *solid lines*; C40-C40 bonds are *dashed
lines*. (B) WT and a Δ4Cys quadruple mutant (C38S/C40S/C42S/C83S) were
expressed in HEK 293 cells. The cellular and secreted fractions were separated by
SDS-gel electrophoresis under reducing and nonreducing conditions for detection by
Western blotting. The Δ4Cys mutant forms an octamer in the absence of dimer
formation, consistent with the first model shown in (A).

Figure 2.11B shows that the secreted C38S/C40S/C42S/C83S mutant, like WT RS1, migrated as a 24-kDa monomer under reducing conditions and as a 180-kDa octamer under nonreducing conditions. Similar results were obtained for the C40S single mutant (Fig. 2.1B). These results support the first model in which an octamer is formed via C59-C223 disulfide bonds even in the absence of C40-mediated dimer formation.

Another interesting finding from this study is that the secreted quadruple cysteine mutant (C38S/C40S/C42S/C83S) in Figure 2.11 does not contain oligomers smaller than the octamer as was found for the triple cysteine mutant (C38S/C40S/C42S) in Figure 2.9. This may be because the extra C83S mutation of the quadruple mutant more severely disrupts folding and assembly such that less abundant species (monomers, dimers, trimers, etc.) show reduced, undetectable levels of secretion. In both cases, however, enough octamer is properly folded and assembled to be secreted.

2.3.9 RS1 is cleaved by signal peptidase between S23 and S24

RS1 contains an N-terminal leader sequence predicted to be cleaved by a signal peptidase as part of the protein secretion process (Gehrig et al., 1999b; Reid et al., 1999; Sauer et al., 1997). To confirm that the leader signal peptide is cleaved in native RS1 and identify the site of cleavage, the N-terminal sequence of immunoaffinity-purified RS1 from retinal tissue was determined by standard Edman degradation methods. The first five amino acid residues were identified as [24]Ser-

Thr-Glu-Asp-Glu[28], indicating that the signal peptidase had removed the N-terminal 23-amino acid leader sequence to produce the mature secreted protein.

This was site of cleavage was confirmed by MALDI mass spectrometry (Figs. 2.4 and 2.5; Table 2.1). Peptide A (m/z of 1592.6 for bovine RS1 and m/z of 1583.6 for human RS1 [not shown]) corresponds to the N-terminal tryptic peptide of the processed RS1 polypeptide, confirming that signal peptidase cleavage had occurred at S23 as part of the protein secretion pathway.

2.4 Discussion

In this study, the structural properties of RS1 have been analyzed as an important step in understanding how this extracellular protein functions in retinal cell adhesion and how mutations in *RS1* cause X-linked retinoschisis. RS1 is composed of eight identical subunits that are linked together through intermolecular disulfide bonds between C59 and C223 residues on adjacent subunits. These disulfide bonds are required for octamer assembly because substitution of C59 or C223 with a serine abolishes octamerization of RS1 under nonreducing denaturing conditions, as observed by SDS-gel electrophoresis, and under native conditions, as analyzed by velocity sedimentation. In addition to the C59-C223 intermolecular disulfide bond, RS1 contains a C40-C40 disulfide bond responsible for dimer formation (Fig. 2.12). Dimerization is independent of octamerization, and octamerization is independent of dimerization because each multimeric species forms in the absence of the other. Accordingly, RS1 is composed of four disulfide-linked dimers within a
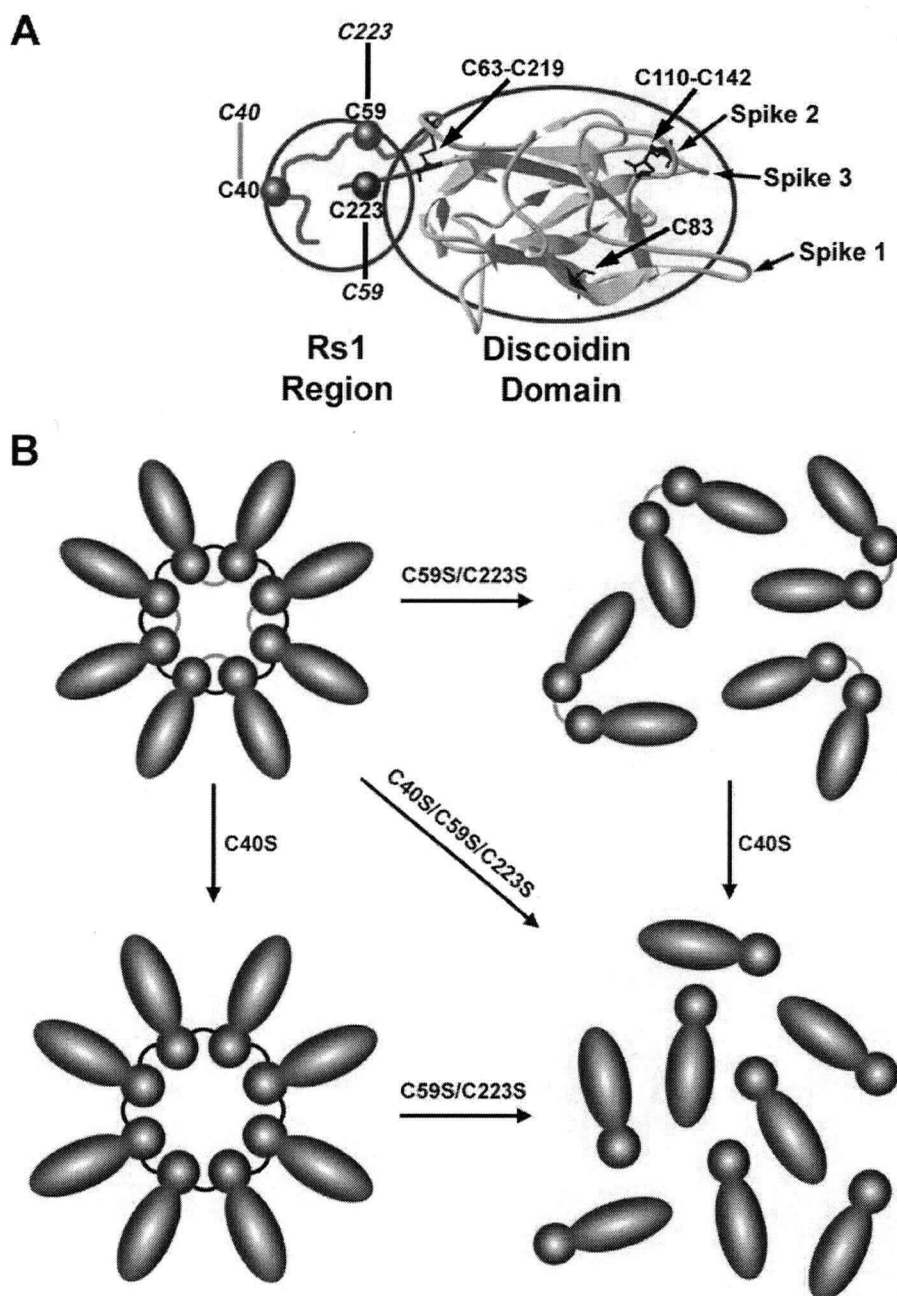
Figure 2.12. Schematic representations of RS1. **(A)** The RS1 polypeptide is shown, with the Rs1 region (*circle*), consisting of both the 39-amino acid Rs1 domain and the 5-amino acid C-terminal segment, joined to the discoidin domain (*ellipsoid*). A structural model of the RS1 discoidin domain is shown within the *ellipsoid*. Cysteines involved in intramolecular (*blue*) and intermolecular (*black* or *gray*) disulfide bonds are shown. C83 exists in its reduced state. **(B)** Schematic showing the effect of intermolecular cysteine mutations on the subunit assembly of RS1. For simplicity, C40-C40 (*gray*) intermolecular disulfide bonds are shown to join adjacent subunits, although the exact arrangement is not known. The C59-C223 disulfide bonds are shown in *black*.

disulfide-linked octameric structure. The exact arrangement of the subunits, however, awaits determination of the high-resolution structure of RS1.

The cysteine residues involved in these intermolecular disulfide bonds are located in segments that flank the discoidin domain, i.e. the 39-amino acid Rs1 domain upstream and a 5-amino acid segment downstream of the discoidin domain, which has been collectively termed the Rs1 region (Fig. 2.12A). Therefore, a principal function of this Rs1 region flanking the discoidin domain is to assemble RS1 into a disulfide-linked octamer. Octamerization appears to be essential for the function of RS1 in retinal cell adhesion because the C59S and C223R mutations, which do not significantly affect the folding and secretion of dimeric RS1, are known to cause X-linked retinoschisis (see Chapter 3). However, it is unclear if C40-mediated dimerization is critical for RS1 function, because substitution of C40 with serine does not affect folding, secretion, or octamerization of RS1 (Fig. 2.1B), and to date no disease-linked missense mutations at position 40 have been found. It is possible that C40-linked dimerization may simply contribute to the stability of the octameric complex but not be critical for its function. A biochemical assay for retinal cell adhesion would help to resolve this issue. For example, one could coat wells with pure, nondenatured protein, apply cells to let them attach to the protein, and then count how many cells remain adhered to the wells after washing. A range of washing conditions (from stringent to weaker washes) and a range of dilutions of the initial number of cells would aid in the precision of the assay.

In addition to cysteine at position 40, the RS1 domain contains two additional cysteine residues at positions 38 and 42. Substitution of these residues with serine

does not significantly affect octamerization and only partially affects dimerization, as shown here (Figs. 2.1B and 2.3). We were unable to determine the redox state of C38 and C42 by mass spectrometry. It is possible that these residues form an intramolecular disulfide bond, or perhaps additional intermolecular disulfide bonds that facilitate dimer formation. Alternatively, C38 and C42 may exist in their reduced state. Interestingly, this ^{38}CKCDC^{42} motif is highly conserved in all vertebrate RS1 proteins that have been sequenced to date (Fig. 1.6).

The discoidin domain is the main functional part of the RS1 protein. Like the discoidin domains of other proteins, RS1 contains conserved cysteine residues marking the beginning (C63) and the end (C219) of its discoidin domain that form an intramolecular disulfide bond, clamping together the N- and C- termini of the discoidin domain. In addition to C63 and C219, the RS1 discoidin domain contains 3 additional cysteine residues. The C110 and C142 cysteines, located in spikes 2 and 3, respectively, have been shown to form another intramolecular disulfide bond within the discoidin domain based on molecular modeling, site-directed mutagenesis, and mass spectrometry studies (Figs. 2.2, 2.5, 2.7). The function of the spike regions in the RS1 discoidin domain has yet to be determined, but in other discoidin domain-containing proteins, it has been implicated in binding to their interacting ligands (Fuentes-Prior et al., 2002). On this basis, the C110-C142 disulfide bond may be important in stabilizing the spike regions of RS1 for insertion into its interacting ligands.

An additional cysteine residue, not found in the discoidin domains of other family members, is present at position 83 of the RS1 discoidin domain. Mass

spectrometric analysis of nonreduced and alkylated proteolytic fragments indicates that this cysteine exists in its reduced state. This is consistent with molecular modeling analysis, which indicates that this residue is largely buried within the protein structure. In fact, C83 is occupied by an alanine in most other discoidin family proteins. Substitution of C83 with serine also has little effect on the folding, secretion, or oligomeric assembly of RS1, suggesting that this cysteine residue may not be essential for the structure or function of RS1. Furthermore, to date no disease-linked missense mutations at position 83 have been reported. A model depicting the role of various cysteines in disulfide bonding is shown in Fig. 2.12.

Functionally, the cysteines in RS1 can therefore be divided into 3 classes based on their potential to form intramolecular or intermolecular disulfide bonds and their effect on RS1 structure. One class consists of 4 cysteines (C63, C110, C142, and C219) in the discoidin domain that are essential for proper folding and efficient protein secretion. When any one of these is substituted with a serine, a major portion of expressed protein is retained in the ER as misfolded, disulfide-linked protein aggregates. A second class of cysteines consists of C59 and C223, lying just outside the discoidin domain. A large fraction of both single and double C59, C223 cysteine mutants fold properly as indicated by their ability to effectively pass through the ER quality control system (Ellgaard et al., 1999), but unlike WT RS1, they are unable to form the octameric complex. Accordingly, C59 and C223 are not critical for the folding of the RS1 subunit, but instead are responsible for intermolecular disulfide bonds that mediate RS1 octamerization. The third class of cysteines, comprised of C38, C40, C42, and C83, has a limited effect on RS1

structure and secretion. Since mutating these cysteines has no significant effect on protein expression, secretion, or oligomer formation, these residues do not appear to play a critical role in protein structure or subunit assembly. However, C40, which mediates dimeric assembly, may be critical for stabilization of the octamer.

The results from these studies suggest a sequence of events leading to the secretion of RS1 from cells (Fig. 2.13). As in the case of many secreted proteins, the leader sequence initiates the insertion and translocation of the nascent RS1 polypeptide chain across the ER membrane. The signal peptidase in the ER cleaves the leader peptide at S23 to produce the processed RS1 polypeptide. Folding of the discoidin domain occurs, with the formation of the C63-C219 and C110-C142 intramolecular disulfide bonds. Subsequently, intermolecular disulfide bonds C40-C40 and C59-C223 within the segments flanking the discoidin domain form to produce the final RS1 octamer for secretion from cells. A portion of RS1 in retinal tissue undergoes additional post-translational modification, the nature of which remains to be determined. Mutational studies also indicate that the monomeric and dimeric forms of RS1 can pass through the ER quality control system for secretion. This suggests that the proper folding of the RS1 discoidin domain occurs independently of disulfide-linked subunit assembly. However, the function of RS1 as a cell adhesion protein requires proper octamerization, as patients with mutations showing defective octameric assembly display X-linked retinoschisis (see Chapter 3). The multivalent nature of the RS1 homo-octamer may facilitate cell-cell adhesion by binding to the surfaces of adjacent cells, acting like a crosslinker. Alternatively, the multisubunit nature of RS1 may enhance its binding
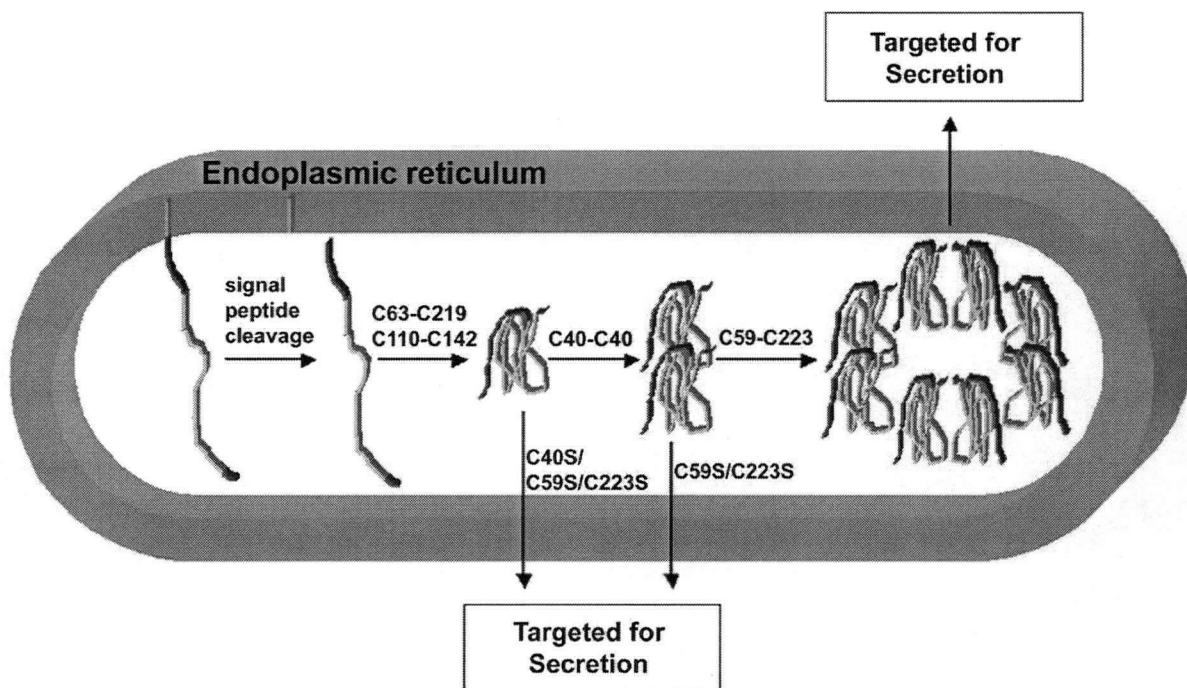
Figure 2.13. Pathway for RS1 ER insertion, disulfide-mediated octameric assembly, and secretion. RS1 inserts into the ER membrane through the leader sequence, enabling the nascent polypeptide chain to be translocated into the ER lumen. Signal peptidase cleaves off the 23-amino acid leader sequence, and folding of the RS1 subunit occurs with the formation of intramolecular disulfide bonds (C63-C219 and C110-C142). WT RS1 assembles into a dimer mediated by C40-C40, and an octamer mediated by C59-C223 intermolecular disulfide bonds. The WT protein is subsequently targeted for secretion into the extracellular space. Dimer and octamer formation can occur independently. Monomers (C40S/C59S/C223S mutant) and dimers (C59S/C223S mutant) can be still secreted even if octamer formation is defective.

to a cell surface by providing multiple subunits that would strengthen an interaction. In either case, RS1 may interact either directly with components of the plasma membrane or indirectly via other extracellular proteins or carbohydrates to promote cell adhesion and stabilize the cellular architecture of the surrounding retinal tissue.

CHAPTER 3: MOLECULAR BASIS OF X-LINKED RETINOSCHISIS [2]

3.1 Introduction

X-linked retinoschisis is a common form of early onset macular degeneration in males (Forsius et al., 1973; Sieving, 1998). It is characterized by a mild to severe decrease in visual acuity, radial streaks extending from the central retina due to a splitting of the inner retina, progressive macular atrophy, and reduction in the electroretinogram b-wave (George et al., 1995b; Hiriyanna et al., 1999; Peachey et al., 1987; Sieving, 1998). Lesions in the peripheral retina associated with impairment in peripheral vision are observed in half the cases. During the course of the disease, complications can arise, which include retinal detachment, vitreal haemorrhaging, and neovascular glaucoma leading to a poor outcome. The *RS1* gene responsible for X-linked retinoschisis was identified by positional cloning and found to encode RS1 (Sauer et al., 1997), which is secreted from photoreceptor and bipolar cells as a disulfide-linked oligomeric complex (Molday et al., 2001).

The RS1 polypeptide chain consists of a leader sequence and a discoidin domain that spans most of the protein (Sauer et al., 1997). Discoidin domains, first identified in discoidin I from *Dictyostelium discoidium* (Rosen et al., 1973; Simpson et al., 1974), have now been found in many secreted and transmembrane proteins, including blood coagulation factors, tyrosine kinase receptors, and proteins involved in neural development (Baumgartner et al., 1998; Fuentes-Prior et al., 2002; Vogel,

---

[2] A version of this chapter has been published.

Wu, WWH and Molday, RS. (2003). Defective discoidin domain structure, subunit assembly, and endoplasmic reticulum processing of retinoschisin are primary mechanisms responsible for X-linked retinoschisis. J Biol Chem *278*, 28139-28146.

1999). The function of the discoidin domain is not well understood, but it has been implicated in cell adhesion and cell signaling. The three-dimensional crystal structures of the C2 discoidin domain of blood coagulation Factors V and VIII and the b1 discoidin domain of neuropilin 1 have been determined, providing insight into the molecular interactions that contribute to its structure and function (Lee et al., 2003; Macedo-Ribeiro et al., 1999; Pratt et al., 1999).

More than 133 different missense, nonsense, insertions, deletions, and splice-site mutations associated with X-linked retinoschisis have now been catalogued (http://www.dmd.nl/rs/; Consortium, 1998). Most missense mutations are located in the discoidin domain of RS1, with over 25% involving the loss or gain of a cysteine residue. Disease-causing missense mutations are also found in regions flanking the discoidin domain as well as within the leader sequence (Gehrig et al., 1999a; Hiriyanna et al., 1999). To determine the structure-function relationships of RS1, and define molecular and cellular mechanisms responsible for X-linked retinoschisis, the effect of various disease-linked missense mutations on the expression, structural properties, intracellular localization, and secretion of RS1 was determined.

Results showed that mutations in the leader sequence prevent insertion of RS1 into the ER membrane, resulting in mislocalization of these mutant polypeptides to the cytoplasm and proteolytic degradation. Most mutations in the RS1 discoidin domain result in severe misfolding of the protein and retention in the ER. Two disease-linked cysteine mutations (C59S and C223R) outside the discoidin domain

do not significantly affect protein folding or secretion from cells. However, these

mutant proteins fail to assemble into an octameric complex. Finally, the R141H

mutant protein is also secreted, but forms multiple aberrant oligomeric structures.

3.2 Methods

3.2.1 Mutagenesis, transfections, protein preparation, and Western blotting

The QuikChange site-directed mutagenesis kit was used to introduce 12

disease-linked mutations within various regions of RS1 (L13P, C59S, E72K, G109E,

C110Y, R141C, C142W, D143V, R182C, P203L, C219R, C223R), 6 additional

disease-linked, non-cysteine mutations found in the spike regions of the RS1

discoidin domain (N104K, R141G, R141H, E146D, E146K, T185K), and 1 suspected

polymorphism (D158N). Constructs were sequenced to verify the presence of the

desired mutations and absence of random mutations. Transfections, harvesting of

the cellular and secreted fractions, SDS-PAGE, and Western blotting were

performed as described in Section 2.2.

3.2.2 Immunofluorescence microscopy

COS-1 or EBNA HEK 293 cells grown on glass cover slips were fixed with 4%

paraformaldehyde in 0.1 M phosphate buffer (pH 7.4) for 20 min. After blocking with

PBS-0.2% Triton X-100 containing 10% goat serum for 15 min, the cells were

double-labelled for 2 h with an RS1 polyclonal antibody (a gift from Dr. B.H.F.

Weber) and the GRP94 monoclonal antibody (Stressgene, Victoria, Canada) as an

ER marker, or the golgin-97 monoclonal antibody (Invitrogen-Molecular Probes) as a

Golgi marker. After rinsing in PBS-0.2% Triton X-100, the cells were labelled for 30 min with the secondary antibody tagged with Alexa 594 (RS1) or Alexa 488 (GRP94 or golgin-97) for visualization with a Zeiss Axioplan 2 microscope using epifluorescence (Zeiss, Oberkochen, Germany) and an Eclipse digital imaging system.

3.3 Results

3.3.1 Mutations within the leader sequence prevent the targeting of RS1 to the ER

To assess the effect of disease-linked mutations on the expression, folding, oligomerization, and secretion of RS1, we analyzed various missense mutations associated with X-linked retinoschisis (Fig. 3.1A). All mutants, with the exception of the L13P variant, were expressed in the cellular fraction at levels comparable with WT RS1 when analyzed under reducing conditions (Fig. 3.1B).

The subcellular localization of WT and mutant RS1 proteins was also examined by immunofluorescence microscopy. WT and disease-linked variants, with the exception of L13P, partially co-localized with the GRP94 chaperone protein to the ER of COS-1 cells (Fig. 3.2). In contrast, the L13P variant with the mutation in the leader sequence did not co-localize with GRP94, but instead showed a less abundant, more punctate type of labelling pattern. This indicates that the L13P mutant, unlike WT RS1, cannot properly target to the ER as the initial step in the secretion process. Similar results were obtained with immunofluorescence microscopy of transfected EBNA HEK 293 cells. In addition, Wang et al. (2002)
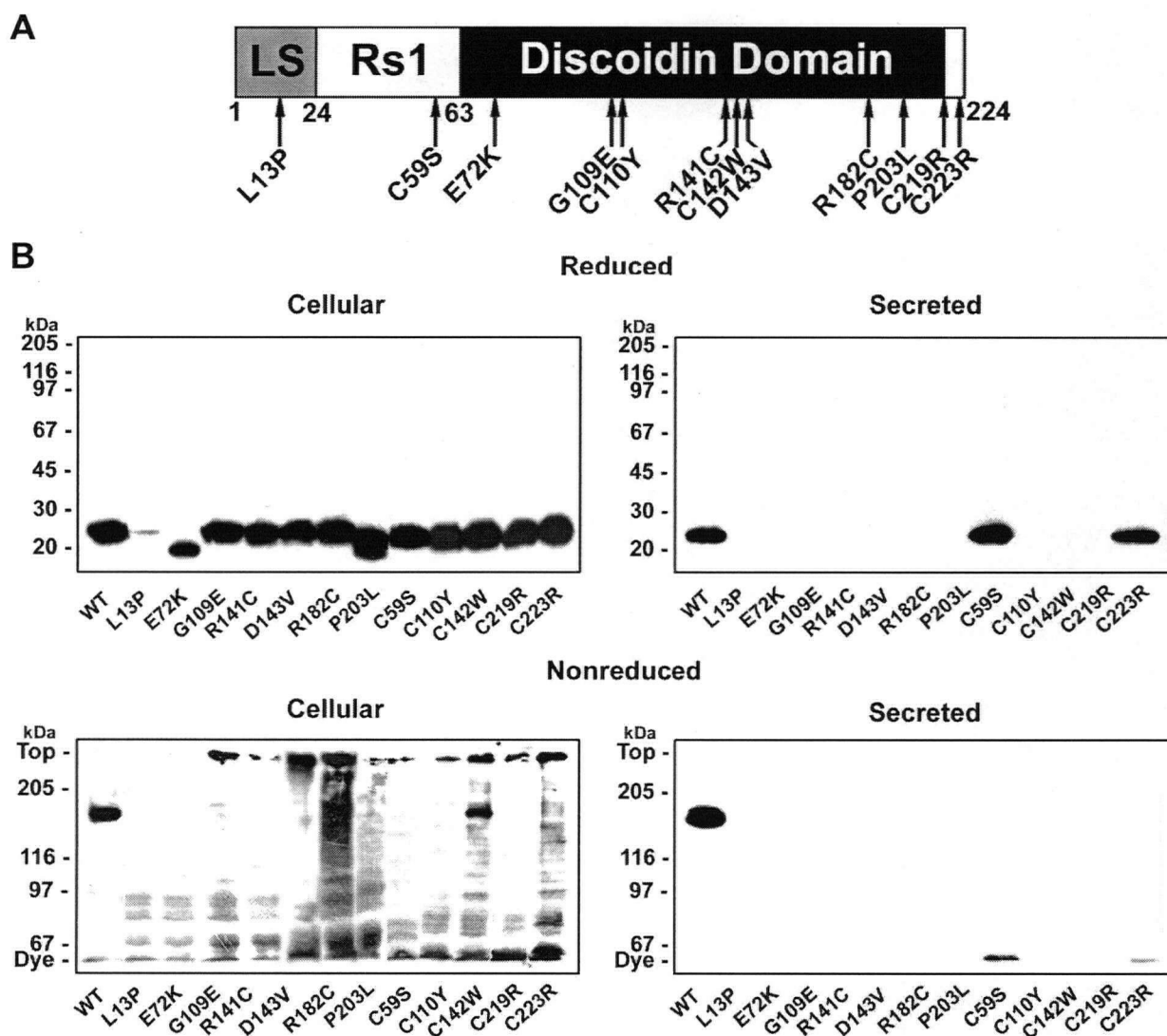
Figure 3.1. Expression and analysis of WT RS1 and disease-linked mutants.
(A) Domain schematic of RS1 showing the relative locations of X-linked retinoschisis missense mutations examined in this study. **(B)** Cellular and secreted fractions of RS1 disease mutants. Cells expressing WT or disease-linked mutant RS1 were divided into the cellular (cells) and secreted (media) fractions. The expressed proteins were run on a 10% or 6.5% SDS-polyacrylamide gel under reducing or nonreducing conditions, respectively, and analyzed on Western blots labelled with the RS1 monoclonal antibody.
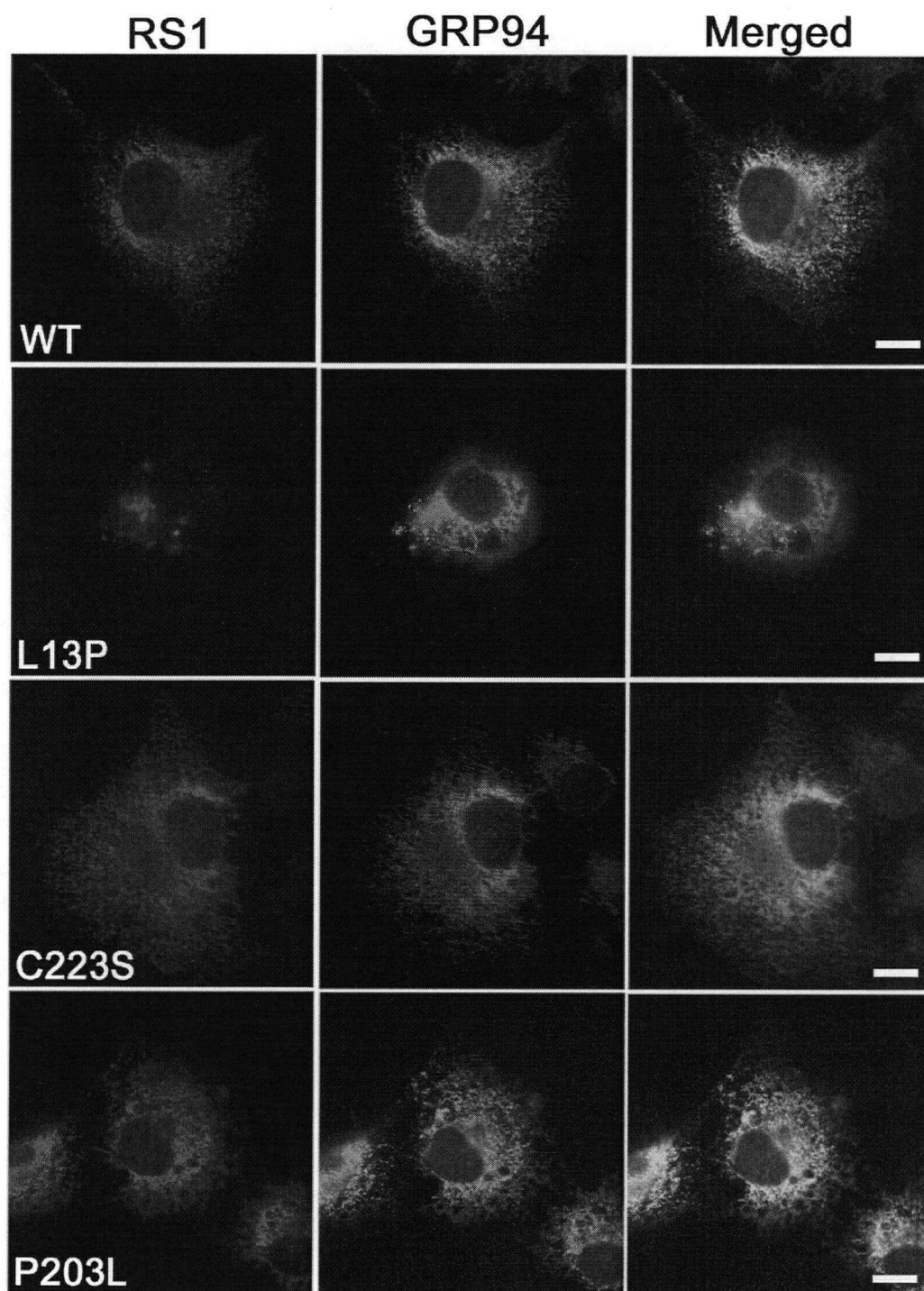
Figure 3.2. Immunofluorescence of WT and mutant RS1 expressed in COS-1 cells doubled labelled with an ER Marker. Transfected cells were fixed and double labelled with the RS1 polyclonal antibody (*red*) and the GRP94 (ER marker) monoclonal antibody (*green*) for visualization by immunofluorescence microscopy. The merged images of labelled cells are also shown. Scale bar is 12μm.

have observed broadly similar labelling patterns for a different set of RS1 disease-linked mutants.

Besides having lower levels of expression, there were also fewer cells expressing detectable amounts of the L13P mutant as viewed by immunofluorescence microscopy. Only 10% of transfected cells expressed the L13P mutant compared with over 30% for WT and the other mutants.

3.3.2 Mutations within the discoidin domain cause protein misfolding and retention in the ER

All discoidin domain mutants expressed at levels comparable to WT when analyzed under disulfide-reducing conditions (Fig. 3.1B). However, the E72K and P203L mutants migrated more rapidly than WT protein and most other mutants in the cellular fraction, possibly due to limited proteolysis. Under nonreducing conditions, all discoidin domain mutants in the cellular fraction were retained at the top of the gel or migrated anomalously as protein aggregates, indicative of misfolded, aggregated protein. These mutant proteins, unlike WT, were not secreted from the cells. Instead, they were retained in the ER, presumably by the ER quality control system. As viewed by immunofluorescence microscopy, P203L, a representative discoidin domain mutant, colocalizes with an ER marker (Fig. 3.2), but does not colocalize with a Golgi marker (Fig. 3.3).

3.3.3 Mutations in C59 and C223 disrupt homo-octamerization

Of the disease-linked mutants examined in Figure 3.1B, only the C59S and C223R mutants were detected in the secreted fraction. The ability of these mutants
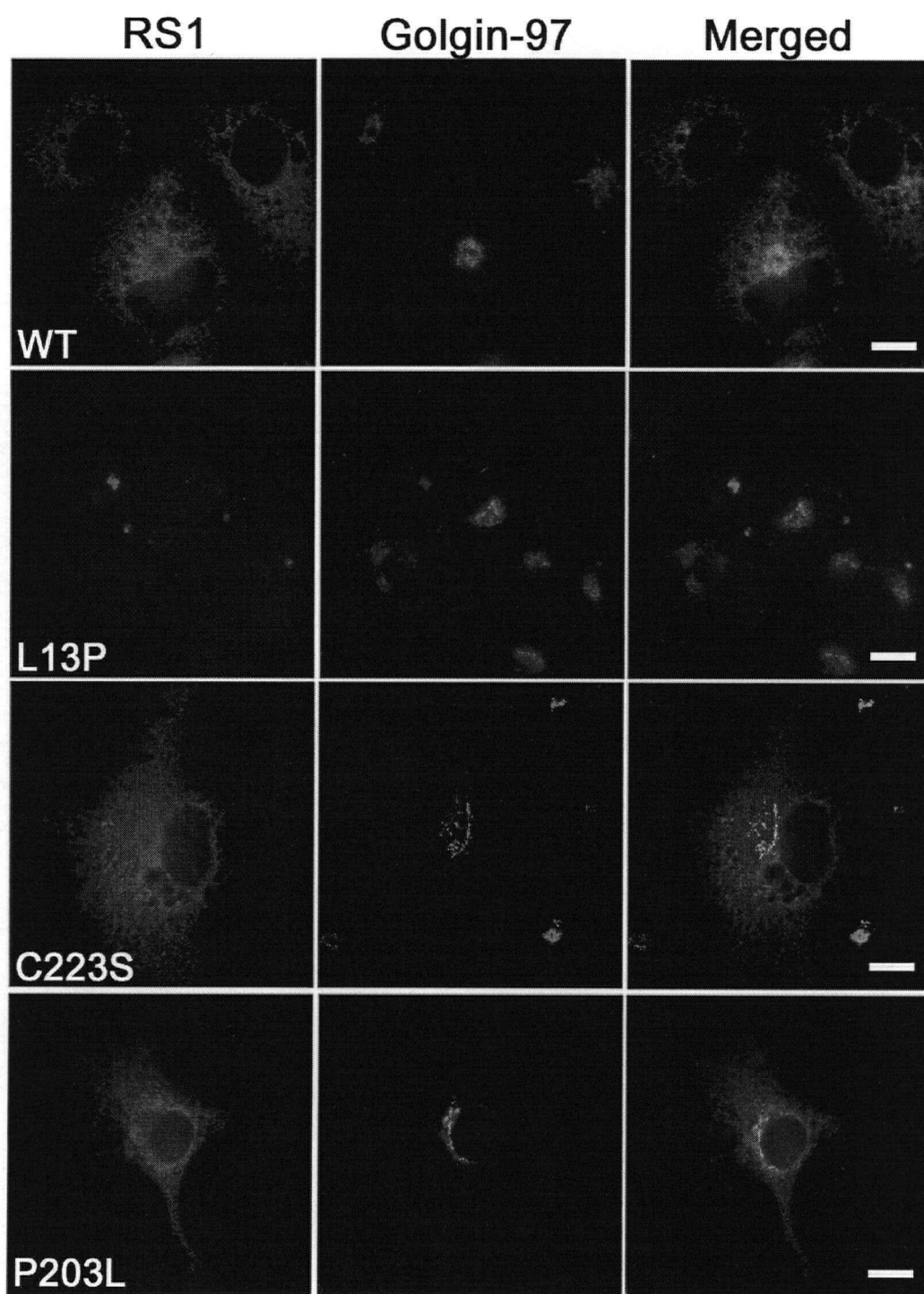
Figure 3.3. Immunofluorescence of WT and mutant RS1 expressed in COS-1 cells doubled labelled with a Golgi marker. Double labelling was performed with the RS1 polyclonal antibody (*red*) and the golgin-97 (Golgi marker) monoclonal antibody (*green*). The merged images of labelled cells are also shown. Scale bar is 12μm.

to traverse from the ER to the Golgi for secretion is similar to that of WT as viewed by immunofluorescence microscopy. Figures 3.2 and 3.3 show the partial co-localization of WT and C223S with GRP94, an ER marker, or with golgin-97, a Golgi marker that labels all of the cis, medial, and trans Golgi compartments. A similar pattern of ER and Golgi labelling was observed for the disease mutants C59S and C223R (not shown). This is consistent with the view that these proteins translocate from the ER to the Golgi as part of the secretion process. In contrast, the L13P, P203L, and other nonsecreted mutants did not colocalize with the Golgi marker.

The major difference between WT RS1 and these two cysteine disease variants, C59S and C223R, is their migration on SDS gels under nonreducing conditions. Whereas WT RS1 migrates as a 180-kDa protein complex under these conditions, the secreted C59S and C223R mutant proteins migrate as lower molecular weight species. This is consistent with the role of C223 and C59 in disulfide-linked octamerization (see Chapter 2).

3.3.4 R141H in spike 3 causes aggregation

Additional non-cysteine, disease-linked mutants in the spike region of the RS1 discoidin domain were generated to determine their ability to be secreted and form an octamer (Fig. 3.4). As shown in Figure 3.5, all these spike mutants expressed in the cellular fraction at levels similar to WT under reducing conditions. However, only the R141H mutant protein was secreted at levels comparable to WT as analyzed under reducing conditions. In contrast to their similar secretion levels under reducing conditions, the R141H mutant differed from WT and migrated as a broad band under nonreducing conditions.
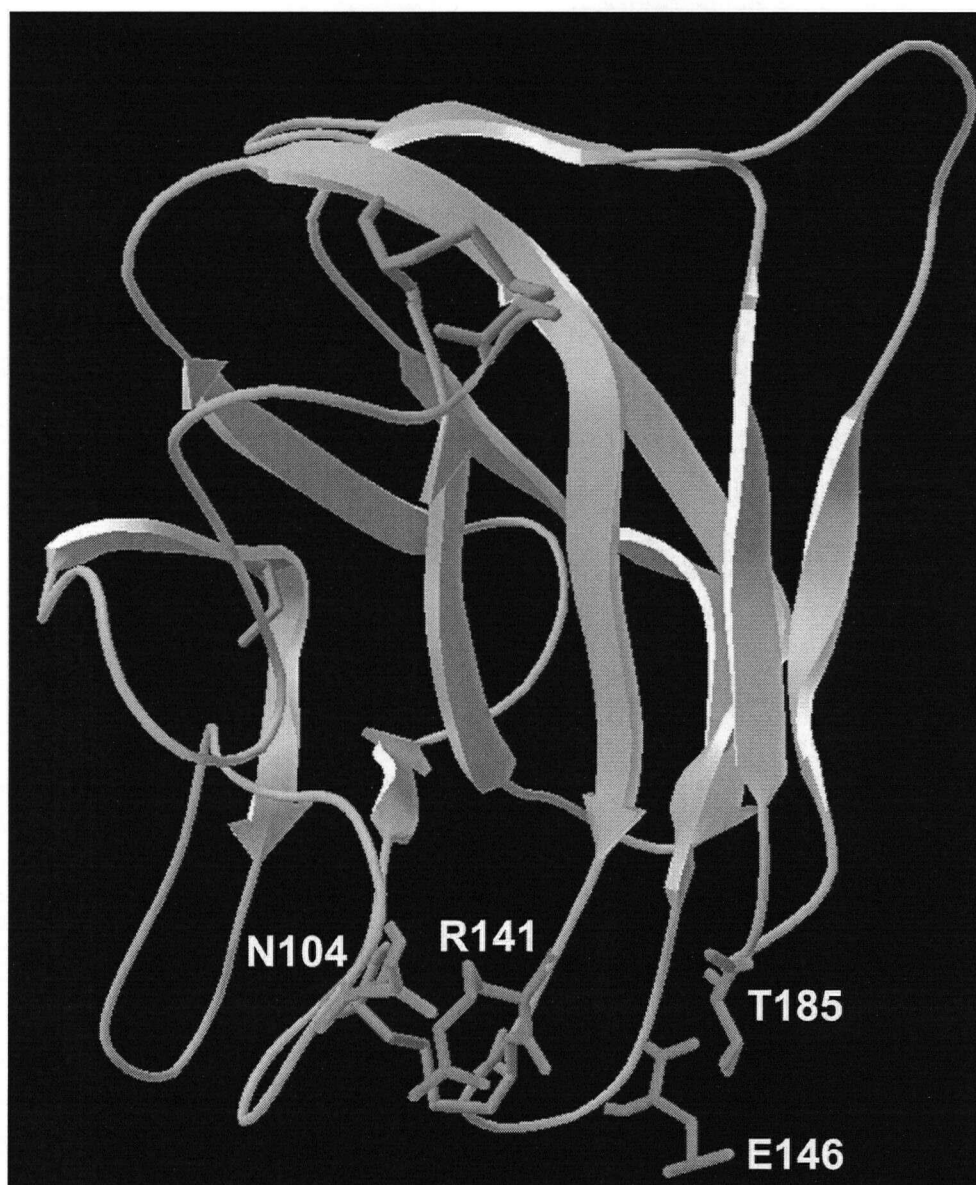
Figure 3.4. Locations of mutated discoidin domain spike residues. Ribbon diagram of the RS1 discoidin domain molecular model, showing the location of the spike residues (*green*) mutated.
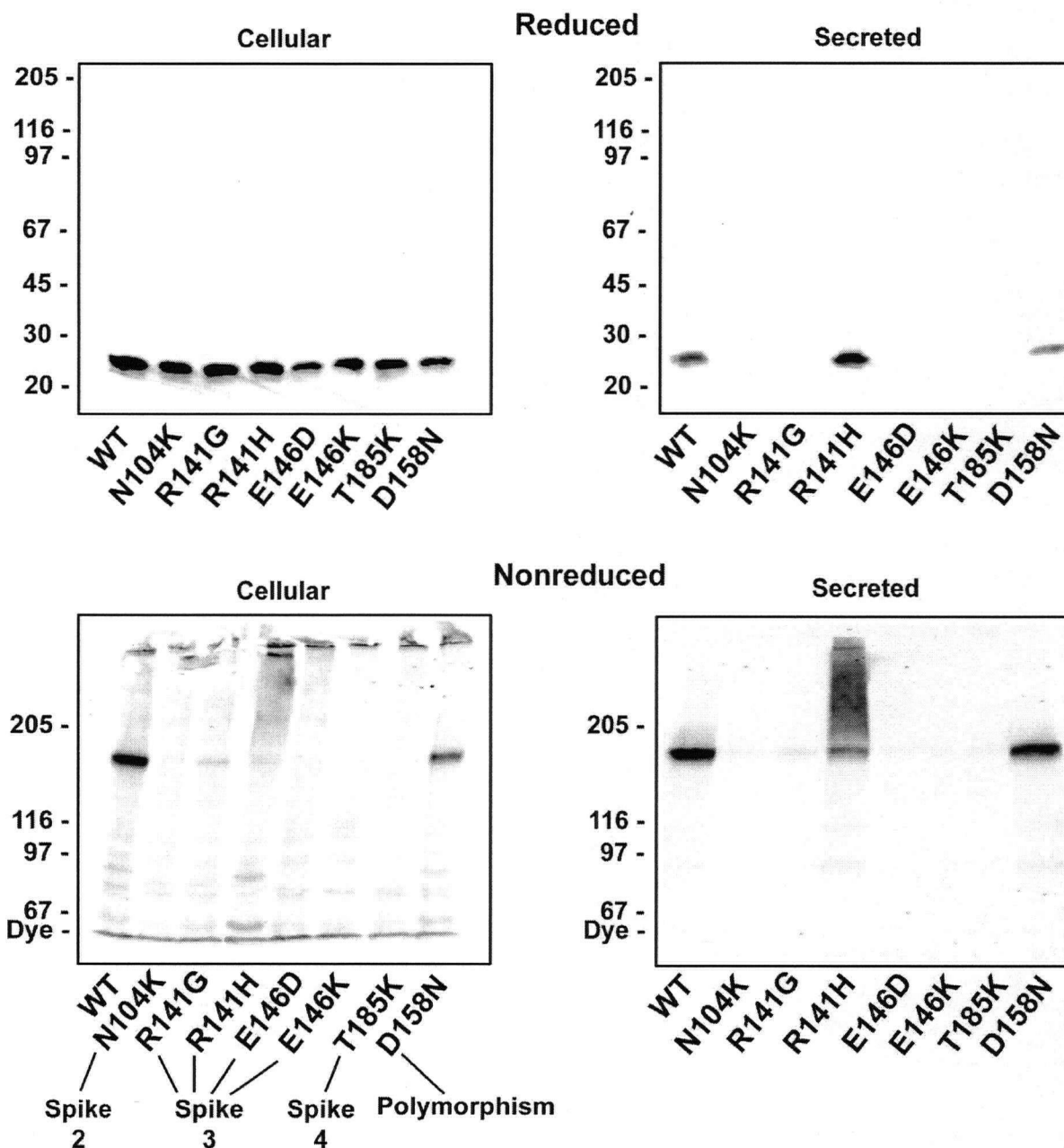
Figure 3.5. Expression and analysis of disease-linked spike mutants and RS1 polymorphism. Cells expressing WT or mutant RS1 were divided into the cellular (cells) and secreted (secreted) fractions. The expressed proteins were run on a 10% or 6.5% SDS-polyacrylamide gel under reducing or nonreducing conditions, respectively, and analyzed on Western blots labelled with the RS1 monoclonal antibody.

3.3.5 D158N polymorphism shows decreased expression and secretion, but normal octamerization

To determine the effect of a polymorphism in the *RS1* gene on RS1 expression, oligomeric assembly, and secretion, a suspected polymorphism (D158N) was created. This mutation had previously been identified from a screen of the *RS1* sequence in more than one hundred healthy individuals, so individuals with this mutation do not possess the X-linked retinoschisis phenotype (Consortium, 1998). This mutant protein behaved similarly to WT, as the nonreducing gels from both the cellular and secreted fractions show that D158N was able to properly form the octamer (Fig. 3.5). The only difference was its apparently lower levels of expression and secretion compared to WT.

3.4 Discussion

Although mutations in *RS1* play a crucial role in the pathogenesis of X-linked retinoschisis, little is known about the structural and molecular determinants in RS1 responsible for the pathogenesis of X-linked retinoschisis. To address this issue, WT RS1 and disease-linked variants were compared with respect to their expression, cellular localization, molecular properties, and secretion. A high percentage of disease-linked missense mutations involving cysteines also led us to examine the role of removing or creating cysteines linked to disease in RS1. These studies show that ineffective insertion of the nascent polypeptide chain into the ER membrane, discoidin domain misfolding, defective disulfide-linked subunit assembly,

and aggregation into higher-order oligomers of RS1 are the primary molecular mechanisms underlying X-linked retinoschisis that is associated with missense mutations in the *RS1* gene.

The ten cysteines found in human RS1 are conserved between mammalian RS1 orthologues and RS1 in the evolutionarily distant pufferfish, *Fugu rubripes* (Brunner et al., 1999; Gehrig et al., 1999b; Sauer et al., 1997), although the pufferfish has additional cysteines near the N-terminus. This conservation, together with the importance of the C63-C219 and C110-C142 intramolecular disulfide bonds and the C59-C223 intermolecular disulfide bond is further highlighted by the finding that mutations in five of these six cysteines within and just flanking the discoidin domain (C59S, C110Y, C142W, C219R, C223R) result in X-linked retinoschisis (Consortium, 1998; Hiriyanna et al., 1999). As indicated in this study, mutations in these cysteines either cause protein misfolding, aggregation, and retention in the ER, or prevent disulfide-linked octamerization. It is likely that a missense mutation in the cysteine marking the beginning of the discoidin domain, C63, would also cause X-linked retinoschisis. Indeed, missense mutations in the analogous residue of Factor VIII are associated with hemophilia A (Kemball-Cook et al., 1998).

From the studies in this chapter, missense mutations associated with X-linked retinoschisis can be divided into four classes based on their location in the RS1 sequence and effect on RS1 expression, structure, and cellular localization. One class comprises mutations in the hydrophobic leader sequence (Hiriyanna et al., 1999). As shown here, the L13P mutation in the leader sequence results in a marked decrease in protein expression and irregular cellular localization. The

decrease in protein expression observed by SDS gel electrophoresis and Western blotting appears to be due in part to the lower number of cells expressing detectable levels of the L13P mutant and in part to the lower protein levels in the individual cells as visualized by immunofluorescence microscopy. A similar localization pattern has been reported for the L12H mutation, another disease-linked mutation located in the RS1 leader sequence (Wang et al., 2002). Their studies further showed that the mutated leader peptide is not cleaved by signal peptidase, and the mutant protein is readily degraded by proteasomes. Together, these studies suggest that substitution of hydrophobic residues in the leader sequence with a proline or with hydrophilic/charged residues prevents the leader peptide from adopting an α-helical secondary structure required for insertion into the ER membrane. Instead, the newly synthesized polypeptide chain remains as a misfolded protein in the reducing environment of the cytoplasm, where it is rapidly degraded by proteasomes.

The second and largest class of disease-linked missense mutations consists of mutations found in the discoidin domain. Insight into how these discoidin domain mutations cause protein misfolding, leading to aggregation and defective secretion, can be deduced from molecular modeling. Like the discoidin domain of Factors V and VIII, the RS1 discoidin domain model consists of a β-barrel core formed by 8 antiparallel strands (Fig. 2.7). Noncovalent interactions within the core structure, together with the C63-C219 and C110-C142 disulfide bonds, play essential roles in generating and maintaining this structure. Mutations in core, solvent inaccessible residues prevent proper protein packing, resulting in protein misfolding and aggregation. This, in turn, results in the mutant protein being retained in the ER as

visualized by immunofluorescence. To further confirm whether these mutants are truly misfolded or whether they have just undergone some sort of conformational change, one could perform experiments to determine changes in the secondary structure of the protein. These may include circular dichroism spectroscopy or nuclear magnetic resonance analysis.

One subset of these discoidin domain mutations directly involves the loss of cysteine residues. As mentioned above, C110Y, C142W, and C219R involve the replacement of key cysteines required for intramolecular disulfide bonding and proper folding of the discoidin domain. The misfolded protein, together with the formation of abnormal disulfide bonds in the oxidizing environment of the ER lumen, results in protein aggregation and defective secretion. Introduction of a cysteine, such as for the R141C and R182C mutations, would similarly create such misfolded proteins.

Another subset of discoidin domain disease mutants involves missense mutations in highly conserved, solvent-inaccessible core residues not involved in disulfide bonds. For example, P203 is a highly conserved residue among discoidin domain family members. It is also a highly buried residue, interrupting the $\beta 7$ strand, and thus contributing to the overall fold and stability of the discoidin domain (Fig. 2.7). Substitution with a leucine residue (P203L) will thus cause a marked change in the secondary structure of the protein, which in turn affects protein packing. Other disease-linked mutations in core residues likely cause disruption in key noncovalent interactions crucial for the formation or stability of the RS1 discoidin domain. For instance, the G109E mutation involves substituting a charged residue for a highly

buried glycine. The negatively-charged glutamate introduced may interfere with normal interactions that stabilize the core of the discoidin domain.

It is a curiosity as to why there are so many mutations affecting the stability of the discoidin domain and few mutations affecting ligand-binding interactions (Fuentes-Prior et al., 2002). One explanation is that there may be redundancy built into the discoidin domain surface-exposed spike regions, which are responsible for ligand binding (Fuentes-Prior et al., 2002; Pratt et al., 1999). This redundancy means that several spike residues may participate in the binding of a ligand. Therefore, if a mutation occurred on one of the spike residues, the disrupted binding would be compensated for by another residue on a different spike or by a different residue on the same spike. This may explain why most disease-linked mutations in *RS1*, such as the discoidin domain mutations mentioned above, and in the coagulation factors do not appear to affect binding. Instead, they result in destabilization of the discoidin domain structure, which appears to be highly susceptible to amino acid substitutions.

A third class of missense mutations associated with X-linked retinoschisis consists of the C59S and C223R disease-linked mutations in the regions flanking the discoidin domain. A significant fraction of these mutant proteins can pass through the Golgi and is secreted into the extracellular medium, indicating that these cysteine substitutions have only a limited effect on protein folding. However, as discussed above, the C59S and C223R mutants, unlike WT RS1, cannot assemble into disulfide-linked octamers. In this instance, failure to form disulfide-linked octamers, and not defective secretion as noted for the first two classes of mutations,

is responsible for the inability of RS1 to function as a cell adhesion protein, thereby resulting in the X-linked retinoschisis phenotype.

A fourth class of missense mutations includes the mutation in the third spike of the RS1 discoidin domain, R141H. This mutant protein appears to be secreted properly, likely due to proper protein folding of its discoidin domain. However, unlike WT, the secreted R141H mutant forms higher-order oligomers or aggregates when analyzed under nonreducing conditions. The effect of these higher-order oligomers on RS1 function is unclear.

Park et al. have examined a family of patients with the R141H mutation (Park et al., 2000). In that study, they examined two unaffected carriers, a mother and a daughter, as well as the mother's two affected sons, who had the X-linked retinoschisis phenotype. With respect to the carriers, only the mother had a slightly reduced, but still within normal range, b-wave, and no retinoschisis. The daughter was normal. This lack of a disease phenotype in the carriers indicates that this mutant does not act through a dominant negative mechanism. Interestingly, when an eight-amino acid synthetic peptide in spike 3 of the lactadherin discoidin domain was dissolved in DMSO, followed by addition of water, that peptide formed a gel-like aggregate (Haggqvist et al., 1999). Since R141 in RS1 is also located at spike 3, the introduction of a histidine may disrupt the C110-C142 disulfide bond in RS1 and expose residues in spike 3 resulting in aberrant oligomerization.

As expected, this study also showed that a suspected polymorphism D158N behaves similarly to WT RS1. Running nonreducing SDS-PAGE of both the secreted and cellular fractions would be a useful tool to predict if a given mutation in

RS1 would result in retinoschisis, as all other disease mutants examined appeared to be different from WT and the D158N polymorphism when analyzed by nonreducing gels.

In summary, our results indicate that the cysteines in RS1 play a key role in RS1 structure and function. Removing key cysteines within the discoidin domain (C63, C110, C142, and C219) or creating extra cysteines result in misfolding of the discoidin domain and retention of RS1 in the ER (Fig. 3.6A). We have also identified four molecular mechanisms responsible for X-linked retinoschisis (Fig. 3.6B). Disease-linked mutations in the leader sequence of RS1 prevent proper insertion of the polypeptide chain into the ER membrane, resulting in cellular mislocalization and defective secretion; mutations in the discoidin domain of RS1 cause protein misfolding and retention in the ER; mutations in C59 or C223 result in defective disulfide-linked octameric assembly, but do not significantly affect secretion; and the R141H mutation in spike 3 of the discoidin domain causes aberrant oligomeric assembly. In each case, there is a loss in the ability of RS1 to function as an extracellular retinal adhesion protein required to maintain the cellular architecture of the retina (Weber et al., 2002).

97
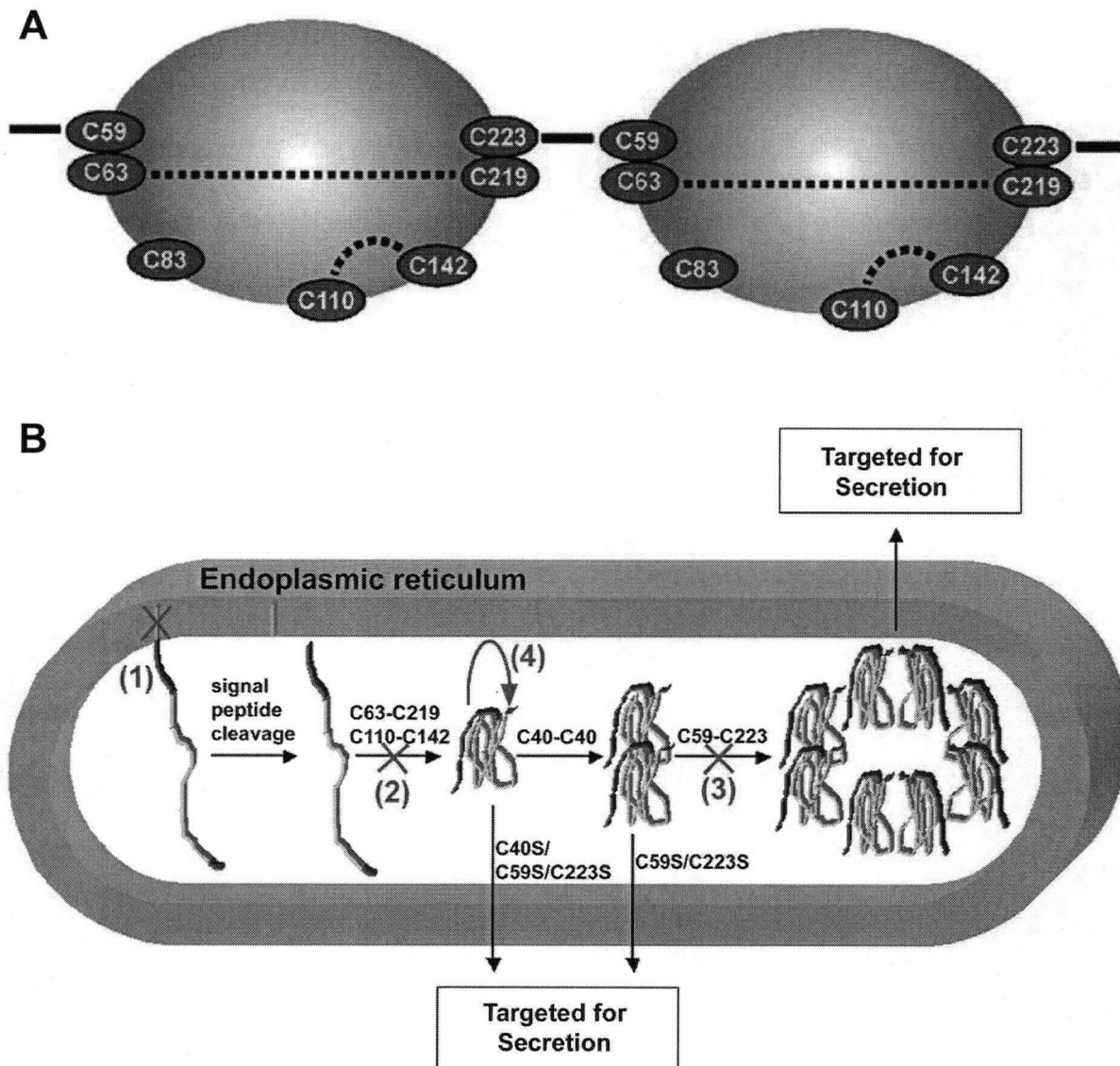
Figure 3.6. Molecular mechanisms responsible for X-linked retinoschisis.
(A) Key cysteines in RS1. Mutations in any of C59, C63, C110, C142, C219, or
C223 are likely to result in the X-linked retinoschisis phenotype. **(B)** Molecular
mechanisms resulting in defective RS1. The X-linked retinoschisis phenotype is due
to improper insertion of the RS1 leader sequence into the ER membrane, improper
folding of the discoidin domain, defective disulfide-linked octamerization, or
generation of aberrant higher-order oligomers.

CHAPTER 4: RS1 IS A LECTIN THAT BINDS

PREFERENTIALLY TO GALACTOSE

4.1 Introduction

RS1 is a retina-specific protein expressed and secreted from photoreceptor cells of the outer retina and bipolar cells of the inner retina as a disulfide-linked homo-oligomer (Grayson et al., 2000; Molday et al., 2001; Reid et al., 1999). The secreted protein associates with the surface of rod and cone photoreceptors at the level of the inner segment, the surface of bipolar cells within the inner nuclear layer, and the outer and inner plexiform layers of the retinal synapses (Molday et al., 2001; Weber et al., 2002). Biochemical studies further demonstrate that RS1 associates tightly with the membrane fraction of retinal cell homogenates (Molday et al., 2001).

The role of RS1 in retinal cell adhesion is supported by studies on WT and *RS1* knockout mice. Mice hemizygous for the disrupted *RS1* gene show general retinal tissue disorganization with irregular displacement of cells in various retinal layers, splitting of the inner retina with gaps between bipolar cells, and disruption of the synapses between the photoreceptors and bipolar cells (Weber et al., 2002). Progressive rod and cone photoreceptor degeneration and a preferential loss in the electroretinogram b-wave are additional characteristic features of these knockout mice. *RS1* mutations in humans can also lead to X-linked retinoschisis, a form of juvenile macular degeneration (Consortium, 1998; Sauer et al., 1997).

Each RS1 subunit consists as its major component a discoidin domain implicated in cell-cell adhesion (Sauer et al., 1997). Discoidin domains are present in many membrane and extracellular proteins (Baumgartner et al., 1998; Fuentes-

Prior et al., 2002; Vogel, 1999). The function of the discoidin domain is not well understood, but it has been implicated in cell adhesion and cell signaling through protein-protein, protein-carbohydrate, or protein-lipid interactions. Some proteins that contain discoidin domains are Factors V and VIII, which are involved in blood coagulation; neuropilins 1 and 2, which mediate nervous system regeneration and degeneration; and discoidin I, involved in cellular adhesion during slime mold differentiation and development (Baumgartner et al., 1998; Fuentes-Prior et al., 2002; Lee et al., 2003; Vogel, 1999).

The crystal structures of several discoidin family proteins have been determined: the C2 discoidin domains of Factors V and VIII, and the b1 discoidin domain of neuropilin 1 (Lee et al., 2003; Macedo-Ribeiro et al., 1999; Pratt et al., 1999). These domains consist of eight antiparallel β-strands arranged in a barrel-like structure with several loops, or "spikes," which project from one end of the core structure. In the case of Factors V and VIII, the spikes are involved in the attachment of these proteins to the phosphatidylserine-rich surface of platelets as a key step in the blood coagulation process (Fuentes-Prior et al., 2002). These spikes also play a crucial role in ligand binding for other discoidin family members (Abdulhussein et al., 2004; Leitinger, 2003; Shimizu et al., 2000).

To begin to elucidate how RS1 functions as an adhesion protein, the ability of RS1 to bind to ligands that bind to discoidin domain family proteins was tested. It is well established that the coagulation Factors V and VIII bind phospholipids, while discoidin and neuropilin bind carbohydrates. Phospholipid binding studies and carbohydrate affinity chromatography were used to test these interactions. No

binding of RS1 to phospholipids was observed. However, results showed that the octameric form of RS1, and not disulfide-disrupted dissociated dimers or monomers, bind with high affinity to D-galactose. Finally, IPTG, an isopropylthiol analogue of galactose, elutes RS1 from a D-galactose column, and extracts RS1 from the surfaces of retinal membranes.

4.2 Methods

4.2.1 Preparation of RS1 protein for lipid and carbohydrate binding studies

Human WT RS1, the C59S/C223S dimeric RS1 mutant, and the C40S/C59S/C223S monomeric RS1 mutant were produced by transfection as described in Section 2.2.2. The media containing 10% fetal calf serum was replaced the following day after transfection with fresh media. One week later, protein was harvested. The secreted RS1 protein was concentrated by precipitation with 40% ammonium sulfate at 4°C, washed with a 40% saturated ammonium sulfate solution, and then resuspended in 1/40th the volume of the cell culture media. The protein was incubated with 10mM NEM for 10 min, and then dialyzed using dialysis tubing with a 100-kDa molecular weight cutoff (Spectrum Laboratories, Los Angeles, CA) overnight against 2mM Tris, pH 7.4. The next day, the protein solution was centrifuged at 100,000 x g for 10 min. The resulting supernatant was supplemented with NaCl and Tris to a final concentration of 20mM Tris, pH 7.4 and 150mM NaCl, and retained for binding studies. RS1 secreted by Weri-Rb1 cells was similarly isolated by ammonium sulfate precipitation and dialysis.

Frozen bovine retinas were thawed and washed twice in low salt containing 10 mM Tris, pH 7.4, by centrifugation at 14,000 x g in an SS-34 Sorvall rotor. The retinal cells were then disrupted as follows: the pellet of cells was resuspended in lysis buffer consisting of 10 mM Tris, pH 7.4, 10 mM NEM, and Complete Protease Inhibitor. The cells were incubated for 10 min on ice, followed by several passages through a 26-gauge needle attached to a syringe. To obtain the membrane fraction, the lysed cells were applied to the top of a solution of 60% sucrose containing 10mM Tris, pH 7.4, and centrifuged for 30 min at 38,000 x g in a Beckman TLS 55 rotor. The membranes were collected from the layer on top of the 60% sucrose, and washed with 10 mM Tris, pH 7.4, by centrifugation at 100,000 x g for 10 min in a Beckman TLA 100.4 rotor. The retinal membranes were then solubilized for 20 min with buffer containing 18 mM CHAPS, 20 mM Tris, pH 7.4, 150 mM NaCl, 10 mM NEM, and Complete Protease Inhibitor. To remove any unsolubilized material, the sample was centrifuged at 100,000 x g for 10 min. The supernatant was then dialyzed overnight against 2mM Tris, pH 7.4, using dialysis tubing with a 100 kDa molecular weight cutoff, and centrifuged again the next day at 100,000 x g for 10 min. The resulting supernatant containing the retinal RS1 protein was supplemented with NaCl and Tris to a final concentration of 20mM Tris, pH 7.4 and 150mM NaCl, and retained for binding studies.

4.2.2 SDS-PAGE, Coomassie and silver staining, and Western blotting

SDS-PAGE and Western blotting were performed as described in Section 2.2. Blots for the Factor Va samples were labelled with the AHV5146 monoclonal antibody, a kind gift from Dr. E. Pryzdial (UBC), against the heavy chain of

coagulation Factor Va. SDS gels that were not transferred for blotting were stained with Coomassie blue for total protein detection. The Coomassie stain contained 0.025% R250 Coomassie dye, 25% isopropanol, and 10% acetic acid. Gels were destained with 10% acetic acid. Silver staining was performed by fixing the gel in 50% methanol and 0.038% formaldehyde for 1 h. The fixed gel was then washed with several changes of nanopure water, and subsequently immersed in staining solution (0.24% silver nitrate, 0.076% sodium hydroxide, 1.4% ammonium hydroxide) for 15 min. After another 5 min wash with water, the gel was developed with developing solution (0.005% citric acid, 0.019% formaldehyde) for 5-10 min. The reaction was stopped by several washes with stop buffer containing 45% methanol and 10% acetic acid.

4.2.3 Generation of phospholipid vesicles

Large unilamellar phospholipid vesicles were prepared as described by Hope et al. (Hope et al., 1985). Synthetic phospholipids (DOPC, DOPE, or DOPS [Avanti Polar Lipids, Alabaster, AL]) or phospholipids extracted from retina were dissolved in a 1:1 ratio of chloroform:methanol. Lipid mixtures consisting of a 3:1 ratio of DOPC:DOPS, a 1:1:1 ratio of DOPC:DOPS:DOPE, or phospholipids extracted from retina were dried to a homogeneous film under a stream of nitrogen gas. The resulting mixture was resuspended in 20mM Tris, pH 7.4 and 150mM NaCl. These multilamellar vesicles were then freeze-thawed five times with liquid nitrogen and at room temperature to promote lipid hydration and equal transmembrane solute distribution. The multilamellar vesicles were then extruded ten times through a 1000nm pore polycarbonate membrane (Whatman Nuclepore, Middlesex, UK)

employing an extrusion device (Lipex Biomembranes, Vancouver, Canada) to produce large unilamellar vesicles.

For extraction of total lipids, retinal membranes were prepared as described above in Section 4.2.1. Total lipids were extracted from retinal membranes according to the method of Bligh and Dyer (Bligh and Dyer, 1959). Briefly, chloroform:methanol in a 1:2 ratio was added to the membranes, and the mixture was then vortexed. After adding a 1:1 ratio of chloroform:water, the solution was vortexed again and centrifuged at 1000 x g for 10 min. The bottom organic phase, which contained the lipids, was recovered and used to make vesicles.

4.2.4 Phospholipid vesicle binding studies

Binding of phospholipid vesicles to Factor Va or RS1 was performed in TBS (20mM Tris, pH 7.4, and 150mM NaCl) with 2mM calcium chloride for 10 min at 25°C. Vesicles were prepared according to Section 4.2.3. Purified Factor Va was obtained from Haematologic Technologies (Essex Junction, VT). RS1 protein was obtained from bovine retina or from Weri-Rb1 retinoblastoma cells as described above in Section 4.2.1. After the 10-min incubation to allow for binding of protein to vesicles, the mixture was centrifuged at 10,000 x g for 10 min to pellet the vesicles and any bound protein. The supernatant containing the unbound protein was saved for analysis on an SDS gel. The vesicles were then washed with TBS containing 2mM calcium chloride to remove any protein bound non-specifically to them, and centrifuged again at 10,000 x g for 10 min. The wash buffer was removed, and the resulting vesicles, which constituted the bound protein fraction, were resuspended in 4% SDS.

4.2.5 Carbohydrate affinity chromatography

RS1 or Factor Va was incubated with agarose beads conjugated to various carbohydrates for 1 h at 4°C in TBS. These agarose-carbohydrate conjugates were galactose-agarose (Pierce, Rockford, IL), and other agarose carbohydrate conjugates (Sigma): lactose-agarose, N-acetylglucosamine-agarose, N-acetylgalactosamine-agarose, heparin-agarose, or mannose-agarose. 6% beaded agarose (Amersham, Buckinghamshire, UK) was used as a control. After incubation, the unbound fraction was removed for analysis and the beads were washed with TBS. Elution of protein to obtain the bound fraction was performed with 4% SDS in TBS, except in studies using elution with other compounds. These other eluting compounds (Sigma) were isopropyl β-D-1-thiogalactopyranoside (IPTG), galactose, and lactose.

4.2.6 Extraction of RS1 from membranes

Bovine retinal membranes or membranes obtained from HEK 293 cells transfected with RS1 were prepared on a 60% sucrose gradient as described above. The membranes were then incubated with TBS, or various compounds dissolved in TBS, and shaken at 25°C for 10 min. The membranes were then centrifuged at 100,000 x g for 10 min, and the extracted protein in the supernatant was removed and saved for analysis. This extraction procedure was repeated two more times, with the resultant protein supernatant being pooled at the end. The pellet, or membrane fraction, was solubilized in 4% SDS to determine the amount of unextracted protein. The pooled supernatant protein was centrifuged one more time

at 100,000 x g for 10 min to ensure any insoluble membranes were removed, and the supernatant was saved for analysis on an SDS gel.

4.3 Results

4.3.1 Coagulation Factor Va, but not RS1, binds phospholipid vesicles

To assess the ability of RS1 to bind phospholipids, large unilamellar vesicles were incubated with RS1. The prebound, unbound, and bound protein samples were saved for analysis by SDS-PAGE. Discoidin family member coagulation Factor V was used as a positive control, since it binds strongly to negatively-charged phospholipids such as phosphatidylserine (Ortel et al., 1992). The activated form of Factor V, called Factor Va, was used in these studies.

As shown in Figure 4.1, Factor Va binds strongly to phospholipid vesicles containing a 3:1 ratio of DOPC:DOPS. The bound fraction contains an abundant amount of Factor Va, whereas the unbound fraction had a relatively small amount. In contrast, essentially all of the RS1 was present in the unbound fraction, indicating that RS1 does not bind strongly to these vesicles. Similar results were obtained using phospholipid vesicles that contained a 1:1:1 ratio of DOPC:DOPS:DOPE, or from phospholipid vesicles generated from extracting total lipid from retinal membranes.
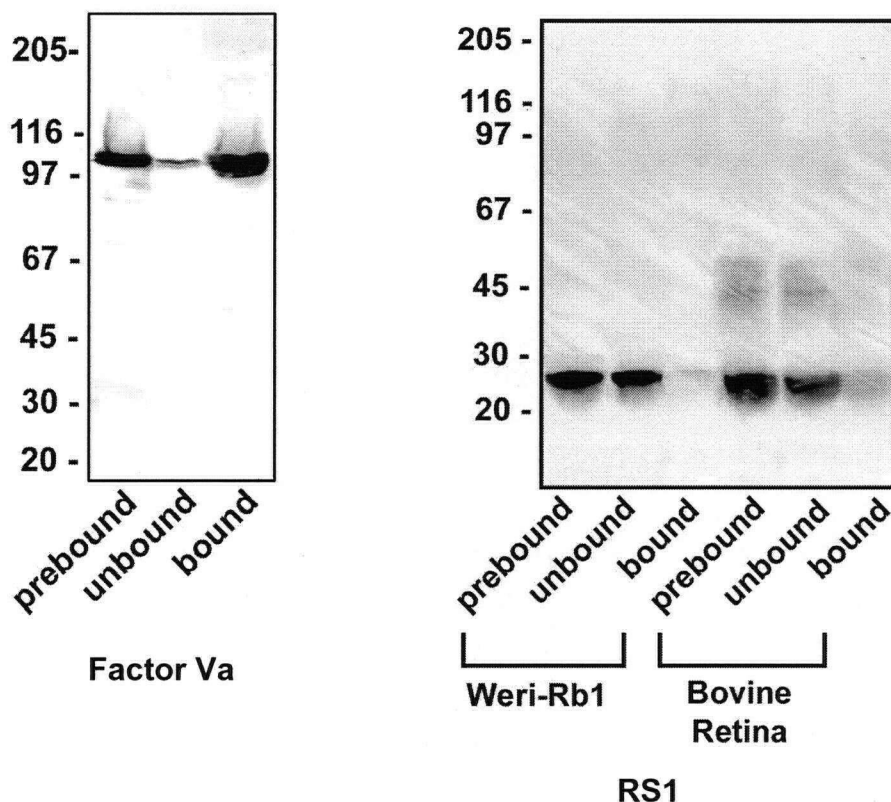
Figure 4.1. Binding of Factor Va and RS1 to phospholipid vesicles. Factor Va or RS1 was incubated with large unilamellar vesicles composed of a 3:1 ratio of DOPC:DOPS. After incubation, vesicles were centrifuged at 10,000 x g for 10 min. The supernatant containing unbound protein was saved for analysis. The vesicles were then washed, centrifuged again, and the pellet resuspended in 4% SDS for analysis of bound Factor Va or RS1 by Western blotting. Samples were run on a 10% SDS-polyacrylamide gel under reducing conditions, and analyzed on Western blots. The RS1 blot was labelled with the RS1 monoclonal antibody and the Factor Va blot was labelled with a monoclonal antibody against the heavy chain of Factor Va. Similar results were obtained using phospholipid vesicles containing a 1:1:1 ratio of DOPC:DOPS:DOPE, or from phospholipid vesicles generated from extraction of total lipid from retinal membranes.

4.3.2 RS1 binds with high affinity to D-galactose

The ability of RS1 to bind carbohydrates was examined with carbohydrate affinity chromatography by incubating RS1 with various carbohydrates coupled to agarose. As shown in Figures 4.2-4.4, RS1 from retinoblastoma cells and retinal membranes bound to galactose-agarose with high affinity. Almost no RS1 protein is in the unbound fraction when incubated with galactose-agarose beads, indicating nearly complete depletion of RS1 from the prebound sample. In contrast, RS1 showed only moderate binding to lactose, as the bound and unbound fractions contain similar amounts of RS1. RS1 showed little binding to N-acetylglucosamine, N-acetylgalactosamine, D-mannose, heparin, or agarose alone. Its weak binding to D-mannose is especially significant, as D-mannose is one of the diastereomers of D-galactose. Together, these studies suggest that RS1 specifically binds D-galactose.

4.3.3 Coagulation Factor Va and RS1 can both act as lectins

Coagulation Factor Va also bound to galactose-agarose, although much less efficiently than RS1 (Fig. 4.5). To ensure that all proteins do not bind galactose-agarose, galactose-agarose beads were incubated with mouse IgG. As shown in Figure 4.5, little binding was observed.

4.3.4 RS1 can be eluted from a galactose column with IPTG, and can be extracted from retinal membranes with IPTG

In order to develop a method to purify RS1 and to examine the specificity of

Weri-Rb1
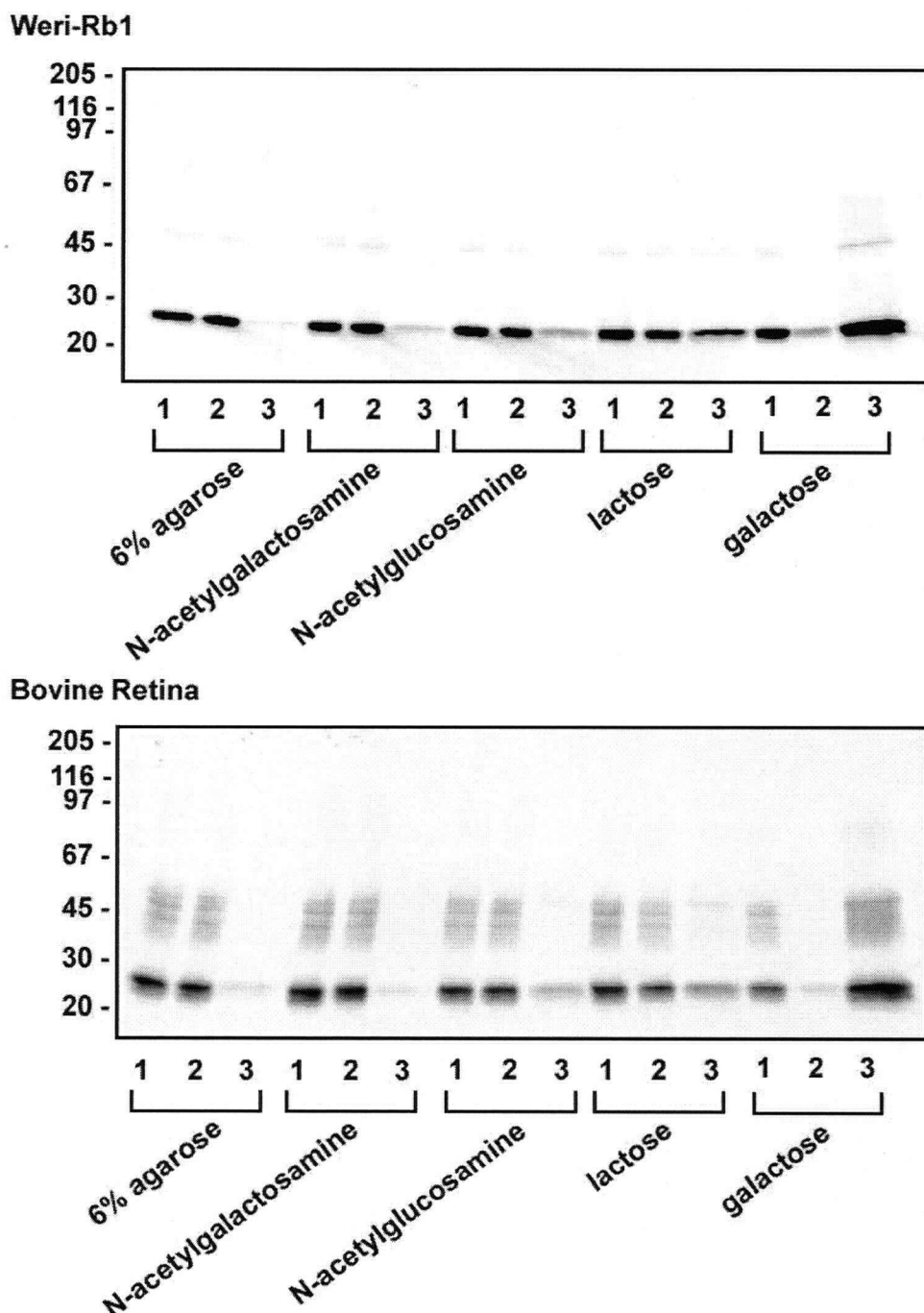
Bovine Retina

Figure 4.2. Carbohydrate affinity chromatography I. RS1 was obtained from the secreted fraction of Weri-Rb1 retinoblastoma cells or from bovine retinal membranes. Binding of RS1 to agarose coupled to various carbohydrates was performed for 1 h at 4°C. Each set of three lanes indicate the prebound (1), unbound (2), and bound (3) fractions, where the bound fraction was eluted with 4% SDS. Samples were run on a 10% SDS-polyacrylamide gel under reducing conditions, and analyzed on Western blots labelled with the RS1 monoclonal antibody.
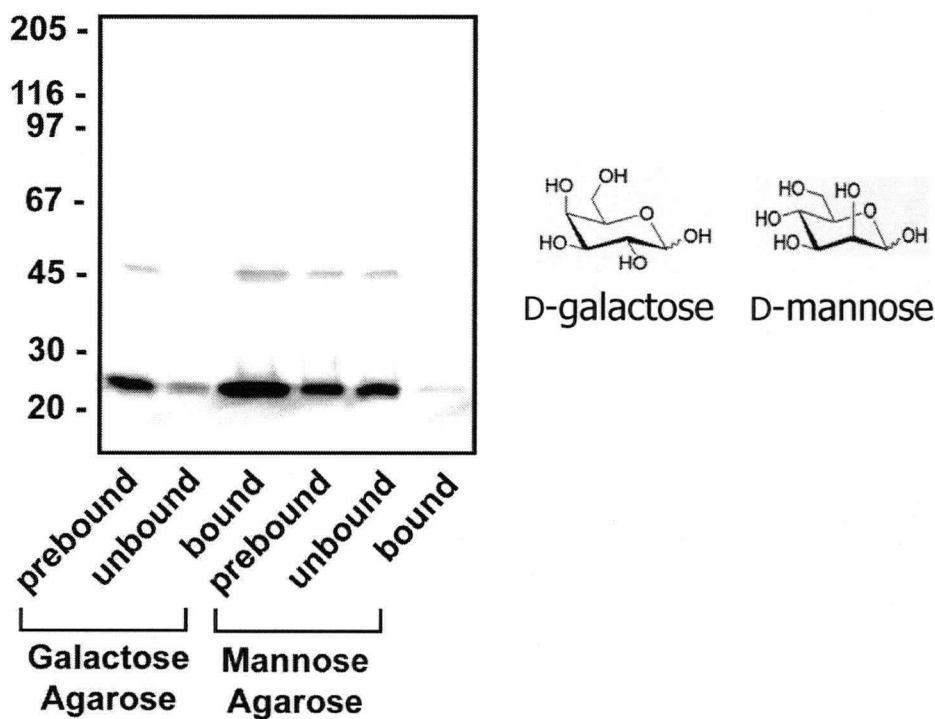
Figure 4.3. Carbohydrate affinity chromatography II. Binding of RS1 secreted from Weri-Rb1 retinoblastoma cells to galactose-agarose or mannose-agarose was performed for 1 h at 4°C. The bound fraction was eluted with 4% SDS. Samples were run on a 10% SDS-polyacrylamide gel under reducing conditions, and analyzed on Western blots labelled with the RS1 monoclonal antibody. Similar results were obtained for RS1 samples from bovine retina.
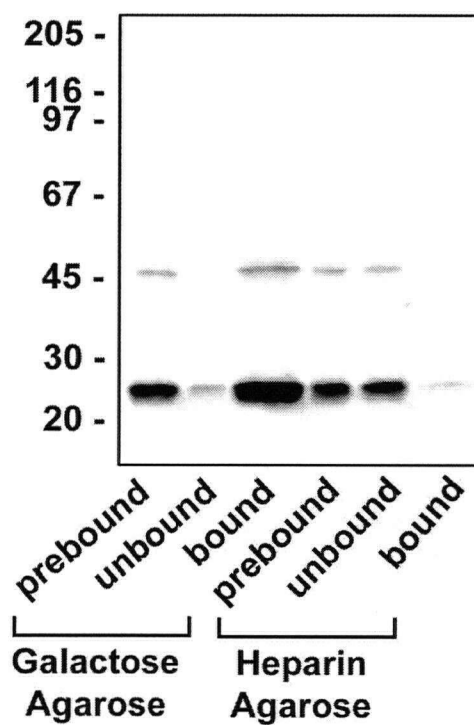
Figure 4.4. Carbohydrate affinity chromatography III. Binding of RS1 secreted from Weri-Rb1 retinoblastoma cells to galactose-agarose or heparin-agarose was performed for 1 h at 4°C. The bound fraction was eluted with 4% SDS. Samples were run on a 10% SDS-polyacrylamide gel under reducing conditions, and analyzed on Western blots labelled with the RS1 monoclonal antibody. Similar results were obtained for RS1 samples from bovine retina.
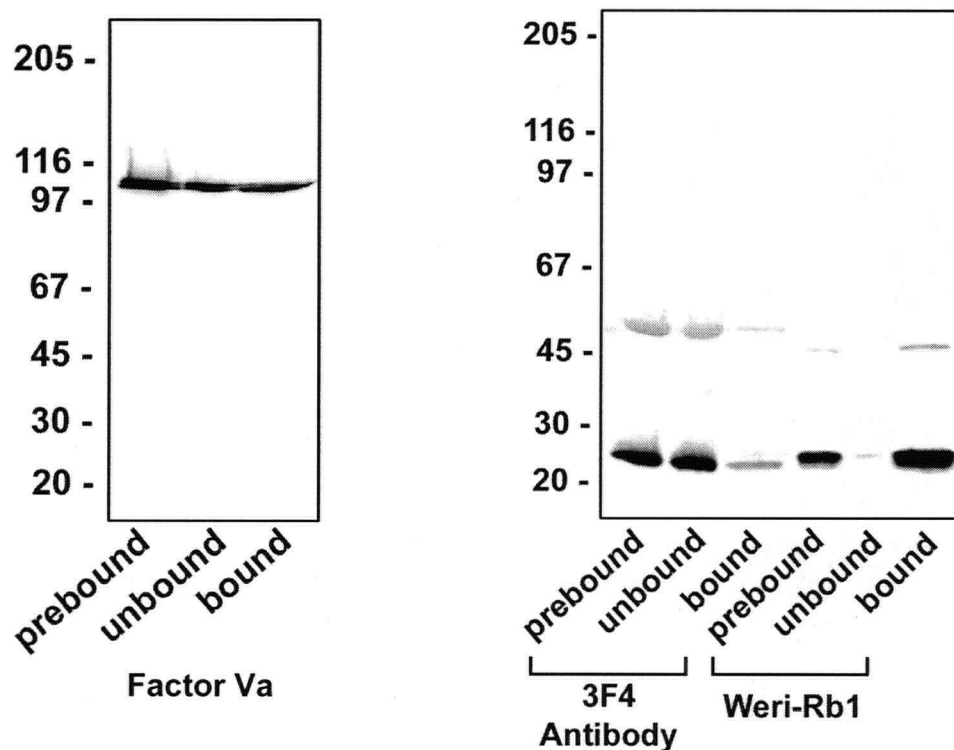
Figure 4.5. Carbohydrate affinity chromatography IV. Binding of coagulation Factor Va, RS1 secreted from Weri-Rb1 retinoblastoma cells, or the 3F4 mouse immunogloubilin to galactose-agarose was performed for 1 h at 4°C. The bound fraction of each of those incubations was eluted with 4% SDS. The prebound, unbound, and bound samples were run on a 10% SDS-polyacrylamide gel under reducing conditions, and analyzed on Western blots labelled with the RS1 monoclonal antibody for the RS1 blot and a monoclonal antibody against the heavy chain of Factor Va for the Factor Va blot.

the binding of RS1 to the galactose-agarose column, various compounds were tested for their ability to elute RS1 from the galactose column. Lactose and galactose could be dissolved only at 0.275M and 0.55M, respectively. As shown in Figure 4.6, neither 0.275M lactose nor 0.55M galactose eluted RS1 from the column. Subsequent elution with SDS released almost all of the RS1 from the column. In contrast, IPTG, which has an extra isopropyl thiol group attached to a galactose moiety, eluted RS1 from the galactose column in a concentration-dependent manner. A significant fraction of RS1 was eluted at 1M compared to 0.275M IPTG.

Various compounds were also tested for their ability to extract RS1 from retinal membranes. This was performed by incubating retinal membranes with various compounds and subsequently analyzing the amount of RS1 in the membrane and supernatant after centrifugation (Fig. 4.7). Similar to the elution experiments above, 1M IPTG in TBS was the most effective extraction agent of RS1 (Fig. 4.7A). The other extraction compounds, including TBS buffer itself, 0.55M galactose, 1M glucose, or 0.55M IPTG, extracted a similar amount of total protein, as displayed by Coomassie blue Staining (Fig. 4.7B), but little or no RS1 was extracted as analyzed by Western blotting (Fig. 4.7A). A final extraction with SDS for each of the samples showed that a similar amount of RS1 was present in each sample (Fig. 4.7A).

Since so many contaminating proteins were present in the extraction, an attempt was made to obtain as pure a preparation as possible by removing nonspecific proteins extracted from the retinal membranes. Therefore, an initial 1M glucose wash in TBS was also performed prior to extraction with 1M IPTG (last
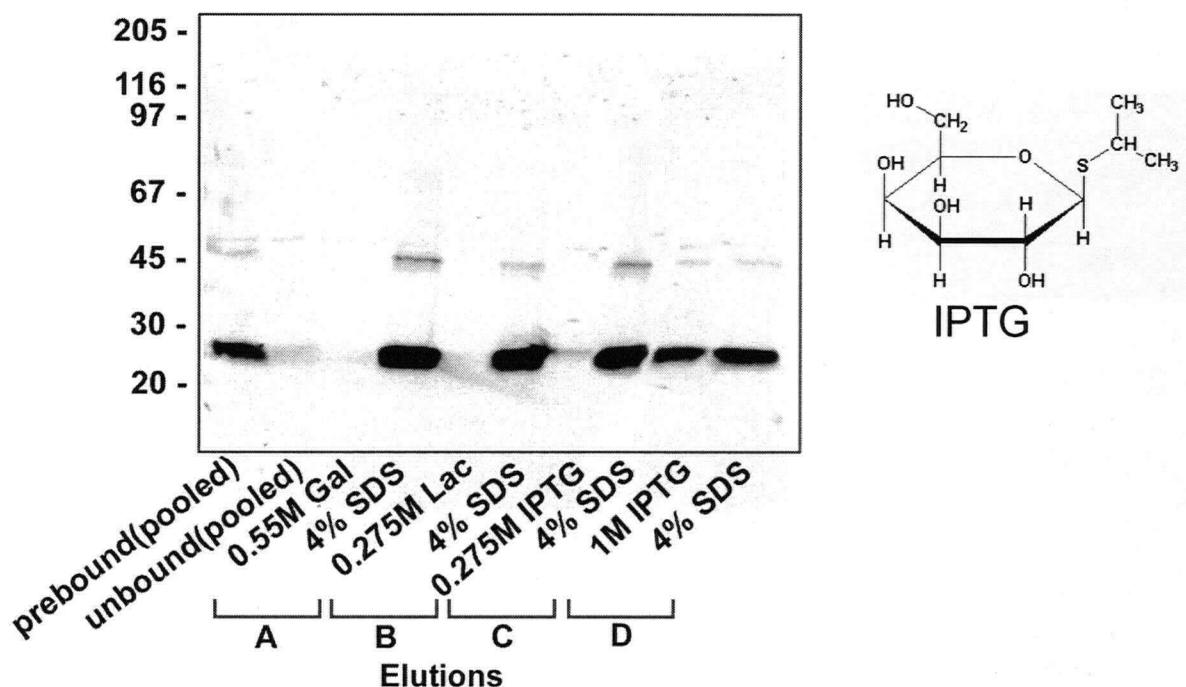
Figure 4.6. Carbohydrate affinity chromatography V. Binding of RS1 secreted from Weri-Rb1 retinoblastoma cells to agarose coupled to various carbohydrates was performed for 1 h at 4°C. The bound fraction was eluted with either 0.55M galactose, 0.275M lactose, 0.275M IPTG, or 1M IPTG (elutions A through D). Each of these elutions was further eluted with 4% SDS. Samples were run on a 10% SDS-polyacrylamide gel under reducing conditions and analyzed on Western blots labelled with the RS1 monoclonal antibody.

A Western Blot - Retinal Membrane Extraction

205 -
116 -
97 -
67 -
45 -
30 -
20 -

TBS
0.55M Galactose
1M Glucose
0.55M IPTG
1M IPTG
TBS
0.55M Galactose
1M Glucose
0.55M IPTG
1M IPTG
1M IPTG after Glucose

Extraction with Compound   Subsequent SDS Extraction

B Coomassie Blue Stain - Retinal Membrane Extraction

205 -
116 -
97 -
67 -
45 -
30 -
20 -

TBS
0.55M Galactose
1M Glucose
0.55M IPTG
1M IPTG
1M IPTG after Glucose

Extraction with Compound

C Western Blot - Retinal or Recombinant Membrane Extraction

205 -
116 -
97 -
67 -
45 -
30 -
20 -

Retina
rWT
C59S/C223S
Retina
rWT
C59S/C223S

IPTG Extraction   SDS Extraction

Figure 4.7. Extraction of RS1 from retinal membranes with various compounds. (A) Western blot of retinal membrane extraction. The membrane fraction of bovine retina was obtained from a 60% sucrose gradient as described in Section 4.2.1. Protein was extracted with various compounds by shaking at 25°C for 10 min. Membranes were centrifuged, and this extraction was repeated twice more, with the resulting supernatant of each sample being pooled at the end. A final SDS extraction was also performed. Samples were run on a 10% SDS-polyacrylamide gel under reducing conditions, and analyzed on Western blots labelled with the RS1 monoclonal antibody. **(B)** Coomassie blue of extracted total protein. The retinal membrane samples extracted with compounds other than SDS were also subjected to Coomassie blue staining to analyze total protein. **(C)** Extraction of retinal and transfected membranes. The membrane fraction of retinal, recombinant wildtype (rWT), and dimeric (C59S/C223S) RS1 were obtained from a 60% sucrose gradient as described in Section 4.2.1. The membranes were incubated with IPTG and the amount of RS1 in the membrane and supernatant was subsequently analyzed as described in (A).

lanes in Figs. 4.7A and B). A significant amount of RS1 was still extracted by IPTG after the glucose wash, as viewed on the Western blot. On the Coomassie blue-stained gel, that sample was also cleaner than extraction with IPTG alone, as there was a more selective spectrum of bands. One of the bands in that lane, at about 35kDa, seemed to be especially abundant when performing an initial glucose wash compared to extraction with only IPTG. The identity of this protein remains to be determined.

The extent to which IPTG extracted WT RS1 or C59S/C223S from membranes of transfected EBNA HEK 293 cells was examined (Fig. 4.7C). Since RS1 is not present on the extracellular surfaces of RS1-transfected cells (immunofluorescence labelling of RS1-transfected cells in the absence of Triton X-100 shows limited RS1 labelling – data not shown), no RS1 should be extracted with 1M IPTG from membranes obtained from transfected cells. As shown in Figure 4.7C, RS1, which is present on the extracellular surfaces of retinal cells, is extracted from retinal membranes with 1M IPTG. In contrast, recombinant RS1 is not extracted from membranes of HEK 293 cells transfected with RS1.

The ability of RS1 to be eluted from the galactose-agarose column was used to purify RS1 from retinal membranes. As shown by silver staining, RS1 eluted from a galactose-agarose column with 1M IPTG was quite pure, showing the typical monomeric RS1 band and broad dimeric band under reducing conditions, with no other detectable bands, especially for elution at 25°C (Fig. 4.8). A few additional minor contaminants were detected for the 37°C elution, but more RS1 was also eluted at this temperature. A blot from a nonreducing gel also showed that RS1 was

Reducing Western Blot

205 -
116 -
97 -
67 -
45 -
30 -
20 -

retinal membranes
solubilized, dialyzed
unbound
25°C IPTG Elution
37°C IPTG Elution

Nonreducing Western Blot

205 -
116 -
97 -
67 -
Dye -

25°C IPTG Elution
37°C IPTG Elution

Silver Stain

205 -
116 -
97 -
67 -
45 -
30 -
20 -

←RS1
←RS1

25°C IPTG Elution
37°C IPTG Elution

Coomassie Blue Stain

205 -
116 -
97 -
67 -
45 -
30 -
20 -

←RS1

retinal membranes
solubilized, dialyzed
DEAE 0.5M NaCl Elution
galactose-agarose 1M IPTG elution

Figure 4.8. Purification of RS1 from bovine retinal membranes. Retinal membranes were prepared by separation of lysed cellular components on a 60% sucrose gradient. The membranes were then solubilized with CHAPS, and the CHAPS was removed by dialysis. The resulting supernatant was then incubated with galactose-agarose at 4°C for 1 h, washed, and eluted with 1M IPTG. For the Coomassie blue stained gel, the sample was additionally incubated with DEAE at pH 8.5, washed with 0.3M NaCl, and eluted with 0.5M NaCl before incubation with galactose-agarose beads.

present in its oligomeric form. For the 37°C elution, Coomassie blue staining was also performed. In this case, DEAE chromatography was introduced prior to galactose affinity chromatography. The retinal protein was loaded on a DEAE-Sephacel column in 20mM Tris, pH 8.5 and 20mM NaCl. The column was first washed with 0.3M NaCl to remove contaminating proteins and subsequently, RS1 was eluted at 0.5M NaCl before loading onto the galactose-agarose column. As shown in Figure 4.8, the Coomassie blue-stained gel run under reducing conditions shows the monomeric form of RS1 as the major band present.

4.3.5 The R141H spike 3 disease mutant binds as well as WT to galactose

To determine if the R141H disease mutant in spike 3 of the RS1 discoidin domain binds galactose, R141H, a suspected polymorphism D158N, and WT RS1, were expressed in EBNA HEK 293 cells. The secreted fractions were concentrated ten-fold by ammonium sulfate precipitation, and applied to a galactose-agarose column. As displayed in Figure 4.9, WT, the R141H mutant, and the D158N polymorphism were all found primarily in the fraction that bound to the matrix. Therefore, the inability of R141H to oligomerize properly does not affect its ability to bind galactose.

4.3.6 Octameric RS1 binds with greater affinity to galactose-agarose than dimeric or monomeric RS1

The binding of the other secreted RS1 mutants (dimer C59S/C223S and monomer C40S/C59S/C223S) to galactose-agarose was also studied. The left panel in Figure 4.10 shows the relative mobilities of the prebound protein samples
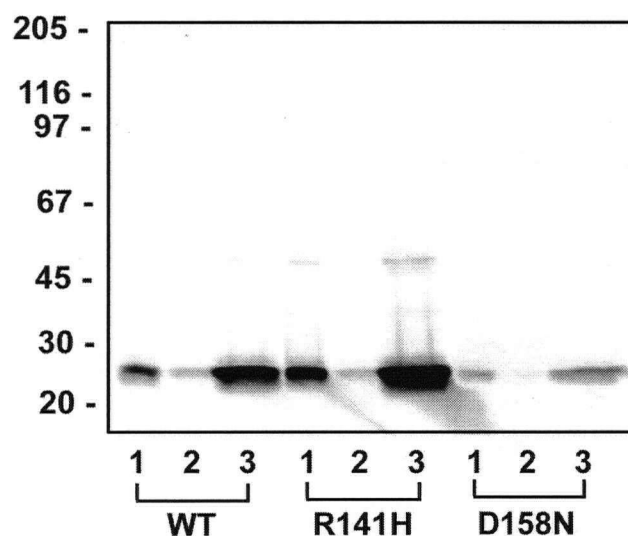
Figure 4.9. Binding of the secreted fractions of WT RS1, spike mutant R141H, and polymorphism mutant D158N to galactose-agarose. Protein was produced from transfection of EBNA HEK 293 cells. The secreted fraction was concentrated ten fold by 40% ammonium sulfate, and incubated with galactose-agarose. After washing, protein was eluted with 4% SDS. Each set of three lanes indicate the prebound (1), unbound (2), and bound fractions (3), where the bound fraction is eluted with 4% SDS. Samples were run on a 10% SDS-polyacrylamide gel under reducing conditions, and analyzed on Western blots labelled with the RS1 monoclonal antibody.

119
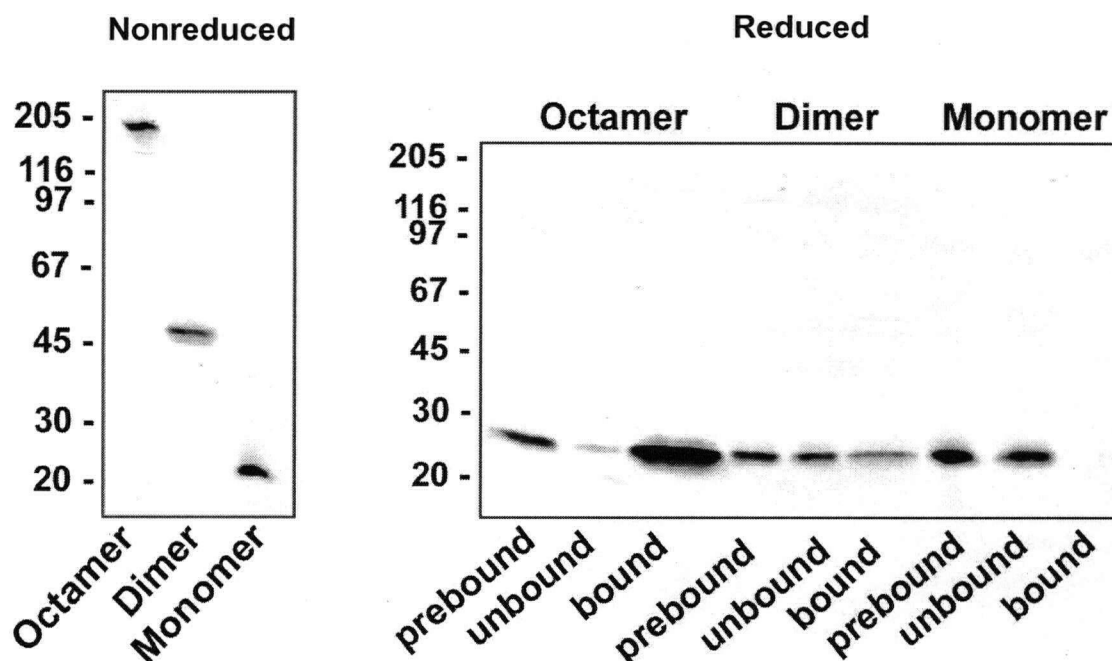
Figure 4.10. Carbohydrate affinity chromatography of octameric, dimeric, and monomeric RS1. Protein was expressed from transfection of EBNA HEK 293 cells. The proteins expressed were octameric WT RS1, dimeric C59S/C223S RS1, and monomeric C40S/C59S/C223S RS1. The secreted fraction of each sample was concentrated ten fold by 40% ammonium sulfate, and incubated with galactose-agarose. After washing, protein was eluted with 4% SDS. Samples on the left panel represent prebound protein run on a 10% SDS-polyacrylamide gel under nonreducing conditions. Samples on the right panel were run on a 10% SDS-polyacrylamide gel under reducing conditions. The gels were transferred and analyzed on Western blots labelled with the RS1 monoclonal antibody.

(octamer, dimer, and monomer) under nonreducing conditions. The right panel shows their binding abilities, with the samples run under reducing conditions. Only the octameric form of RS1 bound to galactose in significant amounts (Fig. 4.10). Both dimeric and monomeric RS1 displayed much weaker binding as evidenced by the large amount of RS1 left in the unbound fraction and the extremely low levels of RS1 in the bound fraction.

4.4 Discussion

In this study, ligands known to bind other members of the discoidin domain family were tested for their ability to interact with RS1. RS1 possesses a high degree of similarity in spike 1 of its discoidin domain to the corresponding region in coagulation Factors V and VIII and milk fat globule membrane protein, which bind negatively-charged phospholipids (Fuentes-Prior et al., 2002). Molecular modeling also suggested that RS1 contains hydrophobic feet that could insert into phospholipid membranes (Fraternali et al., 2003). Therefore, the binding of RS1 to vesicles containing the negatively-charged phospholipid phosphatidylserine and vesicles derived from retinal phospholipids was investigated. Whereas Factor Va bound to phosphatidylserine-containing vesicles, RS1 showed no binding.

A search for other interacting ligands was performed. Since RS1, like discoidin I, is the only discoidin family member known to exist as an oligomeric complex consisting of mainly discoidin domains, the binding of RS1 to carbohydrates was investigated. Discoidin I was initially shown to interact strongly with D-galactose (Rosen et al., 1973). Therefore, RS1 was tested for its ability to bind galactose, as

well as other carbohydrates. As shown in this study, RS1 from Weri-Rb1 retinoblastoma cells, bovine retina, and transfected EBNA HEK 293 cells interacted strongly with D-galactose. In contrast, RS1 did not interact with D-mannose, one of the diastereomers of galactose. This indicates a high degree of specificity for galactose. Lactose showed moderate binding to RS1, likely due to the galactose group present in lactose. Other carbohydrates found in the extracellular matrix, such as N-acetylglucosamine and N-acetylgalactosamine, showed only limited binding to RS1. As neuropilin 1 can interact with heparin via its b1b2 discoidin domains (Mamluk et al., 2002), RS1 was also tested for its ability to bind heparin. However, only limited binding was observed. Interestingly, though, for the first time, it was shown in this study that coagulation Factor V could also bind galactose.

Besides RS1, Factor V, and discoidin I, other discoidin family members also possess lectin-like activity. For example, hemocytin, expressed in the silkworm, possesses carbohydrate-binding and agglutinating properties that may be key to its function both as an immune protein and as a silkworm developmental protein (Yamakawa and Tanaka, 1999). Echinonectin from sea urchin also shows a specificity for galactose (Alliegro and Alliegro, 1991). Another recently-discovered D-galactose lectin, SLL-2 from the octocoral, has been also reported to possess sequence homology to the discoidin family members (Jimbo et al., 2005). Furthermore, when the carbohydrates were removed from collagen, discoidin domain receptor 2 was unable to activate its tyrosine receptor kinase, suggesting that binding to carbohydrates is essential to the function of discoidin domain receptor 2 (Vogel et al., 1997). In addition, galactose oxidase, a distant homologue of the

discoidin domain family, binds galactose as a substrate (Baumgartner et al., 1998). Therefore discoidin I, hemocytin, echinonectin, and SLL-2 from invertebrates, in addition to RS1, Factor V, discoidin domain receptor 2 and neuropilin from vertebrates appear to possess glycan-binding capabilities.

The binding pocket for discoidin family members has been suggested to be located in the spike regions of the discoidin domain. This has been demonstrated in experiments with the coagulation factors, neuropilin 1, and the discoidin domain receptors (Abdulhussein et al., 2004; Gilbert et al., 2002; Kim et al., 2000; Leitinger, 2003; Shimizu et al., 2000; Srivastava et al., 2001). Furthermore, the spike regions of the discoidin domain crystal structures solved to date indicate that this region is the most highly-variable region within the structures of the different proteins (Fuentes-Prior et al., 2002; Lee et al., 2003; Macedo-Ribeiro et al., 1999; Pratt et al., 1999). This variability may exist to allow different discoidin family members to bind different ligands.

One unresolved question is whether the ability of proteins, such as RS1 and to a lesser extent Factor V, to bind carbohydrates such as galactose and lactose, is a residual function remaining from the ability of ancestor proteins such as discoidin I to bind carbohydrates. Alternatively, this lectin-like property may actually play a key physiological role in the organism. One possibility is that during development, these discoidin proteins may be required to bind to carbohydrates. In mature organisms, though, this binding may be no longer relevant (Kilpatrick, 2002). Another possibility is negative feedback mechanisms, which occur during certain situations, may render such carbohydrate-binding abilities relevant. Examples include removal of adhesive

contacts or allowing for remodeling of the organism and the extracellular matrix. However, the ability of lectins to bind not only carbohydrates, but also other macromolecules such as proteins, lipids, or nucleic acids, has been extensively documented (Hinek et al., 1988; Kilpatrick, 1998; Pepys and Butler, 1987). This ability may simply be a general feature of lectins.

In the case of RS1, its ability to act as a lectin is further highlighted by its ability to be eluted by a galactoside, IPTG. This supports the specificity of RS1 for galactose, or more specifically, for a galactoside. The ability of IPTG to extract RS1 from retinal membranes also suggests that RS1 may interact with some galactoside group on the surface of retinal membranes. Possible interacting molecules include glycolipids or glycoproteins. Alternatively, it is possible that IPTG competes for the same binding site as some other ligand that interacts with RS1, enabling IPTG to extract RS1 from retinal membranes. Since 1M glucose was unable to extract any RS1 from retinal membranes, it is unlikely that the extraction was due to possible chaotropic effects from a high molarity of IPTG. It more likely indicates that RS1 is tightly bound to membranes, and thus requires a high concentration of IPTG for extraction.

Similarly, the high concentration of IPTG required to elute RS1 from the galactose-agarose column indicates the strong affinity that RS1 has for galactose-agarose. In addition, the finding that IPTG can be used to elute RS1 from the column is a useful method to purify RS1 under nondenaturing conditions.

A general property of lectins is their cooperativity of binding effect, where several subunits of a protein bind much more strongly to a carbohydrate than a

single subunit (Loris, 2002). RS1 also possesses this property, since dissociated RS1, consisting of dimers or monomers, showed much weaker binding to galactose than octameric RS1. The dimers, in turn, seemed to be stronger than monomers in their binding, but significantly weaker than octameric RS1. Since mutations that disrupt octamer formation result in X-linked retinoschisis (Chapter 3), the inability of octamer-defective mutants to bind galactose-agarose may therefore provide a biochemical basis for the pathogenesis linked to subunit assembly-defective mutations.

Figure 4.11 depicts a model where each subunit of RS1 binds to a single galactose moiety. Even though only the octameric form of RS1 interacts strongly with galactose, each RS1 subunit would likely interact with a single galactose group because there was still a small amount of binding with the dimeric and monomeric forms. This indicates that the interaction of one RS1 subunit enhances the binding of subsequent subunits probably because it brings the other subunits closer to the other galactose groups. The more subunits, the stronger the interaction, culminating in the high affinity of the octameric form for galactose. This is, therefore, a diagrammatic representation of the cooperativity of binding effect mentioned above.

In summary, this study has demonstrated that RS1 interacts strongly with D-galactose. RS1 also displays moderate affinity to lactose, but weak affinity to N-acetylglucosamine, N-acetylgalactosamine, D-mannose, heparin, or agarose alone. Binding to galactose is dependent on the formation of the RS1 octamer, as monomers and dimers display much weaker binding. IPTG can be used to elute RS1 from the galactose-agarose column, a useful tool to purify RS1 in a
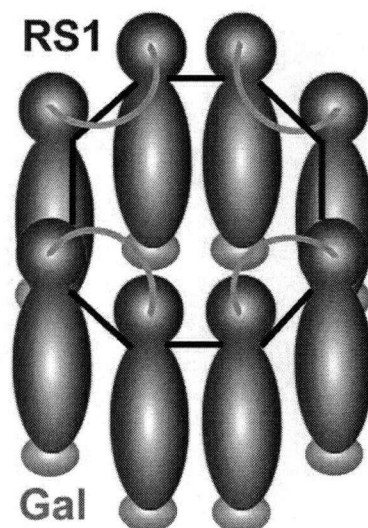
Figure 4.11. Model of RS1 binding to galactose-agarose. **Each RS1 subunit (*blue*) binds to a galactose molecule (abbreviated Gal, *green*). The binding of each additional subunit enhances the strength of the binding to the column. Whether this type of interaction also occurs in the retina remains to be seen. The black and grey lines represent intermolecular disulfide bonds between RS1 subunits.**

nondenaturing manner. In addition, IPTG can extract RS1 from retinal membranes, but not from membranes of transfected cells. These findings thus serve as a basis to probe in further detail the structural properties of RS1 and how it functions as a retinal cell adhesion protein.

CHAPTER 5: SUMMARY AND FUTURE DIRECTIONS

5.1 Summary

Maintaining adhesion between the various cell layers of the retina is a prerequisite for the normal relaying of messages from photoreceptors through to ganglion cells and eventually to the brain. Compromises in this cellular architecture of the retina due to dysfunctional or an absence of RS1 are detrimental to vision, as displayed in patients with the X-linked retinoschisis phenotype. Thus, understanding the mechanism of how RS1 functions as a retinal cell adhesion protein is vital to understanding how the retina maintains its structural integrity. One of the most obvious approaches in understanding this retinal structural organization required for preservation of vision is to dissect the structural properties of RS1, which may hopefully also elucidate its functional properties. Hence, studies on the structure-function relationships in RS1 were conducted in this thesis to investigate how RS1 acts as a retinal cell adhesion protein and how this is compromised in patients with X-linked retinoschisis.

Findings showed that RS1 is a disulfide-linked homo-octamer linked by C59-C223 intermolecular disulfide bonds. Within this octamer, are C40-C40 intermolecular disulfide bonds, which maintain disulfide-linked dimer formation, and possibly further stabilize the RS1 octameric state. RS1 does not assemble into higher ordered structures. C59-C223 disulfide bonds are especially critical since elimination of these intermolecular bonds through mutations in either C59 or C223, reduces RS1 to a dimer. Disrupting dimeric assembly (by disruption of C40-C40 bonds without disrupting C59-C223 bonds) does not affect RS1 octameric structure.

However, dimeric assembly may be critical for stabilizing the octamer or critical during octamer formation.

RS1 obtained directly from the retina, in contrast to RS1 from cultured cells, is heterogeneous. It migrates more slowly by SDS-PAGE than recombinant RS1 or RS1 from Weri-Rb1 cells, and sediments more rapidly by velocity centrifugation. This indicates that retinal cells *in vivo* likely introduce additional post-translational modifications that may be crucial for the function of RS1 as a retinal cell adhesion protein.

Studies from this thesis to probe RS1 structure also determined experimentally the site of leader peptide cleavage that allows RS1 to be secreted. This cleavage site occurs between S23 and S24 of each RS1 subunit. Hence the leader sequence in RS1 is composed of the first 23 amino acids, which is consistent with the length of other leader sequences (Briggs and Gierasch, 1986).

The main functional region within each RS1 subunit is most likely the discoidin domain, a domain implicated in maintaining cell adhesion. Molecular modeling developed from high-resolution crystal structures indicates that the RS1 discoidin domain consists of a core barrel composed predominantly of β strands with spike regions extending from one end of the core structure. An intramolecular disulfide bond exists between C110 and C142, clamping spikes 2 and 3 together. As well, RS1 contains the hallmark disulfide bond found in discoidin family members marking the beginning and end of the discoidin domain. In RS1, this corresponds to the C63-C219 disulfide bond. C83, the remaining cysteine in the discoidin domain, exists as a free cysteine.

Various mutations in *RS1* have been catalogued, as these can lead to X-linked retinoschisis in males with the defective gene or in females with both genes defective. Missense mutations are particularly useful tools to analyze small changes in protein structure. Thus, a variety of missense mutations were generated to examine their effect on RS1 expression, oligomeric assembly, secretion, and localization.

Disease-associated missense mutations can be divided into four categories. The first category comprises mutations in the leader sequence. These mutations cause RS1 to be mistargeted to the cytoplasm leading to rapid degradation and a low steady state level of expression.

The second category of missense mutations affect protein folding. All of these mutations studied thus far were in residues within the discoidin domain. Thus, perturbing the structure of the discoidin domain has a drastic effect on protein folding and stability. These discoidin domain mutants were not secreted from cells, but instead retained in the ER as misfolded aggregated proteins. Many of these missense mutations involve altering a critically conserved residue (e.g. proline), introducing or removing a cysteine that would cause abnormal disulfide bond formation, or changing the charge of a residue. The structure of the discoidin domain apparently cannot tolerate these types of changes and is thus grossly misfolded. A similar mechanism of disease would likely occur for other discoidin domain family members. In particular, mutations in the discoidin domain of Factors VIII and V that lead to hemophilia A or parahemophilia most likely also cause protein misfolding and a loss of function.

The third category of missense mutations involves mutations that disrupt the octameric assembly of RS1. Mutations in either C59 or C223, which mediate octameric assembly fall into this category. Monomeric (C40S/C59S/C223S) or dimeric (C59S/C223S) RS1 can be secreted by cells due to proper protein folding of their discoidin domain. However, the inability to assemble into an octamer compromises the function of RS1. The octamer thus appears to be critical for the function of RS1 as a retinal cell adhesion protein.

The fourth category of missense mutations, of which only one has been found thus far, involves proteins secreted in an aggregated state. The R141H mutant appears to be properly folded since it is secreted from cells. However, abnormal oligomers were observed when analyzed by SDS-PAGE. These abnormal oligomers may have been due to misfolding of the discoidin domain in such a way that it was able to pass through the ER quality control, but unable to form a more discrete quaternary structure as seen normally for WT RS1.

A suspected polymorphism D158N displayed similar characteristics as WT RS1 with respect to oligomerization. The only minor difference was its apparently lower levels of expression and secretion compared to WT RS1. Thus, the lack of a disease phenotype clinically is consistent with the mutant protein having similar cellular and biochemical properties as WT RS1.

The correlation of these missense mutations associated with X-linked retinoschisis with various cellular and biochemical properties thus represents a first step to understanding the disease and hopefully developing a rational therapy for it. The tools and methods used to probe the structural and cellular properties of RS1

can also be used as a diagnostic or a predictive tool to analyze other mutants in the future, or as a mechanism to analyze models of X-linked retinoschisis when designing therapies.

As a step to further understanding how RS1 structure relates to its function, various ligands were tested for their ability to interact with RS1. These ligands were chosen from ligands that interacted with other discoidin family member proteins. Phospholipids were one of these ligands tested, but unlike coagulation Factors V and VIII or the milk fat globule membrane proteins, phospholipids did not interact with RS1. However, RS1, like discoidin I, interacted strongly with D-galactose. RS1 also showed moderate affinity for lactose, but limited affinity for N-acetylglucosamine, N-acetylgalactosamine, heparin, or D-mannose, a diastereomer of D-galactose. Furthermore, IPTG eluted RS1 from the galactose-agarose column, and could be used as a tool to purify RS1 in a nondenaturing manner. IPTG also extracted RS1 from retinal membranes but not from membranes of cells transfected with RS1. This indicates that RS1 may be interacting with some galactoside structure, or perhaps some other molecule, on the extracellular surfaces of retinal cells. Finally, only the octameric form of RS1 was shown to bind to galactose with high affinity. This ability of RS1 to bind carbohydrate as an oligomeric complex is similar to that of other lectins, which often bind carbohydrates with much higher affinity as a protein complex than as a single subunit.

A model of how RS1 may interact with its ligands and maintain retinal adhesion is displayed in Figure 5.1. One model, termed "crosslinking," is when RS1 forms an apparent bridge across components of the extracellular matrix or plasma

A Crosslinking

RS1

Hypothetical RS1 Receptors

B Cooperating

RS1

Hypothetical
RS1 Receptor
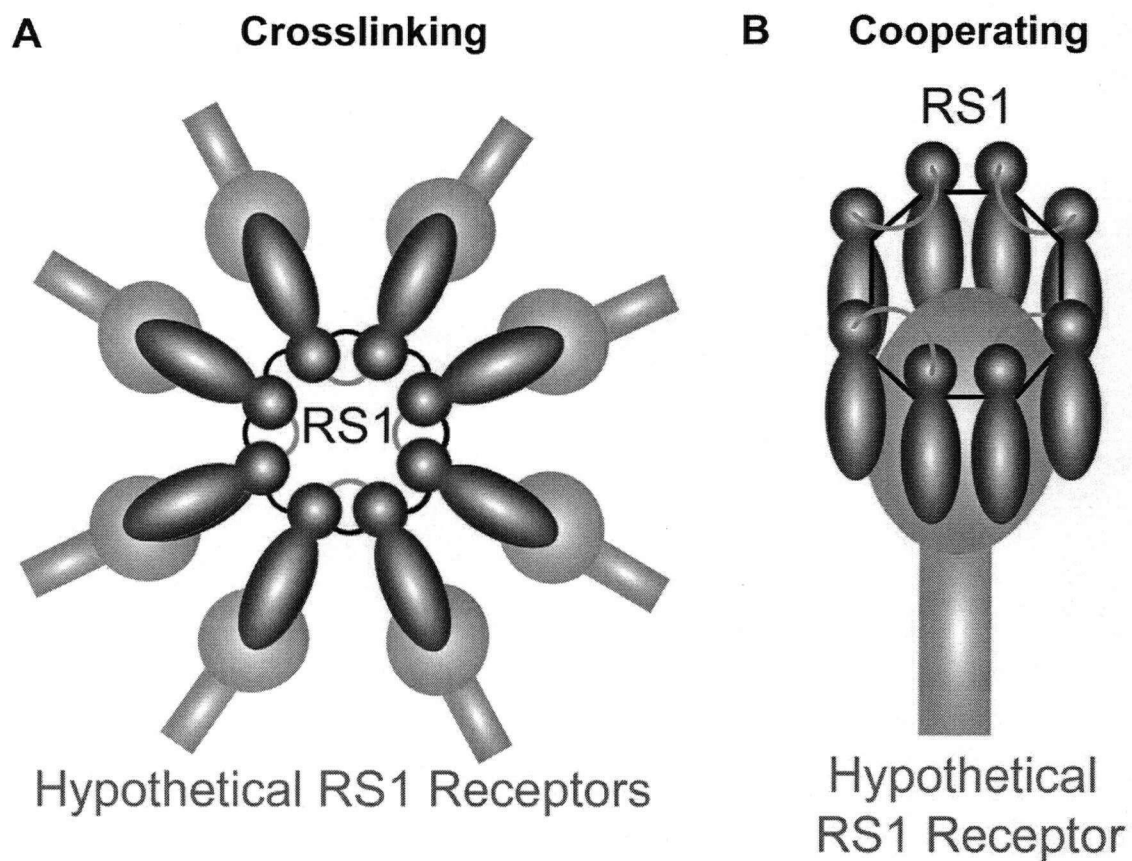
Figure 5.1. Models of retinal adhesion. (A) RS1 may function in retinal adhesion by crosslinking components of the extracellular matrix or plasma membrane. **(B)** The eight subunits of RS1 cooperate to facilitate binding.

membrane, thus linking them together (Fig. 5.1A). Another model, termed "cooperating," is when individual RS1 subunits cooperate to generate a higher-affinity binding site in order to interact with its ligand (Fig. 5.1B). In this model, another binding site elsewhere on RS1 would likely be present to allow for adhesion to occur. Figure 4.11 also shows a similar cooperating model, but in that model, each subunit interacts with a single ligand. More studies are needed to determine which model most closely resembles the process by which RS1 acts as a retinal cell adhesion protein.

5.2 Future Directions

Results from this thesis investigation will hopefully serve as a basis for more exciting discoveries in the future. For example, X-ray crystallography of the entire RS1 oligomeric complex would be important in confirming the intermolecular and intramolecular disulfide bonds found in this study, and in providing insight into the arrangement of individual RS1 subunits within the octameric structure. For these studies, it may be necessary to use either RS1 from retinoblastoma cells or recombinant RS1 since retinal RS1 is much more heterogeneous. NMR studies may also be possible with a single RS1 subunit by using the C40S/C59S/C223S monomer. Alternatively, the structure of just the RS1 discoidin domain could be determined to confirm and refine the model developed here.

The heterogeneous nature of retinal RS1 leads to the question: "What post-translational modifications are present in the retinal form of RS1 and how do these modifications affect its function as an extracellular adhesion protein?" During

the course of these studies, attempts were made to determine if RS1 was glycosylated. However, no post-translational glycosylation was detected by fluorescent staining of periodate-treated RS1 in contrast to control glycosylated proteins. More experimentation will be required to determine the nature and site of post-translational modification responsible for the differences between the retinal and recombinant forms of RS1. Mass spectrometry of peptides and sequencing may help to resolve this issue.

Perhaps one of the most important issues that remains and that may help explain how RS1 functions as an extracellular adhesion protein is to determine what RS1 interacts with in the extracellular matrix and on the surface of photoreceptors and bipolar cells. Co-immunoprecipitation studies were employed during the course of these studies, but these studies failed to reveal any interacting proteins. It is possible that these interacting proteins are present in such small quantities that were under the limits of detection. Scaled-up co-immunoprecipitation studies can be performed in an attempt to detect and characterize any interacting proteins. Another possibility is to isolate RS1 from the retina and couple it to a solid-phase support to identify the interacting ligands. Since RS1 is present on the surfaces of photoreceptors, bipolar cells, and synapses, it would also be interesting to determine if RS1 interacts with different ligands in different parts of the retina. Of course, if the interacting ligand does not contain a protein component, but instead a lipid, glycolipid, or glycosaminoglycan, other methods of detection will have to be employed.

In addition to determining the components that RS1 interacts with in the

extracellular matrix, it would be of interest to determine what RS1 interacts with in the intracellular compartments. In particular, it would be of interest to determine the intracellular chaperone that facilitates protein folding and formation of disulfide bonds. The binding of chaperones to mutant proteins would also be of interest.

Finally, genotype-phenotype correlations have not been extensively carried out on patients with the disease since the gene was only recently discovered. Even though patients with the same mutation display varying phenotypes, it nevertheless may be fruitful to carry out further genotype-phenotype studies on a larger number of patients to determine if any correlations can be drawn. The availability of a knockout mouse also allows for the development and improvement of gene therapy regimes. This X-linked retinoschisis phenotype, which can potentially be extremely debilitating, will hopefully be cured or managed at a sufficient level so that patients can preserve or improve their vision. By more actively engaging in the study of RS1, this hopefully will be achieved.

REFERENCES

Abdulhussein, R., McFadden, C., Fuentes-Prior, P., and Vogel, W. F. (2004). Exploring the collagen-binding site of the DDR1 tyrosine kinase receptor. J Biol Chem *279*, 31462-31470.

Ali, A., Feroze, A. H., Rizvi, Z. H., and Rehman, T. U. (2003). Consanguineous marriage resulting in homozygous occurrence of X-linked retinoschisis in girls. Am J Ophthalmol *136*, 767-769.

Ali, R. R., Sarra, G. M., Stephens, C., Alwis, M. D., Bainbridge, J. W., Munro, P. M., Fauser, S., Reichel, M. B., Kinnon, C., Hunt, D. M., et al. (2000). Restoration of photoreceptor ultrastructure and function in retinal degeneration slow mice by gene therapy. Nat Genet *25*, 306-310.

Alliegro, M. C., and Alliegro, M. A. (1991). The structure and activities of echinonectin: a developmentally regulated cell adhesion glycoprotein with galactose-specific lectin activity. Glycobiology *1*, 253-256.

Allikmets, R., Shroyer, N. F., Singh, N., Seddon, J. M., Lewis, R. A., Bernstein, P. S., Peiffer, A., Zabriskie, N. A., Li, Y., Hutchinson, A., et al. (1997). Mutation of the Stargardt disease gene (ABCR) in age-related macular degeneration. Science *277*, 1805-1807.

Antonarakis, S. E., Kazazian, H. H., and Tuddenham, E. G. (1995). Molecular etiology of factor VIII deficiency in hemophilia A. Hum Mutat *5*, 1-22.

Apushkin, M. A., Fishman, G. A., and Janowicz, M. J. (2005). Correlation of optical coherence tomography findings with visual acuity and macular lesions in patients with X-linked retinoschisis. Ophthalmology *112*, 495-501.

Arai, M., Scandella, D., and Hoyer, L. W. (1989). Molecular basis of factor VIII inhibition by human antibodies. Antibodies that bind to the factor VIII light chain prevent the interaction of factor VIII with phospholipid. J Clin Invest *83*, 1978-1984.

Arnaout, M. A., Goodman, S. L., and Xiong, J. P. (2002). Coming to grips with integrin binding to ligands. Curr Opin Cell Biol *14*, 641-651.

Aumailley, M., and Smyth, N. (1998). The role of laminins in basement membrane function. J Anat *193 (Pt 1)*, 1-21.

Azzolini, C., Pierro, L., Codenotti, M., and Brancato, R. (1997). OCT images and surgery of juvenile Macular retinoschisis. Eur J Ophthalmol *7*, 196-200.

Barclay, A. N. (2003). Membrane proteins with immunoglobulin-like domains--a master superfamily of interaction molecules. Semin Immunol *15*, 215-223.

Bascom, R. A., Manara, S., Collins, L., Molday, R. S., Kalnins, V. I., and McInnes, R. R. (1992). Cloning of the cDNA for a novel photoreceptor membrane protein (rom-1) identifies a disk rim protein family implicated in human retinopathies. Neuron 8, 1171-1184.

Baumgartner, S., Hofmann, K., Chiquet-Ehrismann, R., and Bucher, P. (1998). The discoidin domain family revisited: new members from prokaryotes and a homology-based fold prediction. Protein Sci 7, 1626-1631.

Beharry, S., Zhong, M., and Molday, R. S. (2004). N-retinylidene-phosphatidylethanolamine is the preferred retinoid substrate for the photoreceptor-specific ABC transporter ABCA4 (ABCR). J Biol Chem 279, 53972-53979.

Berson, E. L., Rosner, B., Weigel-DiFranco, C., Dryja, T. P., and Sandberg, M. A. (2002). Disease progression in patients with dominant retinitis pigmentosa and rhodopsin mutations. Invest Ophthalmol Vis Sci 43, 3027-3036.

Bessant, D. A., Ali, R. R., and Bhattacharya, S. S. (2001). Molecular genetics and prospects for therapy of the inherited retinal dystrophies. Curr Opin Genet Dev 11, 307-316.

Bligh, E. G., and Dyer, W. J. (1959). A rapid method of total lipid extraction and purification. Can J Biochem Physiol 37, 911-917.

Boggon, T. J., Murray, J., Chappuis-Flament, S., Wong, E., Gumbiner, B. M., and Shapiro, L. (2002). C-cadherin ectodomain structure and implications for cell adhesion mechanisms. Science 296, 1308-1313.

Bork, P., Downing, A. K., Kieffer, B., and Campbell, I. D. (1996). Structure and distribution of modules in extracellular proteins. Q Rev Biophys 29, 119-167.

Bradshaw, K., George, N., Moore, A., and Trump, D. (1999). Mutations of the XLRS1 gene cause abnormalities of photoreceptor as well as inner retinal responses of the ERG. Doc Ophthalmol 98, 153-173.

Briggs, M. S., and Gierasch, L. M. (1986). Molecular mechanisms of protein secretion: the role of the signal sequence. Adv Protein Chem 38, 109-180.

Brunger, A. T., Adams, P. D., Clore, G. M., DeLano, W. L., Gros, P., Grosse-Kunstleve, R. W., Jiang, J. S., Kuszewski, J., Nilges, M., Pannu, N. S., et al. (1998). Crystallography & NMR system: A new software suite for macromolecular structure determination. Acta Crystallogr D Biol Crystallogr 54 (Pt 5), 905-921.

Brunner, B., Todt, T., Lenzner, S., Stout, K., Schulz, U., Ropers, H. H., and Kalscheuer, V. M. (1999). Genomic structure and comparative analysis of

nine Fugu genes: conservation of synteny with human chromosome Xp22.2-p22.1. Genome Res *9*, 437-448.

Buckland, A. G., and Wilton, D. C. (2000). Anionic phospholipids, interfacial binding and the regulation of cell functions. Biochim Biophys Acta *1483*, 199-216.

Buser, P. A., and Imbert, M. (1992). Vision (Cambridge, Massachusetts, MIT Press).

Carson, D. D. (2004). Extracellular matrix: forum introduction. Reprod Biol Endocrinol *2*, 1.

Cavallerano, A. A. (1992). Retinal detachment. Optom Clin *2*, 25-70.

Chang, G. Q., Hao, Y., and Wong, F. (1993). Apoptosis: final common pathway of photoreceptor death in rd, rds, and rhodopsin mutant mice. Neuron *11*, 595-605.

Chen, C., and Okayama, H. (1987). High-efficiency transformation of mammalian cells by plasmid DNA. Mol Cell Biol *7*, 2745-2752.

Chiquet-Ehrismann, R. (2004). Tenascins. Int J Biochem Cell Biol *36*, 986-990.

Cohen, A. I. (1963). Vertebrate retinal cells and their organization. Biol Rev Cambridge Phil Soc *38*, 427-459.

Colognato, H., and Yurchenco, P. D. (2000). Form and function: the laminin family of heterotrimers. Dev Dyn *218*, 213-234.

Comer, G. M., Ciulla, T. A., Criswell, M. H., and Tolentino, M. (2004). Current and future treatment options for nonexudative and exudative age-related macular degeneration. Drugs Aging *21*, 967-992.

Congdon, N., O'Colmain, B., Klaver, C. C., Klein, R., Munoz, B., Friedman, D. S., Kempen, J., Taylor, H. R., and Mitchell, P. (2004). Causes and prevalence of visual impairment among adults in the United States. Arch Ophthalmol *122*, 477-485.

Connell, G., Bascom, R., Molday, L., Reid, D., McInnes, R. R., and Molday, R. S. (1991). Photoreceptor peripherin is the normal product of the gene responsible for retinal degeneration in the rds mouse. Proc Natl Acad Sci U S A *88*, 723-726.

Consortium, R. (1998). Functional implications of the spectrum of mutations found in 234 cases with X-linked juvenile retinoschisis. Hum Mol Genet *7*, 1185-1192.

Cremers, F. P., van de Pol, D. J., van Driel, M., den Hollander, A. I., van Haren, F. J., Knoers, N. V., Tijmes, N., Bergen, A. A., Rohrschneider, K., Blankenagel, A., et al. (1998). Autosomal recessive retinitis pigmentosa and cone-rod

dystrophy caused by splice site mutations in the Stargardt's disease gene ABCR. Hum Mol Genet *7*, 355-362.

Daiger, S. P., Rossiter, B. J. F., Greenberg, J., Christoffels, A., and Hide, W. (1998). Data services and software for identifying genes and mutations causing retinal degeneration, RetNet, http://www.sph.uth.tmc.edu/RetNet/. Invest Ophthalmol Vis Sci *39*, S295.

Davidson, J. M., Gabriella, G., and Mecham, R. P. (1995). Elastin. In The Extracellular Matrix: A Practical Approach, M. A. Haralson, and J. R. Hassell, eds. (Oxford, Oford University Press), pp. 241-260.

De Wit, J., De Winter, F., Klooster, J., and Verhaagen, J. (2005). Semaphorin 3A displays a punctate distribution on the surface of neuronal cells and interacts with proteoglycans in the extracellular matrix. Mol Cell Neurosci *29*, 40-55.

Dedhar, S. (1999). Integrins and signal transduction. Curr Opin Hematol *6*, 37-43.

Dejmek, J., Dib, K., Jonsson, M., and Andersson, T. (2003). Wnt-5a and G-protein signaling are required for collagen-induced DDR1 receptor activation and normal mammary cell adhesion. Int J Cancer *103*, 344-351.

Delori, F. C., Staurenghi, G., Arend, O., Dorey, C. K., Goger, D. G., and Weiter, J. J. (1995). In vivo measurement of lipofuscin in Stargardt's disease--Fundus flavimaculatus. Invest Ophthalmol Vis Sci *36*, 2327-2331.

Dowling, J. E. (1987). The Retina: An Approachable Part of the Brain (Cambridge, Massachusetts, Harvard University Press).

Edwards, A. O., Ritter, R., 3rd, Abel, K. J., Manning, A., Panhuysen, C., and Farrer, L. A. (2005). Complement factor H polymorphism and age-related macular degeneration. Science *308*, 421-424.

Eksandh, L. C., Ponjavic, V., Ayyagari, R., Bingham, E. L., Hiriyanna, K. T., Andreasson, S., Ehinger, B., and Sieving, P. A. (2000). Phenotypic expression of juvenile X-linked retinoschisis in Swedish families with different mutations in the XLRS1 gene. Arch Ophthalmol *118*, 1098-1104.

Ellgaard, L., Molinari, M., and Helenius, A. (1999). Setting the standards: quality control in the secretory pathway. Science *286*, 1882-1888.

Ensslin, M. A., and Shur, B. D. (2003). Identification of mouse sperm SED1, a bimotif EGF repeat and discoidin-domain protein involved in sperm-egg binding. Cell *114*, 405-417.

Eriksson, U., Larsson, E., and Holmstrom, G. (2004). Optical coherence tomography in the diagnosis of juvenile X-linked retinoschisis. Acta Ophthalmol Scand *82*, 218-223.

Ewing, C. C., and Ives, E. J. (1970). Juvenile hereditary retinoschisis. Trans Ophthalmol Soc U K *89*, 29-39.

Fernald, R. D. (2004). Eyes: variety, development and evolution. Brain Behav Evol *64*, 141-147.

Forsius, H., Krause, U., Helve, J., Vuopala, V., Mustonen, E., Vainio-Mattila, B., Fellman, J., and Eriksson, A. W. (1973). Visual acuity in 183 cases of X-chromosomal retinoschisis. Can J Ophthalmol *8*, 385-393.

Foster, P. A., Fulcher, C. A., Houghten, R. A., and Zimmerman, T. S. (1990). Synthetic factor VIII peptides with amino acid sequences contained within the C2 domain of factor VIII inhibit factor VIII binding to phosphatidylserine. Blood *75*, 1999-2004.

Fraternali, F., Cavallo, L., and Musco, G. (2003). Effects of pathological mutations on the stability of a conserved amino acid triad in retinoschisin. FEBS Lett *544*, 21-26.

Friedburg, C., Allen, C. P., Mason, P. J., and Lamb, T. D. (2004). Contribution of cone photoreceptors and post-receptoral mechanisms to the human photopic electroretinogram. J Physiol *556*, 819-834.

Fuentes-Prior, P., Fujikawa, K., and Pratt, K. P. (2002). New insights into binding interfaces of coagulation factors V and VIII and their homologues lessons from high resolution crystal structures. Curr Protein Pept Sci *3*, 313-339.

Gabius, H. J., Springer, W. R., and Barondes, S. H. (1985). Receptor for the cell binding site of discoidin I. Cell *42*, 449-456.

Gariano, R. F., and Kim, C. H. (2004). Evaluation and management of suspected retinal detachment. Am Fam Physician *69*, 1691-1698.

Gehrig, A., White, K., Lorenz, B., Andrassi, M., Clemens, S., and Weber, B. H. (1999a). Assessment of RS1 in X-linked juvenile retinoschisis and sporadic senile retinoschisis. Clin Genet *55*, 461-465.

Gehrig, A. E., Warneke-Wittstock, R., Sauer, C. G., and Weber, B. H. (1999b). Isolation and characterization of the murine X-linked juvenile retinoschisis (Rs1h) gene. Mamm Genome *10*, 303-307.

Gelse, K., Poschl, E., and Aigner, T. (2003). Collagens--structure, function, and biosynthesis. Adv Drug Deliv Rev *55*, 1531-1546.

George, N. D., Yates, J. R., Bradshaw, K., and Moore, A. T. (1995a). Infantile presentation of X linked retinoschisis. Br J Ophthalmol *79*, 653-657.

George, N. D., Yates, J. R., and Moore, A. T. (1995b). X linked retinoschisis. Br J Ophthalmol *79*, 697-702.

Ghazi, N. G., and Green, W. R. (2002). Pathology and pathogenesis of retinal detachment. Eye *16*, 411-421.

Gilbert, G. E., Kaufman, R. J., Arena, A. A., Miao, H., and Pipe, S. W. (2002). Four hydrophobic amino acids of the factor VIII C2 domain are constituents of both the membrane-binding and von Willebrand factor-binding motifs. J Biol Chem *277*, 6374-6381.

Glazer, L. C., and Dryja, T. P. (2002). Understanding the etiology of Stargardt's disease. Ophthalmol Clin North Am *15*, 93-100, viii.

Goldberg, A. F., and Molday, R. S. (1996). Defective subunit assembly underlies a digenic form of retinitis pigmentosa linked to mutations in peripherin/rds and rom-1. Proc Natl Acad Sci USA *93*, 13726-13730.

Grayson, C., Reid, S. N., Ellis, J. A., Rutherford, A., Sowden, J. C., Yates, J. R., Farber, D. B., and Trump, D. (2000). Retinoschisin, the X-linked retinoschisis protein, is a secreted photoreceptor protein, and is expressed and released by Weri-Rb1 cells. Hum Mol Genet *9*, 1873-1879.

Gross, O., Beirowski, B., Harvey, S. J., McFadden, C., Chen, D., Tam, S., Thorner, P. S., Smyth, N., Addicks, K., Bloch, W., *et al.* (2004). DDR1-deficient mice show localized subepithelial GBM thickening with focal loss of slit diaphragms and proteinuria. Kidney Int *66*, 102-111.

Guex, N., and Peitsch, M. C. (1997). SWISS-MODEL and the Swiss-PdbViewer: an environment for comparative protein modeling. Electrophoresis *18*, 2714-2723.

Haggqvist, B., Naslund, J., Sletten, K., Westermark, G. T., Mucchiano, G., Tjernberg, L. O., Nordstedt, C., Engstrom, U., and Westermark, P. (1999). Medin: an integral fragment of aortic smooth muscle cell-produced lactadherin forms the most common human amyloid. Proc Natl Acad Sci U S A *96*, 8669-8674.

Haines, J. L., Hauser, M. A., Schmidt, S., Scott, W. K., Olson, L. M., Gallins, P., Spencer, K. L., Kwan, S. Y., Noureddine, M., Gilbert, J. R., *et al.* (2005). Complement factor H variant increases the risk of age-related macular degeneration. Science *308*, 419-421.

Hakomori, S. (1990). Bifunctional role of glycosphingolipids. Modulators for transmembrane signaling and mediators for cellular interactions. J Biol Chem *265*, 18713-18716.

Haralson, M. A., and Hassell, J. R. (1995). The Extracellular Matrix - an Overview. In The Extracellular Matrix: A Practical Approach, M. A. Haralson, and J. R. Hassell, eds. (Oxford, Oxford University Press), pp. 1-30.

Harrison, O. J., Corps, E. M., Berge, T., and Kilshaw, P. J. (2005). The mechanism of cell adhesion by classical cadherins: the role of domain 1. J Cell Sci *118*, 711-721.

He, Z., and Tessier-Lavigne, M. (1997). Neuropilin is a receptor for the axonal chemorepellent Semaphorin III. Cell *90*, 739-751.

Heinzelmann-Schwarz, V. A., Gardiner-Garden, M., Henshall, S. M., Scurry, J., Scolyer, R. A., Davies, M. J., Heinzelmann, M., Kalish, L. H., Bali, A., Kench, J. G., *et al.* (2004). Overexpression of the cell adhesion molecules DDR1, Claudin 3, and Ep-CAM in metaplastic ovarian epithelium and ovarian cancer. Clin Cancer Res *10*, 4427-4436.

Hileman, R. E., Fromm, J. R., Weiler, J. M., and Linhardt, R. J. (1998). Glycosaminoglycan-protein interactions: definition of consensus sites in glycosaminoglycan binding proteins. Bioessays *20*, 156-167.

Hinek, A., Wrenn, D. S., Mecham, R. P., and Barondes, S. H. (1988). The elastin receptor: a galactoside-binding protein. Science *239*, 1539-1541.

Hiriyanna, K. T., Bingham, E. L., Yashar, B. M., Ayyagari, R., Fishman, G., Small, K. W., Weinberg, D. V., Weleber, R. G., Lewis, R. A., Andreasson, S., *et al.* (1999). Novel mutations in XLRS1 causing retinoschisis, including first evidence of putative leader sequence change. Hum Mutat *14*, 423-427.

Hogg, R., and Chakravarthy, U. (2004). AMD and micronutrient antioxidants. Curr Eye Res *29*, 387-401.

Hope, M. J., Bally, M. B., Webb, G., and Cullis, P. R. (1985). Production of large unilamellar vesicles by a rapid extrusion procedure. Characterization of size distribution, trapped volume, and ability to maintain a membrane potential. Biochim Biophys Acta *812*, 55-65.

Hricovini, M. (2004). Structural aspects of carbohydrates and the relation with their biological properties. Curr Med Chem *11*, 2565-2583.

Hrynchak, P., and Simpson, T. (2000). Optical coherence tomography: an introduction to the technique and its use. Optom Vis Sci *77*, 347-356.

Humphries, M. J. (2002). Insights into integrin-ligand binding and activation from the first crystal structure. Arthritis Res *4 Suppl 3*, S69-78.

Huopaniemi, L., Fellman, J., Rantala, A., Eriksson, A., Forsius, H., De La, C. A., and Alitalo, T. (1999). Skewed secondary sex ratio in the offspring of carriers of the 214G > A mutation of the RS1 gene. Ann Hum Genet 63, 521-533.

Hvarregaard, J., Andersen, M. H., Berglund, L., Rasmussen, J. T., and Petersen, T. E. (1996). Characterization of glycoprotein PAS-6/7 from membranes of bovine milk fat globules. Eur J Biochem 240, 628-636.

Hynes, R. O. (1999). Fibronectins. In Guidebook to the Extracellular Matrix, Anchor, and Adhesion Proteins, T. Kreiss, and R. Vale, eds. (Oxford, Oxford University Press), pp. 422-425.

Hynes, R. O. (2002). Integrins: bidirectional, allosteric signaling machines. Cell 110, 673-687.

Ikeda, K., Wang, L. H., Torres, R., Zhao, H., Olaso, E., Eng, F. J., Labrador, P., Klein, R., Lovett, D., Yancopoulos, G. D., et al. (2002). Discoidin domain receptor 2 interacts with Src and Shc following its activation by type I collagen. J Biol Chem 277, 19206-19212.

Illing, M., Molday, L. L., and Molday, R. S. (1997). The 220-kDa rim protein of retinal rod outer segments is a member of the ABC transporter superfamily. J Biol Chem 272, 10303-10310.

Iozzo, R. V. (1998). Matrix proteoglycans: from molecular design to cellular function. Annu Rev Biochem 67, 609-652.

Isacke, C. M., and Horton, M. A. (2000). The Adhesion Molecule Factsbook (San Diego, Academic Press).

Jenny, R. J., Pittman, D. D., Toole, J. J., Kriz, R. W., Aldape, R. A., Hewick, R. M., Kaufman, R. J., and Mann, K. G. (1987). Complete cDNA and derived amino acid sequence of human factor V. Proc Natl Acad Sci U S A 84, 4846-4850.

Jimbo, M., Koike, K., Sakai, R., Muramoto, K., and Kamiya, H. (2005). Cloning and characterization of a lectin from the octocoral Sinularia lochmodes. Biochem Biophys Res Commun 330, 157-162.

Joester, A., and Faissner, A. (2001). The structure and function of tenascins in the nervous system. Matrix Biol 20, 13-22.

Kahn, H. A., Leibowitz, H. M., Ganley, J. P., Kini, M. M., Colton, T., Nickerson, R. S., and Dawber, T. R. (1977). The Framingham Eye Study. I. Outline and major prevalence findings. Am J Epidemiol 106, 17-32.

Kajiwara, K., Berson, E. L., and Dryja, T. P. (1994). Digenic retinitis pigmentosa due to mutations at the unlinked peripherin/RDS and ROM1 loci. Science 264, 1604-1608.

Kane, W. H., and Davie, E. W. (1986). Cloning of a cDNA coding for human factor V, a blood coagulation factor homologous to factor VIII and ceruloplasmin. Proc Natl Acad Sci U S A *83*, 6800-6804.

Karecla, P. I., Green, S. J., Bowden, S. J., Coadwell, J., and Kilshaw, P. J. (1996). Identification of a binding site for integrin alphaEbeta7 in the N-terminal domain of E-cadherin. J Biol Chem *271*, 30909-30915.

Kawano, K., Tanaka, K., Murakami, F., and Ohba, N. (1981). Congenital hereditary retinoschisis: evolution at the initial stage. Albrecht Von Graefes Arch Klin Exp Ophthalmol *217*, 315-323.

Kedzierski, W., Lloyd, M., Birch, D. G., Bok, D., and Travis, G. H. (1997). Generation and analysis of transgenic mice expressing P216L-substituted rds/peripherin in rod photoreceptors. Invest Ophthalmol Vis Sci *38*, 498-509.

Keen, T. J., and Inglehearn, C. F. (1996). Mutations and polymorphisms in the human peripherin-RDS gene and their involvement in inherited retinal degeneration. Hum Mutat *8*, 297-303.

Kellner, U., Brummer, S., Foerster, M. H., and Wessing, A. (1990). X-linked congenital retinoschisis. Graefes Arch Clin Exp Ophthalmol *228*, 432-437.

Kemball-Cook, G., Tuddenham, E. G., and Wacey, A. I. (1998). The factor VIII Structure and Mutation Resource Site: HAMSTeRS version 4. Nucleic Acids Res *26*, 216-219.

Kennan, A., Aherne, A., and Humphries, P. (2005). Light in retinitis pigmentosa. Trends Genet *21*, 103-110.

Kilpatrick, D. C. (1998). Phospholipid-binding activity of human mannan-binding lectin. Immunol Lett *61*, 191-195.

Kilpatrick, D. C. (2002). Animal lectins: a historical introduction and overview. Biochim Biophys Acta *1572*, 187-197.

Kim, S. W., Quinn-Allen, M. A., Camp, J. T., Macedo-Ribeiro, S., Fuentes-Prior, P., Bode, W., and Kane, W. H. (2000). Identification of functionally important amino acid residues within the C2-domain of human factor V using alanine-scanning mutagenesis. Biochemistry *39*, 1951-1958.

Klaver, C. C., Wolfs, R. C., Assink, J. J., van Duijn, C. M., Hofman, A., and de Jong, P. T. (1998). Genetic risk of age-related maculopathy. Population-based familial aggregation study. Arch Ophthalmol *116*, 1646-1651.

Klein, R. J., Zeiss, C., Chew, E. Y., Tsai, J. Y., Sackler, R. S., Haynes, C., Henning, A. K., SanGiovanni, J. P., Mane, S. M., Mayne, S. T., *et al.* (2005).

Complement factor H polymorphism in age-related macular degeneration. Science *308*, 385-389.

Klevering, B. J., van Driel, M., van de Pol, D. J., Pinckers, A. J., Cremers, F. P., and Hoyng, C. B. (1999). Phenotypic variations in a family with retinal dystrophy as result of different mutations in the ABCR gene. Br J Ophthalmol *83*, 914-918.

Knapp, A. G., and Schiller, P. H. (1984). The contribution of on-bipolar cells to the electroretinogram of rabbits and monkeys. A study using 2-amino-4-phosphonobutyrate (APB). Vision Res *24*, 1841-1846.

Koch, A. W., Manzur, K. L., and Shan, W. (2004). Structure-based models of cadherin-mediated cell adhesion: the evolution continues. Cell Mol Life Sci *61*, 1884-1895.

Kolb, H. (1994). The architecture of functional neural circuits in the vertebrate retina. The Proctor Lecture. Invest Ophthalmol Vis Sci *35*, 2385-2404.

Kolodkin, A. L., Levengood, D. V., Rowe, E. G., Tai, Y. T., Giger, R. J., and Ginty, D. D. (1997). Neuropilin is a semaphorin III receptor. Cell *90*, 753-762.

Kresse, H., and Schonherr, E. (2001). Proteoglycans of the extracellular matrix and growth control. J Cell Physiol *189*, 266-274.

Laemmli, U. K. (1970). Cleavage of structural proteins during the assembly of the head of bacteriophage T4. Nature *227*, 680-685.

Larocca, D., Peterson, J. A., Urrea, R., Kuniyoshi, J., Bistrain, A. M., and Ceriani, R. L. (1991). A Mr 46,000 human milk fat globule protein that is highly expressed in human breast tumors contains factor VIII-like domains. Cancer Res *51*, 4994-4998.

Layne, M. D., Endege, W. O., Jain, M. K., Yet, S. F., Hsieh, C. M., Chin, M. T., Perrella, M. A., Blanar, M. A., Haber, E., and Lee, M. E. (1998). Aortic carboxypeptidase-like protein, a novel protein with discoidin and carboxypeptidase-like domains, is up-regulated during vascular smooth muscle cell differentiation. J Biol Chem *273*, 15654-15660.

Lee, C. C., Kreusch, A., McMullan, D., Ng, K., and Spraggon, G. (2003). Crystal structure of the human neuropilin-1 b1 domain. Structure (Camb) *11*, 99-108.

Lee, M. H., and Murphy, G. (2004). Matrix metalloproteinases at a glance. J Cell Sci *117*, 4015-4016.

Leitinger, B. (2003). Molecular analysis of collagen binding by the human discoidin domain receptors, DDR1 and DDR2: Identification of collagen binding sites in DDR2. J Biol Chem.

Lewin, A. S., Drenser, K. A., Hauswirth, W. W., Nishikawa, S., Yasumura, D., Flannery, J. G., and LaVail, M. M. (1998). Ribozyme rescue of photoreceptor cells in a transgenic rat model of autosomal dominant retinitis pigmentosa. Nat Med *4*, 967-971.

Liu, M., and Grigoriev, A. (2004). Protein domains correlate strongly with exons in multiple eukaryotic genomes--evidence of exon shuffling? Trends Genet *20*, 399-403.

Loewen, C. J., Moritz, O. L., Tam, B. M., Papermaster, D. S., and Molday, R. S. (2003). The role of subunit assembly in peripherin-2 targeting to rod photoreceptor disk membranes and retinitis pigmentosa. Mol Biol Cell *14*, 3400-3413.

Loris, R. (2002). Principles of structures of animal and plant lectins. Biochim Biophys Acta *1572*, 198-208.

Ma, J., Norton, J. C., Allen, A. C., Burns, J. B., Hasel, K. W., Burns, J. L., Sutcliffe, J. G., and Travis, G. H. (1995). Retinal degeneration slow (rds) in mouse results from simple insertion of a t haplotype-specific element into protein-coding exon II. Genomics *28*, 212-219.

Macedo-Ribeiro, S., Bode, W., Huber, R., Quinn-Allen, M. A., Kim, S. W., Ortel, T. L., Bourenkov, G. P., Bartunik, H. D., Stubbs, M. T., Kane, W. H., and Fuentes-Prior, P. (1999). Crystal structures of the membrane-binding C2 domain of human coagulation factor V. Nature *402*, 434-439.

Madjarov, B., Hilton, G. F., Brinton, D. A., and Lee, S. S. (1995). A new classification of the retinoschises. Retina *15*, 282-285.

Madley, I. C., Cook, M. J., and Hames, B. D. (1982). Cell-surface discoidin in aggregating cells of Dictyostelium discoideum. Biochem J *204*, 787-794.

Mamluk, R., Gechtman, Z., Kutcher, M. E., Gasiunas, N., Gallagher, J., and Klagsbrun, M. (2002). Neuropilin-1 binds vascular endothelial growth factor 165, placenta growth factor-2, and heparin via its b1b2 domain. J Biol Chem *277*, 24818-24825.

Martinez-Mir, A., Paloma, E., Allikmets, R., Ayuso, C., del Rio, T., Dean, M., Vilageliu, L., Gonzalez-Duarte, R., and Balcells, S. (1998). Retinitis pigmentosa caused by a homozygous mutation in the Stargardt disease gene ABCR. Nat Genet *18*, 11-12.

Matese, J. C., Black, S., and McClay, D. R. (1997). Regulated exocytosis and sequential construction of the extracellular matrix surrounding the sea urchin zygote. Dev Biol *186*, 16-26.

Matsuyama, W., Wang, L., Farrar, W. L., Faure, M., and Yoshimura, T. (2004). Activation of discoidin domain receptor 1 isoform b with collagen up-regulates chemokine production in human macrophages: role of p38 mitogen-activated protein kinase and NF-kappa B. J Immunol *172*, 2332-2340.

McIlwain, J. T. (1996). An Introduction to the Biology of Vision (Cambridge, UK, Cambridge University Press).

Mendoza-Londono, R., Hiriyanna, K. T., Bingham, E. L., Rodriguez, F., Shastry, B. S., Rodriguez, A., Sieving, P. A., and Tamayo, M. L. (1999). A Colombian family with X-linked juvenile retinoschisis with three affected females finding of a frameshift mutation. Ophthalmic Genet *20*, 37-43.

Meyers, S. M., and Zachary, A. A. (1988). Monozygotic twins with age-related macular degeneration. Arch Ophthalmol *106*, 651-653.

Miao, H. Q., Soker, S., Feiner, L., Alonso, J. L., Raper, J. A., and Klagsbrun, M. (1999). Neuropilin-1 mediates collapsin-1/semaphorin III inhibition of endothelial cell motility: functional competition of collapsin-1 and vascular endothelial growth factor-165. J Cell Biol *146*, 233-242.

Michaelides, M., Hunt, D. M., and Moore, A. T. (2003). The genetics of inherited macular dystrophies. J Med Genet *40*, 641-650.

Migdal, M., Huppertz, B., Tessler, S., Comforti, A., Shibuya, M., Reich, R., Baumann, H., and Neufeld, G. (1998). Neuropilin-1 is a placenta growth factor-2 receptor. J Biol Chem *273*, 22272-22278.

Miner, J. H., Patton, B. L., Lentz, S. I., Gilbert, D. J., Snider, W. D., Jenkins, N. A., Copeland, N. G., and Sanes, J. R. (1997). The laminin alpha chains: expression, developmental transitions, and chromosomal locations of alpha1-5, identification of heterotrimeric laminins 8-11, and cloning of a novel alpha3 isoform. J Cell Biol *137*, 685-701.

Molday, L. L., Cook, N. J., Kaupp, U. B., and Molday, R. S. (1990). The cGMP-gated cation channel of bovine rod photoreceptor cells is associated with a 240-kDa protein exhibiting immunochemical cross-reactivity with spectrin. J Biol Chem *265*, 18690-18695.

Molday, L. L., Hicks, D., Sauer, C. G., Weber, B. H., and Molday, R. S. (2001). Expression of X-linked retinoschisis protein RS1 in photoreceptor and bipolar cells. Invest Ophthalmol Vis Sci *42*, 816-825.

Molday, L. L., Rabin, A. R., and Molday, R. S. (2000). ABCR expression in foveal cone photoreceptors and its role in stargardt macular dystrophy. Am J Ophthalmol *130*, 689.

Moriarty-Craige, S. E., and Jones, D. P. (2004). Extracellular thiols and thiol/disulfide redox in metabolism. Annu Rev Nutr *24*, 481-509.

Mott, J. D., and Werb, Z. (2004). Regulation of matrix biology by matrix metalloproteinases. Curr Opin Cell Biol *16*, 558-564.

Myllyharju, J., and Kivirikko, K. I. (2004). Collagens, modifying enzymes and their mutations in humans, flies and worms. Trends Genet *20*, 33-43.

Nagar, B., Overduin, M., Ikura, M., and Rini, J. M. (1996). Structural basis of calcium-induced E-cadherin rigidification and dimerization. Nature *380*, 360-364.

Nakamura, F., Tanaka, M., Takahashi, T., Kalb, R. G., and Strittmatter, S. M. (1998). Neuropilin-1 extracellular domains mediate semaphorin D/III-induced growth cone collapse. Neuron *21*, 1093-1100.

Olsen, B. R., and Ninomiya, Y. (1999). Collagens. In Guidebook to the Extracellular Matrix, Anchor, and Adhesion Proteins, T. Kreiss, and R. Vale, eds. (Oxford, Oxford University Press), pp. 380-408.

Ongusaha, P. P., Kim, J. I., Fang, L., Wong, T. W., Yancopoulos, G. D., Aaronson, S. A., and Lee, S. W. (2003). p53 induction and activation of DDR1 kinase counteract p53-mediated apoptosis and influence p53 regulation through a positive feedback loop. Embo J *22*, 1289-1301.

Ortel, T. L., Devore-Carter, D., Quinn-Allen, M., and Kane, W. H. (1992). Deletion analysis of recombinant human factor V. Evidence for a phosphatidylserine binding site in the second C-type domain. J Biol Chem *267*, 4189-4198.

Overall, C. M. (2001). Matrix metalloproteinase substrate binding domains, modules and exosites. Overview and experimental strategies. Methods Mol Biol *151*, 79-120.

Park, J. H., Ott, S. H., Wang, X., Appukuttan, B., Patel, R. J., Van Boemel, G. B., and Stout, J. T. (2000). Clinical phenotype associated with the arg141 his mutation in the X- linked retinoschisis gene. Arch Ophthalmol *118*, 127-129.

Patthy, L. (2003). Modular assembly of genes and the evolution of new functions. Genetica *118*, 217-231.

Peachey, N. S., Fishman, G. A., Derlacki, D. J., and Brigell, M. G. (1987). Psychophysical and electroretinographic findings in X-linked juvenile retinoschisis. Arch Ophthalmol *105*, 513-516.

Peles, E., Nativ, M., Lustig, M., Grumet, M., Schilling, J., Martinez, R., Plowman, G. D., and Schlessinger, J. (1997). Identification of a novel contactin-associated

transmembrane receptor with multiple domains implicated in protein-protein interactions. Embo J *16*, 978-988.

Penfold, P. L., Madigan, M. C., Gillies, M. C., and Provis, J. M. (2001). Immunological and aetiological aspects of macular degeneration. Prog Retin Eye Res *20*, 385-414.

Pepys, M. B., and Butler, P. J. (1987). Serum amyloid P component is the major calcium-dependent specific DNA binding protein of the serum. Biochem Biophys Res Commun *148*, 308-313.

Perret, E., Leung, A., Feracci, H., and Evans, E. (2004). Trans-bonded pairs of E-cadherin exhibit a remarkable hierarchy of mechanical strengths. Proc Natl Acad Sci U S A *101*, 16472-16477.

Pertz, O., Bozic, D., Koch, A. W., Fauser, C., Brancaccio, A., and Engel, J. (1999). A new crystal structure, Ca2+ dependence and mutational analysis reveal molecular details of E-cadherin homoassociation. EMBO J *18*, 1738-1747.

Pierschbacher, M. D., and Ruoslahti, E. (1984). Variants of the cell recognition site of fibronectin that retain attachment-promoting activity. Proc Natl Acad Sci U S A *81*, 5985-5988.

Poole, S., Firtel, R. A., Lamar, E., and Rowekamp, W. (1981). Sequence and expression of the discoidin I gene family in Dictyostelium discoideum. J Mol Biol *153*, 273-289.

Portera-Cailliau, C., Sung, C. H., Nathans, J., and Adler, R. (1994). Apoptotic photoreceptor cell death in mouse models of retinitis pigmentosa. Proc Natl Acad Sci U S A *91*, 974-978.

Pratt, K. P., Shen, B. W., Takeshima, K., Davie, E. W., Fujikawa, K., and Stoddard, B. L. (1999). Structure of the C2 domain of human factor VIII at 1.5 A resolution. Nature *402*, 439-442.

Prydz, K., and Dalen, K. T. (2000). Synthesis and sorting of proteoglycans. J Cell Sci *113 Pt 2*, 193-205.

Puente, X. S., Sanchez, L. M., Overall, C. M., and Lopez-Otin, C. (2003). Human and mouse proteases: a comparative genomic approach. Nat Rev Genet *4*, 544-558.

Quondamatteo, F. (2002). Assembly, stability and integrity of basement membranes in vivo. Histochem J *34*, 369-381.

Rando, R. R. (2001). The biochemistry of the visual cycle. Chem Rev *101*, 1881-1896.

Regillo, C. D., Tasman, W. S., and Brown, G. C. (1993). Surgical management of complications associated with X-linked retinoschisis. Arch Ophthalmol *111*, 1080-1086.

Reichardt, L. F. (1999). Introduction to Extracellular Matrix Molecules and Their Receptors. In Guidebook to the Extracellular Matrix, Anchor, and Adhesion Proteins, T. Kreiss, and R. Vale, eds. (Oxford, Oxford University Press), pp. 335-344.

Reichardt, L. F., Bossy, B., de, C., I, Neugebauer, K. M., Venstrom, K., and Sretavan, D. (1992). Adhesive interactions that regulate development of the retina and primary visual projection. Cold Spring Harb Symp Quant Biol *57*, 419-429.

Reid, S. N., Akhmedov, N. B., Piriev, N. I., Kozak, C. A., Danciger, M., and Farber, D. B. (1999). The mouse X-linked juvenile retinoschisis cDNA: expression in photoreceptors. Gene *227*, 257-266.

Reid, S. N., Yamashita, C., and Farber, D. B. (2003). Retinoschisin, a photoreceptor-secreted protein, and its interaction with bipolar and muller cells. J Neurosci *23*, 6030-6040.

Riccardi, D. (2000). Calcium ions as extracellular, first messengers. Z Kardiol *89 Suppl 2*, 9-14.

Richards, A. J., Scott, J. D., and Snead, M. P. (2002). Molecular genetics of rhegmatogenous retinal detachment. Eye *16*, 388-392.

Rodieck, R. W. (1973). The Vertebrate Retina: Principles of Structure and Function (San Francisco, W. H. Freeman and Company).

Rosen, S. D., Kafka, J. A., Simpson, D. L., and Barondes, S. H. (1973). Developmentally regulated, carbohydrate-binding protein in Dictyostelium discoideum. Proc Natl Acad Sci U S A *70*, 2554-2557.

Roy, S. W. (2003). Recent evidence for the exon theory of genes. Genetica *118*, 251-266.

Saleh, M., Peng, W., Quinn-Allen, M. A., Macedo-Ribeiro, S., Fuentes-Prior, P., Bode, W., and Kane, W. H. (2004). The factor V C1 domain is involved in membrane binding: identification of functionally important amino acid residues within the C1 domain of factor V using alanine scanning mutagenesis. Thromb Haemost *91*, 16-27.

Sanyal, S., and Jansen, H. G. (1981). Absence of receptor outer segments in the retina of rds mutant mice. Neurosci Lett *21*, 23-26.

Sasaki, T., and Timpl, R. (1999). Laminins. In Guidebook to the Extracellular Matrix, Anchor, and Adhesion Proteins, T. Kreiss, and R. Vale, eds. (Oxford, Oxford University Press), pp. 434-443.

Sauer, C. G., Gehrig, A., Warneke-Wittstock, R., Marquardt, A., Ewing, C. C., Gibson, A., Lorenz, B., Jurklies, B., and Weber, B. H. (1997). Positional cloning of the gene associated with X-linked juvenile retinoschisis. Nat Genet *17*, 164-170.

Schlichtenbrede, F. C., da Cruz, L., Stephens, C., Smith, A. J., Georgiadis, A., Thrasher, A. J., Bainbridge, J. W., Seeliger, M. W., and Ali, R. R. (2003). Long-term evaluation of retinal function in Prph2Rd2/Rd2 mice following AAV-mediated gene replacement therapy. J Gene Med *5*, 757-764.

Seddon, J. M., Cote, J., Page, W. F., Aggen, S. H., and Neale, M. C. (2005). The US twin study of age-related macular degeneration: relative roles of genetic and environmental influences. Arch Ophthalmol *123*, 321-327.

See, Y. P., and Jackowski, G. (1989). Estimating molecular weights of polypeptides by SDS gel electrophoresis. In Protein Structure: A Practical Approach, T. E. Creighton, ed. (Oxford, IRL Press).

Shan, W., Yagita, Y., Wang, Z., Koch, A., Svenningsen, A. F., Gruzglin, E., Pedraza, L., and Colman, D. R. (2004). The minimal essential unit for cadherin-mediated intercellular adhesion comprises extracellular domains 1 and 2. J Biol Chem *279*, 55914-55923.

Shan, W. S., Tanaka, H., Phillips, G. R., Arndt, K., Yoshida, M., Colman, D. R., and Shapiro, L. (2000). Functional cis-heterodimers of N- and R-cadherins. J Cell Biol *148*, 579-590.

Shapiro, L., Fannon, A. M., Kwong, P. D., Thompson, A., Lehmann, M. S., Grubel, G., Legrand, J. F., Als-Nielsen, J., Colman, D. R., and Hendrickson, W. A. (1995). Structural basis of cell-cell adhesion by cadherins. Nature *374*, 327-337.

Sharon, N., and Lis, H. (2003). Lectins (Dordrecht, Netherlands, Kluwer Academic).

Shimizu, M., Murakami, Y., Suto, F., and Fujisawa, H. (2000). Determination of cell adhesion sites of neuropilin-1. J Cell Biol *148*, 1283-1293.

Shinoda, K., Ishida, S., Oguchi, Y., and Mashima, Y. (2000). Clinical characteristics of 14 japanese patients with X-linked juvenile retinoschisis associated with XLRS1 mutation. Ophthalmic Genet *21*, 171-180.

Sieving, P. A. (1998). Juvenile Retinoschisis. In Genetic Diseases of the Eye, E. I. Traboulsi, ed. (New York, Oxford University Press).

Sieving, P. A., Bingham, E. L., Kemp, J., Richards, J., and Hiriyanna, K. (1999). Juvenile X-linked retinoschisis from XLRS1 Arg213Trp mutation with preservation of the electroretinogram scotopic b-wave. Am J Ophthalmol *128*, 179-184.

Simpson, D. L., Rosen, S. D., and Barondes, S. H. (1974). Discoidin, a developmentally regulated carbohydrate-binding protein from Dictyostelium discoideum. Purification and characterization. Biochemistry *13*, 3487-3493.

Smith, W., Mitchell, P., and Leeder, S. R. (1996). Smoking and age-related maculopathy. The Blue Mountains Eye Study. Arch Ophthalmol *114*, 1518-1523.

Soker, S., Takashima, S., Miao, H. Q., Neufeld, G., and Klagsbrun, M. (1998). Neuropilin-1 is expressed by endothelial and tumor cells as an isoform-specific receptor for vascular endothelial growth factor. Cell *92*, 735-745.

Springer, W. R., Cooper, D. N., and Barondes, S. H. (1984). Discoidin I is implicated in cell-substratum attachment and ordered cell migration of Dictyostelium discoideum and resembles fibronectin. Cell *39*, 557-564.

Srivastava, A., Quinn-Allen, M. A., Kim, S. W., Kane, W. H., and Lentz, B. R. (2001). Soluble phosphatidylserine binds to a single identified site in the C2 domain of human factor V(a). Biochemistry *40*, 8246-8255.

Sternlicht, M. D., and Werb, Z. (1999). ECM Proteinases. In Guidebook to the Extracellular Matrix, Anchor, and Adhesion Proteins, T. Kreiss, and R. Vale, eds. (Oxford, Oxford University Press), pp. 505-509.

Sun, H., Molday, R. S., and Nathans, J. (1999). Retinal stimulates ATP hydrolysis by purified and reconstituted ABCR, the photoreceptor-specific ATP-binding cassette transporter responsible for Stargardt disease. J Biol Chem *274*, 8269-8281.

Sung, C. H., Makino, C., Baylor, D., and Nathans, J. (1994). A rhodopsin gene mutation responsible for autosomal dominant retinitis pigmentosa results in a protein that is defective in localization to the photoreceptor outer segment. J Neurosci *14*, 5818-5833.

Takeichi, M., Hatta, K., Nose, A., Nagafuchi, A., and Matsunaga, M. (1989). Cadherin-mediated specific cell adhesion and animal morphogenesis. Ciba Found Symp *144*, 243-249; discussion 250-244, 290-245.

Tam, B. M., Moritz, O. L., Hurd, L. B., and Papermaster, D. S. (2000). Identification of an outer segment targeting signal in the COOH terminus of rhodopsin using transgenic Xenopus laevis. J Cell Biol *151*, 1369-1380.

Tantri, A., Vrabec, T. R., Cu-Unjieng, A., Frost, A., Annesley, W. H., Jr., and Donoso, L. A. (2004). X-linked retinoschisis: a clinical and molecular genetic review. Surv Ophthalmol *49*, 214-230.

Thompson, J. D., Higgins, D. G., and Gibson, T. J. (1994). CLUSTAL W: improving the sensitivity of progressive multiple sequence alignment through sequence weighting, position-specific gap penalties and weight matrix choice. Nucleic Acids Res *22*, 4673-4680.

Towbin, H., Staehelin, T., and Gordon, J. (1979). Electrophoretic transfer of proteins from polyacrylamide gels to nitrocellulose sheets: procedure and some applications. Proc Natl Acad Sci U S A *76*, 4350-4354.

Travis, G. H., Brennan, M. B., Danielson, P. E., Kozak, C. A., and Sutcliffe, J. G. (1989). Identification of a photoreceptor-specific mRNA encoded by the gene responsible for retinal degeneration slow (rds). Nature *338*, 70-73.

van Leeuwen, R., Klaver, C. C., Vingerling, J. R., Hofman, A., and de Jong, P. T. (2003). Epidemiology of age-related maculopathy: a review. Eur J Epidemiol *18*, 845-854.

van Wijk, R., Nieuwenhuis, K., van den Berg, M., Huizinga, E. G., van der Meijden, B. B., Kraaijenhagen, R. J., and van Solinge, W. W. (2001). Five novel mutations in the gene for human blood coagulation factor V associated with type I factor V deficiency. Blood *98*, 358-367.

Varki, A., Cummings, R., Esko, J., Freeze, H., Hart, G., and Marth, J. (2000). Essentials of Glycobiology (Cold Spring Harbor, NY, Cold Spring Harbor Laboratory Press).

Venstrom, K. A., and Reichardt, L. F. (1993). Extracellular matrix. 2: Role of extracellular matrix molecules and their receptors in the nervous system. FASEB J *7*, 996-1003.

Vingerling, J. R., Hofman, A., Grobbee, D. E., and de Jong, P. T. (1996). Age-related macular degeneration and smoking. The Rotterdam Study. Arch Ophthalmol *114*, 1193-1196.

Vogel, W. (1999). Discoidin domain receptors: structural relations and functional implications. FASEB J *13 Suppl*, S77-S82.

Vogel, W., Gish, G. D., Alves, F., and Pawson, T. (1997). The discoidin domain receptor tyrosine kinases are activated by collagen. Mol Cell *1*, 13-23.

Wang, T., Waters, C. T., Rothman, A. M., Jakins, T. J., Romisch, K., and Trump, D. (2002). Intracellular retention of mutant retinoschisin is the pathological mechanism underlying X-linked retinoschisis. Hum Mol Genet *11*, 3097-3105.

Weber, B. H., Schrewe, H., Molday, L. L., Gehrig, A., White, K. L., Seeliger, M. W., Jaissle, G. B., Friedburg, C., Tamm, E., and Molday, R. S. (2002). Inactivation of the murine X-linked juvenile retinoschisis gene, Rs1h, suggests a role of retinoschisin in retinal cell layer organization and synaptic structure. Proc Natl Acad Sci USA *99*, 6222-6227.

Weng, J., Mata, N. L., Azarian, S. M., Tzekov, R. T., Birch, D. G., and Travis, G. H. (1999). Insights into the function of Rim protein in photoreceptors and etiology of Stargardt's disease from the phenotype in abcr knockout mice. Cell *98*, 13-23.

Wenzel, A., Grimm, C., Samardzija, M., and Reme, C. E. (2005). Molecular mechanisms of light-induced photoreceptor apoptosis and neuroprotection for retinal degeneration. Prog Retin Eye Res *24*, 275-306.

West, D. C., Rees, C. G., Duchesne, L., Patey, S. J., Terry, C. J., Turnbull, J. E., Delehedde, M., Heegaard, C. W., Allain, F., Vanpouille, C., *et al.* (2005). Interactions of multiple heparin binding growth factors with neuropilin-1 and potentiation of the activity of fibroblast growth factor-2. J Biol Chem *280*, 13457-13464.

Whittard, J. D., Craig, S. E., Mould, A. P., Koch, A., Pertz, O., Engel, J., and Humphries, M. J. (2002). E-cadherin is a ligand for integrin alpha2beta1. Matrix Biol *21*, 525-532.

Wolf, G. (2003). Lipofuscin and macular degeneration. Nutr Rev *61*, 342-346.

Wood, W. I., Capon, D. J., Simonsen, C. C., Eaton, D. L., Gitschier, J., Keyt, B., Seeburg, P. H., Smith, D. H., Hollingshead, P., Wion, K. L., and et al. (1984). Expression of active human factor VIII from recombinant DNA clones. Nature *312*, 330-337.

Wu, W. W. H., and Molday, R. S. (2003). Defective discoidin domain structure, subunit assembly, and endoplasmic reticulum processing of retinoschisin are primary mechanisms responsible for X-linked retinoschisis. J Biol Chem *278*, 28139-28146.

Wu, W. W. H., and Molday, R. S. (2005). Interactions of the synaptic retinal adhesion protein, RS1, with components of the extracellular matrix. Synaptic Function and Plasticity Conference, Vancouver, Canada.

Wu, W. W. H., Wong, J. P., Kast, J., and Molday, R. S. (2005). RS1, a discoidin domain-containing retinal cell adhesion protein associated with X-linked retinoschisis, exists as a novel disulfide-linked octamer. J Biol Chem *280*, 10721-10730.

Xiong, J. P., Stehle, T., Diefenbach, B., Zhang, R., Dunker, R., Scott, D. L., Joachimiak, A., Goodman, S. L., and Arnaout, M. A. (2001). Crystal structure of the extracellular segment of integrin alpha Vbeta3. Science *294*, 339-345.

Xu, L., Peng, H., Wu, D., Hu, K., Goldring, M. B., Olsen, B. R., and Li, Y. (2005). Activation of the discoidin domain receptor 2 induces expression of matrix metalloproteinase 13 associated with osteoarthritis in mice. J Biol Chem *280*, 548-555.

Yamada, E. (1969). Some structural features of the fovea centralis in the human retina. Arch Ophthalmol *82*, 151-159.

Yamakawa, M., and Tanaka, H. (1999). Immune proteins and their gene expression in the silkworm, Bombyx mori. Dev Comp Immunol *23*, 281-289.

Zamir, E., and Geiger, B. (2001). Molecular complexity and dynamics of cell-matrix adhesions. J Cell Sci *114*, 3583-3590.